

NASA TECHNICAL NOTE



NASA TN D-4110

c.1

NASA TN D-4110

LOAN COPY: 1
APR 1967
KURTZ



ALIGNMENT OF INERTIAL SYSTEMS ON A MOVING BASE

by Arthur H. Lipton
Electronics Research Center
Cambridge, Mass.



ALIGNMENT OF INERTIAL SYSTEMS ON A MOVING BASE

By Arthur H. Lipton

Electronics Research Center
Cambridge, Mass.

NATIONAL AERONAUTICS AND SPACE ADMINISTRATION

For sale by the Clearinghouse for Federal Scientific and Technical Information
Springfield, Virginia 22151 - CFSTI price \$3.00

ABSTRACT

A unified theory of alignment is developed which is founded on the two considerations common to all alignment procedures: coordinate frames and measurements. All alignment procedures are viewed as a class of non-dimensional, vector-direction-indication problems which effect a transfer of orientation between two coordinate frames. Part of the present thesis is that the differences among various approaches to the solution of the moving base alignment problem are superficial. A discussion of the essential requirements for alignment is presented in the unified format. The roles of instrument errors and base motion as fundamental limitations on the alignment accuracy are developed in detail. All performance indices are chosen as angular quantities which are invariant under coordinate transformation. This facilitates a comparison and evaluation of techniques independent of the details of system mechanization. The necessary conversion of magnitude-sensitive instrument uncertainties to their angular equivalents is presented in detail.

Purely geometric considerations yield a closed form solution for the sensitivity of platform misalignment to the angle between measured vectors. It is also shown that the magnitude of a rotation specified by the arguments of the principal direction cosines is independent of the skewness of the rotated coordinate frame. The magnitude of a rotation specified by Euler angles is found to be almost completely independent of the order of the rotations. The very important distinctions among "measuring a vector," "measuring a vector's magnitude," and "measuring a vector's direction" are quantified as a function of instrument error parameters and the orientation of the vector with respect to the instruments.

Application of the unified analysis is made to the following specific alignment techniques: Vertical Indication; Gyrocompassing; Star Tracking; Fix Monitored Azimuth; Vector Matching; Gimbal Angle Matching; and Optical Comparison. It is shown for a multiple-system configuration that simultaneous measurements of a single vector by multiple systems do not constitute multiple measurements of a common alignment parameter. An additional measurement is introduced which takes advantage of the multiple system configuration and improves the alignment of each system. The extent to which operational considerations act as a pre-filter on the selection of an alignment scheme is discussed relative to the carrier-borne alignment of aircraft navigation systems.

TABLE OF CONTENTS

<u>Chapter</u>		<u>Page</u>
I.	INTRODUCTION	1
II.	A UNIFIED THEORY OF ALIGNMENT	7
	2.1 Introduction	7
	2.2 Coordinate Frame Considerations	8
	2.2.1 Independent Reference Frame.	8
	2.2.2 Dependent Reference Frame	10
	2.2.3 Intermediate Reference Frame	11
	2.2.4 Transfer Reference Frame.	12
	2.3 Measurement Considerations.	12
	2.3.1 Vectorial Nature of the Measurements.	12
	2.3.2 Two Vector Requirement.	14
	2.4 Error Analysis.	21
	2.4.1 Angular Quantities.	21
	2.4.2 System Measurement Capability.	40
	2.4.2.1 Basic Sensor Errors and Their Equiva- lent Misalignments	42
	2.4.2.2 System Magnitude Measurements	53
	2.4.2.3 System Null-Seeking Measurements	67
	2.4.2.4 System Sensitive Axis Uncertainty.	73
	2.4.2.5 Summary of System Measurement Capability	79
	2.4.3 Composite Misalignment for Two Vector Measurement	85
	2.4.4 Information Transferred From an Ex- ternal Sensor or System	89
	2.5 Summary	91
III.	ANALYSIS OF ALIGNMENT TECHNIQUES	95
	3.1 Introduction	95
	3.2 Vertical Indication	97
	3.2.1 Evaluation of β for Vertical Indication	100
	3.2.2 Evaluation of α for Vertical Indication	106
	3.3 Gyrocompassing	107
	3.3.1 Evaluation of β for Gyrocompassing	108
	3.3.2 Evaluation of α for Gyrocompassing	111
	3.3.3 A Special One-Gyro Situation	113

TABLE OF CONTENTS (Cont)

<u>Chapter</u>	<u>Page</u>
3.4 Star Tracking	113
3.4.1 Discussion of β for Star Tracking . . .	114
3.4.2 Comment on α for Star Tracking . . .	115
3.5 Fix Monitored Azimuth	117
3.6 Vector Matching	122
3.6.1 "Memory" in Transfer Alignments . . .	122
3.6.2 Vector Matching Theory and Mechanizations.	123
3.6.3 Compensation for Platform Separation .	127
3.6.4 The Vector Match Vertical - A Fallacy	127
3.6.5 General Formulation of Vector Matching	129
3.7 Gimbal Angle Matching	132
3.7.1 Coordinate Transformation	133
3.7.2 Error Analysis.	136
3.7.3 An Observation Regarding System Installation	140
3.8 Optical Alignment	140
3.9 Summary	143
IV. EXAMPLES OF UNIQUE OPERATIONAL SITUATIONS	145
4.1 Introduction	145
4.2 Multiple Airborne Systems	145
4.3 A Naval Situation	150
V. SUMMARY AND RECOMMENDATIONS	155
5.1 Summary	155
5.2 Recommendations	157

TABLE OF CONTENTS (Cont)

<u>Appendices</u>	<u>Page</u>
A. INSTRUMENT EXAMPLE - THE LINEAR ACCELEROMETER159
B. A CERTAIN EVALUATION OF THE EQUATION $A^2 = B^2 + C^2 \pm 2 BC \cos \eta$165
C. AN INTERPRETATION OF STATISTICS ASSOCIATED WITH A TRIAD OF SENSORS.169
D. OPTIMAL ESTIMATION APPLIED TO MULTIPLE SYSTEMS173

ALIGNMENT OF INERTIAL SYSTEMS
ON A MOVING BASE *

By Arthur H. Lipton
Electronics Research Center
Cambridge, Massachusetts

CHAPTER I
INTRODUCTION

The preparation of an inertial guidance system for any mission requires:

1. Establishment of a measurement reference frame through initial alignment of the inertial measuring unit (IMU), and
2. Establishment of initial conditions on velocity and position of the system in this frame.

The initialization of a system while its carrying vehicle is stationary relative to the earth has been the subject of a continuing effort to achieve greater accuracies in less time. This effort has met with considerable success in the past, and, in fact, is currently showing significant progress.^{1**}

There has also been a recurring requirement to perform this initialization when the carrying vehicle is non-stationary relative to the earth. The concept of initialization-in-motion is particularly attractive in weapon system technology. Several examples of vehicles which may be used to transport an inertial system together with representative systems which specify (or specified) initialization while in motion are an aircraft (Skybolt, Hound Dog), a train (Minuteman), an aircraft carrier (F-111B) or a submarine (Polaris).

* Submitted to the Massachusetts Institute of Technology, Department of Aeronautics and Astronautics in August 1966 in partial fulfillment of the requirements for the degree of Doctor of Science in Instrumentation.

** Superscript numerals refer to numbered references in the bibliography.

Unfortunately, success in initialization on a moving base has been much more limited than that on a stationary base. The initial alignment portion of the complete initialization task represents a particularly hard core problem. It is to this initial alignment problem that this thesis is addressed, with special emphasis on the problems of aligning on a moving base.

Alignment, for our purposes, is defined as determining the angular orientation of a set of fiducial axes fixed in an IMU with respect to an arbitrarily chosen set of reference axes. This determination is either an analytic evaluation of the relative angular orientation between two coordinate frames or a procedure which seeks to achieve angular coincidence between two coordinate frames. The reference axes to which the IMU is aligned frequently represent a traditional geographic or geocentric coordinate frame. In several moving base alignment techniques, however, the reference axes may well be the fiducial axes of a second IMU. Regardless of the particular frames involved, the error quantity (misalignment) represents an undesired angular discrepancy between the IMU's fiducial axes and the reference coordinate axes. The most general description of misalignment is the "whole angle rotation" described in Chapter II. A familiar and important specialization of this description is the vertical and azimuth specification of an IMU's misalignment relative to a geographic reference frame.

Most alignments depend, to some degree, on measurements of the IMU's inertial sensors²: accelerometers and gyros. Since these sensors are required for guidance and navigation subsequent to initialization, it is desirable to utilize them for alignment. The accelerometers and gyros are able to effect alignment relative to the earth by identifying the earth's gravity

(\bar{g}) and daily rotation rate ($\bar{\omega}_{IE}$) vectors. This identification is straightforward from a base fixed relative to the earth. Motion of a vehicle with respect to the earth, however, effectively decouples the system from these significant inputs by adding inertially indistinguishable vehicle accelerations to \bar{g} and angular vehicle rates to $\bar{\omega}_{IE}$. When this decoupling due to base-motion becomes severe enough to prohibit alignment by standard fixed-base techniques, we have a moving base alignment problem. As used in this thesis, then, a moving base connotes a vehicle which undergoes sufficient translation and rotation relative to the earth to seriously affect the alignment problem.

An examination of the literature ^{3, 4, 5} reveals two basic engineering approaches to the solution of the moving base alignment problem. The first is an extension and/or modification of the techniques used in a stationary situation. The extensions and/or modifications effectively serve to recouple the system to the earth by processing (i. e. filtering, compensating) the moving-base inertial measurements in a manner which obtains an equivalent fixed-base inertial measurement. Often as not, this requires additional non-inertial measurements with respect to the earth.

The second approach is the development of a group of special techniques. Some of these techniques still rely upon measurements of the systems' inertial sensors, but the measured quantities no longer have a unique a priori meaning relative to the earth. In this case, some means of calibrating the measured quantity must be provided, usually in the form of a pre-aligned inertial measurement unit carried on board the same vehicle. Other special techniques introduce non-inertial alignment

measurements as a means of circumventing the base motion disturbance of inertial quantities. Some of these non-inertial measurements identify quantities which have an a priori significance relative to an inertial reference frame (e.g., a star line-of-sight) or even to the earth (e.g., a range measurement relative to an earth-fixed point). Still other non-inertial measurements are merely a means of transferring the alignment of a pre-aligned on-board IMU to the inertial system of an aircraft or missile.

This thesis emphasizes the homogeneity among the superficially distinct approaches to the moving base alignment problem. Among other things, this facilitates the evaluation and comparison of the more significant techniques. The fundamental limitations of moving base alignment are viewed as 1) the errors due to the measurement devices and 2) the errors due to base motion interference with the measurement paths. In this context, base-motion interference relates not only to gross motions of the vehicle relative to the earth but also to the non-rigid behavior of the vehicle structure. That these fundamental limitations may be described in a uniform fashion regardless of the measurement technique is demonstrated in the thesis. The relative contributions of sensor error and base-motion to a composite alignment accuracy are developed, providing a basis for studying the trade-off between instrument errors and disturbing base-motions.

Chapter II of this thesis is devoted to the development of a unified theory of alignment. This theory is founded on the two considerations common to all alignment procedures:

coordinate frames and measurements. All alignment procedures are viewed as the transfer of alignment between two coordinate frames by means of measurements on at least two non-collinear vectors. Individual techniques are seen to vary only in the mechanization of particular measurements. Coordinate frame rotations are treated as whole angle rotations, the latter being developed in terms of all the more usual rotational parameters. Measurements are discussed from the viewpoint of single-degree-of-freedom sensors attempting to locate the direction of a vector input. Both magnitude sensitive and angle sensitive instruments are considered. Base motion is treated as causing an angular deflection of the measured vector from a desired nominal direction. The magnitude of the total platform misalignment resulting from independent measurements of two non-collinear vectors is calculated as a function of the angular uncertainties in determining the nominal direction of each of the vectors.

Chapter III applies the analysis of Chapter II to the following specific alignment techniques: Vertical Indication, Gyrocompassing, Star Tracking, Fix Monitored Azimuth, Vector Matching, Gimbal Angle Matching and Optical Comparison. The mathematical methodology not only provides a common basis for comparing techniques but also is seen in certain instances to be a simpler way of treating old problems (e. g. , Gimbal Angle Matching). Limitations on the use of each technique are discussed as an aid in the appropriate selection of measurement techniques for individual situations. Individual conclusions are necessarily limited in scope but taken together encompass the spectrum of moving base problems associated with acceptable carrying vehicles.

Chapter IV discusses two unique operational situations. The first is that of multiple missile systems carried aboard the same vehicle. The question addressed is whether the simultaneous alignment of all the systems is advantageous from the standpoint of improved individual system alignments. The second situation, that of the carrier-borne alignment of aircraft navigation systems, demonstrates how operational considerations can be a very strong pre-filter on the selection of a particular technique.

A summary and recommendations are presented in Chapter V.

Professor Walter Wrigley, the chairman of my thesis committee, has been a source of encouragement and helpful suggestions throughout my doctoral program. Detailed discussions with him and with Professors Y. T. Li, W. R. Markey and J. E. Potter have contributed greatly to this thesis and are sincerely appreciated.

I thank Mr. Kenneth Fertig for the encouragement and training received while under his supervision and for his continued interest in the author's progress. I am also grateful to my colleagues at the MIT Instrumentation Laboratory and the NASA Electronics Research Center for their many helpful suggestions and discussions. I acknowledge with gratitude the understanding of my supervisors at NASA in providing conditions necessary for completion of this thesis.

CHAPTER II

A UNIFIED THEORY OF ALIGNMENT

2.1 Introduction

The literature devoted to the alignment of inertial systems on a moving base (for example, References 1, 2, 3, 4, 13, 24, 25, 27, 30, 32) is primarily concerned with the analysis of distinct approaches and techniques. In fact, seven specific alignment techniques are discussed in detail in Chapter III of this thesis. Yet no matter how different the various approaches to the solution of the moving base alignment problem may appear, this difference is superficial. There exists a large measure of homogeneity among the various approaches which is not evident from a survey of the literature. Properly emphasized, this homogeneity facilitates a comparison and evaluation of techniques which a preoccupation with disparity might otherwise mask. Hence the development and presentation of this unified theory of alignment.

When reduced to its elementary form, the alignment problem is seen to be concerned with three major considerations: 1) the consideration of coordinate frames and coordinate frame transformations; 2) the consideration of measurements made by sensors integral to a particular inertial system; and 3) the consideration of information transferred from an external sensor or system.

The organization of this chapter is such that these considerations are first discussed separately. This is primarily to minimize the framework necessary for analysis of the problem. It is not to imply that the three (3) considerations are completely independent, for as measurements are made to establish the alignment of coordinate frames, so does the alignment of coordinate frames affect the ability of sensors to make accurate measurements. Dependencies such as this are developed as part of the uniform error analysis in the latter portion of the chapter.

2.2 Coordinate Frame Considerations

The definition of alignment requires only two (2) coordinate frames: a set of fiducial axes fixed in an inertial measuring unit (IMU) and an arbitrary set of reference axes. Yet the physical realization of an alignment procedure frequently requires the consideration of many more than two (2) coordinate frames. By minimizing the required number, one achieves a significant simplification in the associated transformations and manipulations.

It is possible to identify four reference coordinate frames which constitute the absolute minimum necessary to describe every moving base alignment procedure known to this author. This minimum results from considering the stable member of an IMU as simply a rigid body. In order to permit evaluation of the alignment (i. e., orientation or attitude) of this stable member, one need only visualize implanting a reference triad in the stable member. Except for certain purposes of mathematical convenience, the location of this reference set does not have to have a special relationship to instrument axes, computational axes, or the navigational reference frame. It will, however, ordinarily be chosen as an orthogonal set.

Figure 2.1 shows the functional relationships for the required reference coordinate frames. In addition, because the alignment process is always based on a set of measurements and sometimes aided by a transfer of external information, the alternate measurement paths required to describe the complete alignment problem are also indicated. Of the two coordinate frames required for the definition of alignment, the fiducial axes of an IMU form the dependent reference frame of Figure 2.1 and the arbitrary set of reference axes form the independent reference frame.

2.2.1 Independent Reference Frame

The independent reference frame is a purely analytical coordinate frame. As such it is the only required coordinate frame which is not considered rigidly attached to the stable

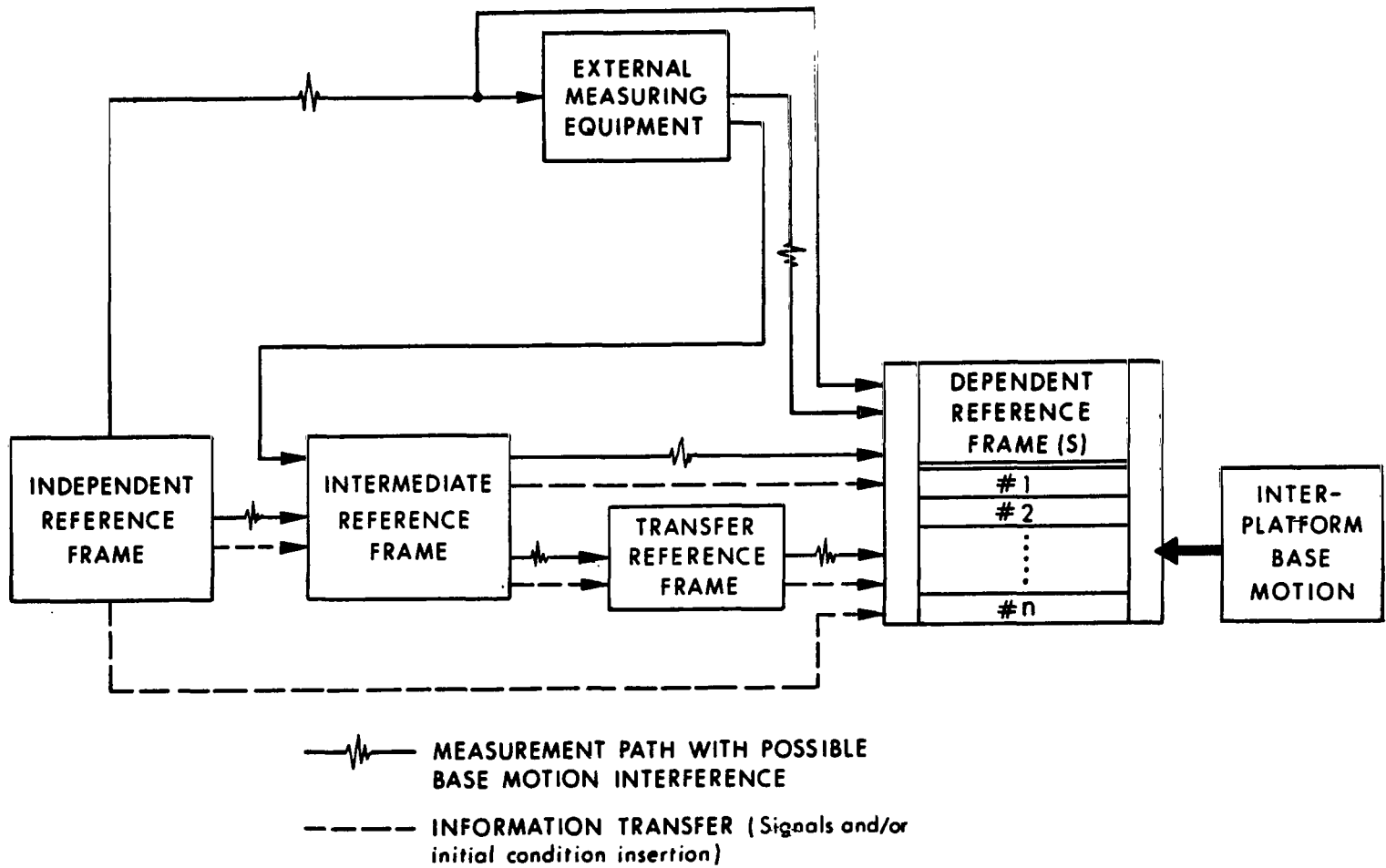


Figure 2-1 Functional Diagram of Coordinate Frames and Measurement Paths Required to Describe the Moving Base Alignment Problem

member of an IMU. It represents the ideal orientation of any of its physically mechanized counterparts and is therefore the ultimate gauge of how well a system has been aligned. The orientation chosen for the independent reference frame usually will be closely related to the geometry of the space chosen for navigation and guidance of the carrying vehicle. The traditional independent reference frames, such as geographic, geocentric, and inertial are described in detail in the literature^{5, 6, 7, 8}

2.2.2 Dependent Reference Frame

Each of the dependent reference frames indicated in Figure 2.1 is associated with one IMU which is to be aligned. The multiplicity recognizes that a single vehicle might carry several systems which require alignment. In the event that these systems are different, the dependent reference frames may be non-identical. Conversely, identical dependent frames are expected for identical systems. Chapter III discusses several techniques whereby each dependent frame is aligned individually. Chapter IV considers the simultaneous alignment of several dependent frames.

The dependent frames are reference frames only insofar as they serve as a measurement reference for the IMU during a mission. They are dependent because they must be aligned with respect to some other reference system. In particular, it is desirable to align the dependent system by a series of measurements made with respect to the independent reference frame. This requires information which can be sensed by the instrument associated with the dependent reference frame to have a unique geometrical relationship to the independent reference frame. For example, the earth's gravity vector (\bar{g}) and angular velocity vector ($\bar{\omega}_{ie}$) are well defined in the geographic frame. If their orientation with respect to the dependent frame can be established by measurements performed in the dependent frame and compared to the known orientation in the geographic frame, the alignment of the dependent frame to the independent frame follows directly. This particular procedure is known as gyrocompassing. It depends upon the capability to measure \bar{g} and $\bar{\omega}_{ie}$ accurately in the dependent reference frame.

2.2.3 Intermediate Reference Frame

When measurements suitable for alignment cannot be made directly with respect to the independent reference frame, an indirect series of measurements may be used. For this purpose a "substitute" independent reference frame, i. e. one which "remembers" the independent reference frame, is provided. This is the intermediate reference frame of Figure 2.1. The use of active intermediate reference frames for moving base alignment is perhaps the most significant dividing point between fixed base and moving base alignment procedures. Although intermediate reference frames are often necessary in both fixed and moving base alignment to circumvent physical disturbance of the measurement, the fixed base procedure will usually employ a static type of intermediate reference. In many proposed moving base alignment techniques, there is made available on board the vehicle an IMU which has previously been aligned with respect to an independent reference frame and to which it is desired to align one or more additional platforms. In other words, it is desired to transfer the alignment of the intermediate reference frame to the dependent frame. In this case the alignment capability is measured with respect to the intermediate reference frame while the total alignment accuracy must include the ability of the intermediate system to remember the orientation obtained from the independent reference frame.

A transfer alignment of the type considered above is sometimes called a Master-Slave alignment. This name derives from mechanizations where the orientation of the dependent system (slave) is physically slaved to match the orientation of the intermediate system³, but is now popularly applied to any transfer method⁵. Gulland⁴ has discussed a naval application involving transfer of the SINS coordinate reference to a remote fire-control device aboard the same vessel. Nauman and Oestreich³ and O'Donnell⁵ indicate the interest in a transfer of coordinates from an airborne auto-navigator to a remote fire-control device aboard the same aircraft.

2.2.4 Transfer Reference Frame

When it is not possible to make suitable measurements between dependent and intermediate reference systems, a transfer reference frame (Figure 2.1) may be used. The proposed carrier-borne alignment of the F-111B navigation equipment¹⁰ employs this technique. The transfer reference frame is an active inertial platform which is first aligned to the intermediate system. Then it is physically transported to where its alignment can be measured by and transferred to the dependent reference frame. Although required to remember its orientation for a much shorter time period than the intermediate system, the transfer system and errors introduced by the alignment procedure are similar to those considered for the intermediate system discussed in Section 2.2.3.

2.3 Measurement Considerations

2.3.1 Vectorial Nature of the Measurements

All alignment techniques depend on the ability to accurately measure naturally existing or artificially introduced quantities. The point of greatest significance to the unification of alignment studies is that regardless of the fact that the measurement of these quantities may proceed by inertial, optical, electromagnetic or other means, the various measurements have a common characteristic of singular importance:

Every quantity measured for the purpose of alignment is vectorial in nature.

The vectorial nature to which we refer is the particular concept of a vector as a geometric entity having characteristics of direction and magnitude. Although every measured quantity relevant to alignment may, in fact, be properly described as a vector, the determination of just its direction supplies conditions which are mathematically sufficient to determine alignment. The determination of magnitude is not a mathematically necessary condition but it may be a practical necessity depending upon the nature of the measured quantity and the sensors employed. When magnitude measurements are made, they are for the purpose of determining the

directional parameters of the input quantity. This concept is sufficiently important to warrant amplification by example.

Consider, first, the fixed base gyrocompassing mode of alignment. Here the system attempts to establish its orientation by determining the vectorial direction of each of two physical quantities: gravity (\bar{g}) and the earth's daily rotation ($\bar{\omega}_{ie}$). Each of these quantities is a vector. The instrumented measurements (using accelerometers and gyros respectively) determine the vector directions in one of two ways. Either they make the best possible estimate of magnitude components of the quantity or they seek the null magnitude plane of the quantity. This presents a choice of four possible measurement combinations, but in each case the full vector nature of gravity and earthrate is being utilized.

Optical measurements provide an example of an alignment measurement which is not a complete vector mechanization but whose basis is indeed vectorial. Optical systems (such as auto-collimators) are concerned with the line of sight from the instrument to an object. This line of sight may be properly considered to represent only the directional aspect of the position vector from the instrument to the object, where in order to measure rotation of the object about some axis the position vector must terminate in a point of the body off the rotational axis. Angular measurements can determine the direction of this position vector (and hence the alignment between object and instrument) without recourse to magnitude measurements. In optics, magnitude considerations relate to the energy of the electromagnetic wave. In this sense, the magnitude of the position vector does weigh heavily on the practical application of optical instruments. Other parameters of the wave, however, carry the intelligence related to direction finding.

It may now be seen that examining the alignment problem in terms of a vector measurement problem permits a

clear understanding of the limitations on the process of moving base alignment implied by the measurement capabilities. It is primarily in the choice of the vectors and the corresponding form of the measurement that the techniques discussed in the literature differ.

2.3.2 Two Vector Requirement

The determination of the angular orientation of an inertial measuring unit by vector measurement requires at a minimum two non-collinear* vectors whose orientation is known with respect to the desired system attitude. This may be proved simply by both mathematical and physical arguments.

Consider a misalignment between the dependent and independent frames of Figure 2-2. A relationship between the observations of the vector \bar{V} in each frame is

$$\bar{V}^i = R_d^i \bar{V}^d \quad 2.3-1$$

where the vector superscripts indicate coordinatization in the respective frames and the rotation matrix R_d^i carries the d-frame into the i-frame. Visualize the misalignment as being developed on an incremental basis beginning with the two frames coincident and having \bar{V} remain constant in the i-frame. Then we may write

$$\begin{aligned} \Delta \bar{V}^i &= R_d^i [\Delta \bar{V}^d + R_i^d \Delta R_d^i \bar{V}^d] \\ &= 0 \end{aligned} \quad 2.3-2$$

from which

$$-\Delta \bar{V}^d = R_i^d \Delta R_d^i \bar{V}^d$$

* In the general case, one merely requires a pair of skew vectors. Because a center of measurement is defined in the IMU, the measured vectors must intersect and define a common plane. Hence the requirement for non-collinear vectors.

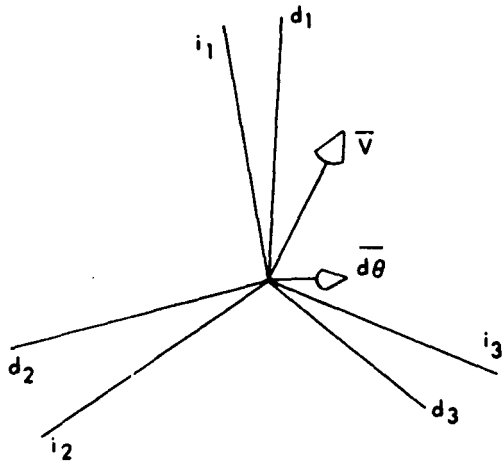


Figure 2-2 Evaluating Misalignment ($\overline{d\theta}$) Between Independent (i) and Dependent (d) Frames by Measurement of a Vector (\vec{V})

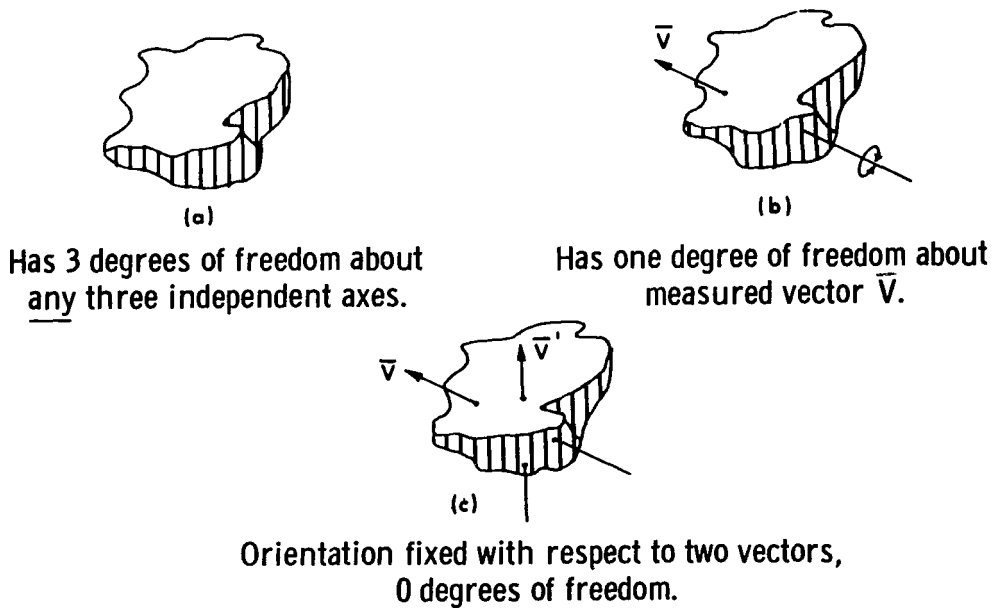


Figure 2-3 A Physical Argument to Establish the Two-Vector Requirement

or

$$\bar{V}^d \Big|_{t=0} - \bar{V}^d = R_i^d \Delta R_d^i \bar{V}^d \quad 2.3-3$$

where we choose $t=0$ as the instant when the d-frame and i-frame are coincident. We ask now whether these observations of the single vector \bar{V} are sufficient to evaluate uniquely the misalignment between the frames.

Under suitable restrictions (which have been discussed by many authors^{11, 12, 13}) the misalignment may be represented by a vector angle $\bar{d}\theta$. The direction of $\bar{d}\theta$ gives the axis about which the misalignment was generated, while the magnitude of $\bar{d}\theta$ specifies the amount of rotation about this axis. Using the vector angle concept, an identification of the right-hand side of Equation 2.3-3 in terms of a vector cross product¹⁴ may be made.

$$R_i^d \Delta R_d^i \Rightarrow \bar{d}\theta \times \quad 2.3-4$$

Substituting 2.3-4 into 2.3-3 gives the desired expression, coordinatized in the d-frame

$$\bar{V}^d \Big|_{t=0} - \bar{V}^d = \bar{d}\theta \times \bar{V} \quad 2.3-5$$

The non-simultaneous measurements of 2.3-5 may be replaced by equivalent simultaneous observations of the same vector from different frames, since

$$\begin{aligned} \bar{V}^d \Big|_{t=0} &= \left[R_i^d \bar{V}^i \right]_{t=0} = I \bar{V}^i \Big|_{t=0} \\ &= \bar{V}^i \end{aligned} \quad 2.3-6$$

The term $\bar{V}^d \Big|_{t=0}$ in Equation 2.3-5 is, therefore, a representation in the d-frame of \bar{V}^i . While the substitution of 2.3-6 into 2.3-5 is rigorously proper, the resulting equation is subject to mis-interpretation and therefore is not written explicitly.

The implication of Equation 2.3-5 is that only the component of $\overline{d\theta}$ perpendicular to \overline{V} can be evaluated by measurements of \overline{V} . Any component of $\overline{d\theta}$ which is parallel to \overline{V} remains indeterminate after a measurement of \overline{V} . The evaluation of this parallel component requires measurement of information which is linearly independent of \overline{V} in three-space, hence has some component orthogonal to \overline{V} . Because the additional information must here be described as a vector, the requirement for linear independence is met by selecting the second vector to be non-collinear with \overline{V} . The component of the second vector which is normal to \overline{V} contains the required intelligence; the component parallel to \overline{V} supplies redundant information which may or may not be used to improve the estimate of the $\overline{d\theta}$ component perpendicular to \overline{V} . Note in this connection that a null-magnitude component of a vector is equally as significant for direction indication as a non-zero projection. However, the greatest sensitivity for evaluation of the parallel component of $\overline{d\theta}$ obviously corresponds to choosing the second vector perpendicular to \overline{V} .

A simple physical argument establishing the two vector requirement proceeds as follows. The stable member of an IMU, considered as a rigid body, has three degrees of rotational freedom (Figure 2-3 a). The determination of the body's orientation with respect to one measured vector is entirely analogous to fixing that vector in the body, much as an axle (Figure 2-3 b). The original three degrees of freedom are thus reduced by two, leaving only the single degree of rotational freedom about the originally measured vector unspecified. The required non-collinear vector (Figure 2-3 c), by supplying a measurement orthogonal to \overline{V} , fixes the orientation of the rigid body.

The visualization of a measured vector as an axis in the body, when specialized to the case of a coordinate set "straddling" a vector input, is of central importance in developments to follow.

It is emphasized that by measuring two non-collinear vectors it is possible only to uniquely specify the orientation of the dependent reference frame with respect to the vectors. The orientation of the vectors must be known with respect to the desired system attitude (as represented in the independent, intermediate or transfer reference frames) in order to complete the measurement portion of the alignment. In most cases it is interesting to make a detailed examination of the accuracy with which a system assumes a new orientation from a measured orientation only when the dynamics of this process affect the measurement problem itself.

An important violation of the non-collinear vector requirement occurs when a gyrocompassing system is operated in the polar regions. The often discussed singular behavior of such systems has a simple physical basis in the near-collinearity of \bar{g} and $\bar{\omega}_{ie}$. Precisely at the poles, where \bar{g} and ω_{ie} become collinear, the vectors no longer provide sufficient information to determine direction uniquely.

Since each measured vector provides two of the three pieces of information required for alignment, a mathematical over-specification of alignment results from the use of two non-collinear vectors. This leads quite naturally to the possibility of measuring more than two vectors in order to take advantage of this redundancy. In fact, measuring a total of three vectors, no two of which are collinear, would provide exactly twice the conditions mathematically sufficient to determine alignment; however, this approach has little practical appeal at present because of the difficulty involved in instrumenting even the two required vector measurements. The specific problem of employing more than two vectors is not pursued in this thesis, but much of the forthcoming analysis is applicable to this concept.

In general, the requirement for two non-collinear vectors cannot be met by two vectors of the same type if the measurements are made simultaneously. The exception to this is represented by the direction vectors involved in optical measurements. This is because two physical vectors with the same units of measure will add

vectorially and appear to a measuring instrument as a single resultant vector . For example, although $\bar{\omega}_{ie}$ and another non-collinear angular velocity vector may exist at the same time, they appear as just a single vector to the gyroscopic sensors. For a simultaneous measurement we must therefore require (with the exception noted above) that the two vectors employed be distinguishable on a dimensional basis in addition to being non-collinear.

Non-simultaneous measurements make it possible not only to use two different vectors of the same type (providing they do not exist simultaneously) but to have a single physical vector satisfy the two vector requirement. This requires, however, that the direction of the vector change as a function of time in both the reference frame to which we are aligning and the dependent frame being aligned. By way of explanation, consider a different viewpoint of fixed base gyrocompassing. If a system's gyros are used to maintain an inertially fixed orientation, observations of the local gravity vector display a uniform change of direction relative to the system. With the aid of a clock, these observations of a single vector provide sufficient information for alignment relative to an inertial independent reference frame. The important point is that the physical vector (\bar{g}) has remained constant; only a carefully calibrated apparent direction change has occurred. It is this apparent change which permits alignment.

Vector matching (Section 3.6) provides an example where non-simultaneous measurements of similar vectors permit alignment. The master and slave systems are both aligned to \bar{g} with the vehicle in a non-maneuvering condition. The systems are then placed in a vertical-hold mode while the vehicle maneuvers in order to generate a significant horizontal acceleration. Although the total specific force vector now lies somewhere between \bar{g} and the horizontal, our "calibration" of \bar{g} at a prior time period allows us to complete the alignment based upon the horizontal acceleration

only. Had we not separated the measurements in time, the components existing at one point in time would be indistinguishable.

It is crucial in these mechanizations that a real or apparent change of vector direction occur in both the dependent and independent frames. If the vector orientation were to remain fixed with respect to either coordinate frame, there would be an unresolved ambiguity in that frame's orientation about the vector. An ambiguity associated with either frame, is, of course, an alignment uncertainty between the two frames. In order for the non-simultaneous vector technique to be considered, the reference frame must be capable of monitoring the vector's direction change very accurately. It should be obvious now that the actual change of vector direction may be accomplished either by rotating the reference frame and dependent frame (called "slewing") with respect to a spatially fixed vector or by spatially fixing the coordinate frames and turning the vector.

The foregoing discussion of the measurement problem has indicated the principal choices available for meeting the minimum vector measurement requirement but has not been concerned with the quantities the input vector represents. If one counts the combination of ways available to meet the two vector requirement while also distinguishing the vector quantities on the basis of dimension (i. e., position, velocity, acceleration . . .), the selection of an appropriate solution of the alignment problem is already seen to be a formidable task. This selection is further complicated by the external measuring equipment and information transfers depicted in Figure 2.1. Separate from the measurements made by sensors integral to the inertial system under consideration, information may also be transferred to the system from a remote sensor or system. This information is considered separately from primary measurements not only because its role is usually auxiliary but also

because the separation between measurement points allows the information link to be corrupted by base motion interference effects. The important point to recognize, and which renders the general analysis of moving base alignment tractable, is that because every input is a vector quantity, the error analysis may be treated by simply relating fixed directional indicating capabilities to a resultant alignment accuracy.

The inaccuracy of the measurement processes, has two major sources: the inherent errors of the measuring instruments and the fact that all measurement paths are subject to interference from base motion. The success (or failure) of present alignment procedures can be said to depend largely on how well base motion is either 1) circumvented, 2) measured, or 3) predicted and filtered, since the instrument quality is usually taken as a fixed item. The approach of this thesis is to show the tradeoff required between the two error sources in order to achieve a desired alignment accuracy.

Based upon a composite figure of merit derived for each measurement system it is possible to relate the expected accuracy of alignment to the expected accuracy of measurement. This includes the necessary conversion of linear measurements and magnitude measurements to their angular equivalents. The derivation of the composite figure of merit will be shown in what follows.

2.4 Error Analysis

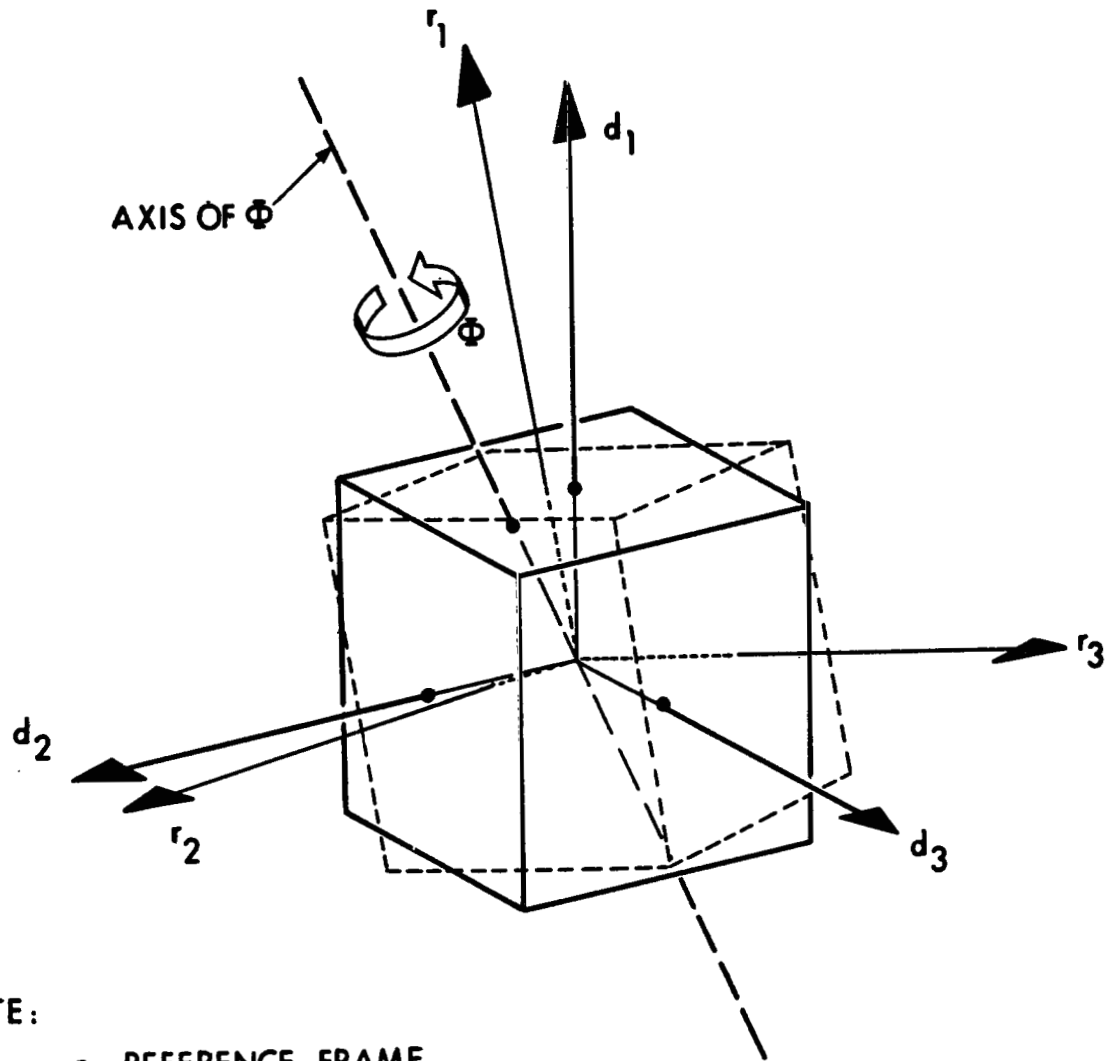
2.4.1 Angular Quantities

In view of our basic definition of alignment, it is natural to speak in terms of error angles as an index of performance. All error sources contributing to the misalignment of a dependent reference frame may be described in terms of misalignments between appropriate pairs of the four basic coordinate frames of Section 2.2. Additional coordinate systems are used as analytical aids when necessary but are not central to the problem.

The magnitude of any quantity properly described as a vector is invariant with respect to the coordinate transformations necessary to characterize it in a particular reference coordinate system. The inputs to alignment measurement processes, as vectors, certainly have this attribute. If the errors resulting from a study of the measurement processes can be shown to have this attribute also, then to a very useful degree the alignment problem may be studied free of the geometry involved in specific hardware mechanizations. Because of the increased emphasis on inter-platform phenomena associated with the moving base alignment problem, the choice of variables influences both the complexity involved in the analysis procedure and the insight afforded by the results. It is desirable that the variables chosen be applicable to all coordinate systems and thereby be independent of any particular mechanization.

While angles cannot be described properly as vector quantities, the simplest description of a misalignment angle nonetheless has invariant properties under coordinate transformations. The simple description referred to reduces any defined difference in the angular orientation of two bodies to a single rotation about a specific axis. That this reduction may be achieved is a consequence of Chasle's Theorem¹² regarding the generalized motion of a rigid body and has been discussed in detail in Ball's¹⁵ treatise on screw motion.

In order to distinguish the single rotation, Φ from its coordinatized representation or the series of distinct rotations employed to arrive at a final orientation, it will be called a "Whole Angle Rotation." Although Φ has the vector characteristics of magnitude and a directional axis, these properties are only necessary to establish the whole angle rotation as a geometric entity in space whose representation is independent of particular coordinate systems. It will be helpful for the reader to visualize the alignment process as one of finding an axis about which one "turns" the dependent reference frame by a finite angle in order



NOTE:

r = REFERENCE FRAME

d = DEPENDENT FRAME

Figure 2-4 Pictorial Representation of the Whole Angle Rotation Required for Alignment

to achieve angular coincidence with the reference coordinate set. This is schematically represented in Figure 2-4. The dependent reference frame, d , and the rectangular parallelepiped to which it is attached are rotated in space from their identical counterparts, the reference frame, r , and its associated parallelepiped. The alignment problem seeks only to achieve angular coincidence between the d and r frames. This may be done in several ways.

In all cases of Euler type rotation, the following information must be recorded: 1) the body which is rotated; 2) the coordinate frame in which the rotations are specified; 3) the order of the three required rotations; and 4) the magnitude of each of the three rotations. On the other hand, if the whole angle representation of alignment is employed the following must be recorded: 1) the body which is rotated; 2) the coordinate frame in which the axis is specified; 3) the axis of rotation; and 4) the magnitude of the rotation, Φ . In terms of simple "bookkeeping", the Euler rotation requires keeping track of eight pieces of information; the whole angle rotation requires only five.

The angle Φ , in addition to being an easily visualized quantity, describes the magnitude of the misalignment by a single number. Until one requires a coordinatized representation of this angle, the location of the rotation axis with respect to a particular reference coordinate set is unimportant. The magnitude Φ is, in fact, an upper bound on the magnitude of the angle ϕ_i between any two corresponding misaligned axes. An original proof of this bound follows. The geometric definition of the ϕ_i is depicted in Figure 2-5. ϕ_1 , ϕ_2 , and ϕ_3 are there seen to be the arguments of the principal direction cosines.

That Φ is an upper bound on the ϕ_i may be proved with the help of Figure 2-6. There the d and r coordinate systems are represented by sets of unit vectors, \bar{r}_i and \bar{d}_i . Beginning with the d and r frames coincident, the d frame has been rotated through the angle Φ about the axis indicated to achieve the

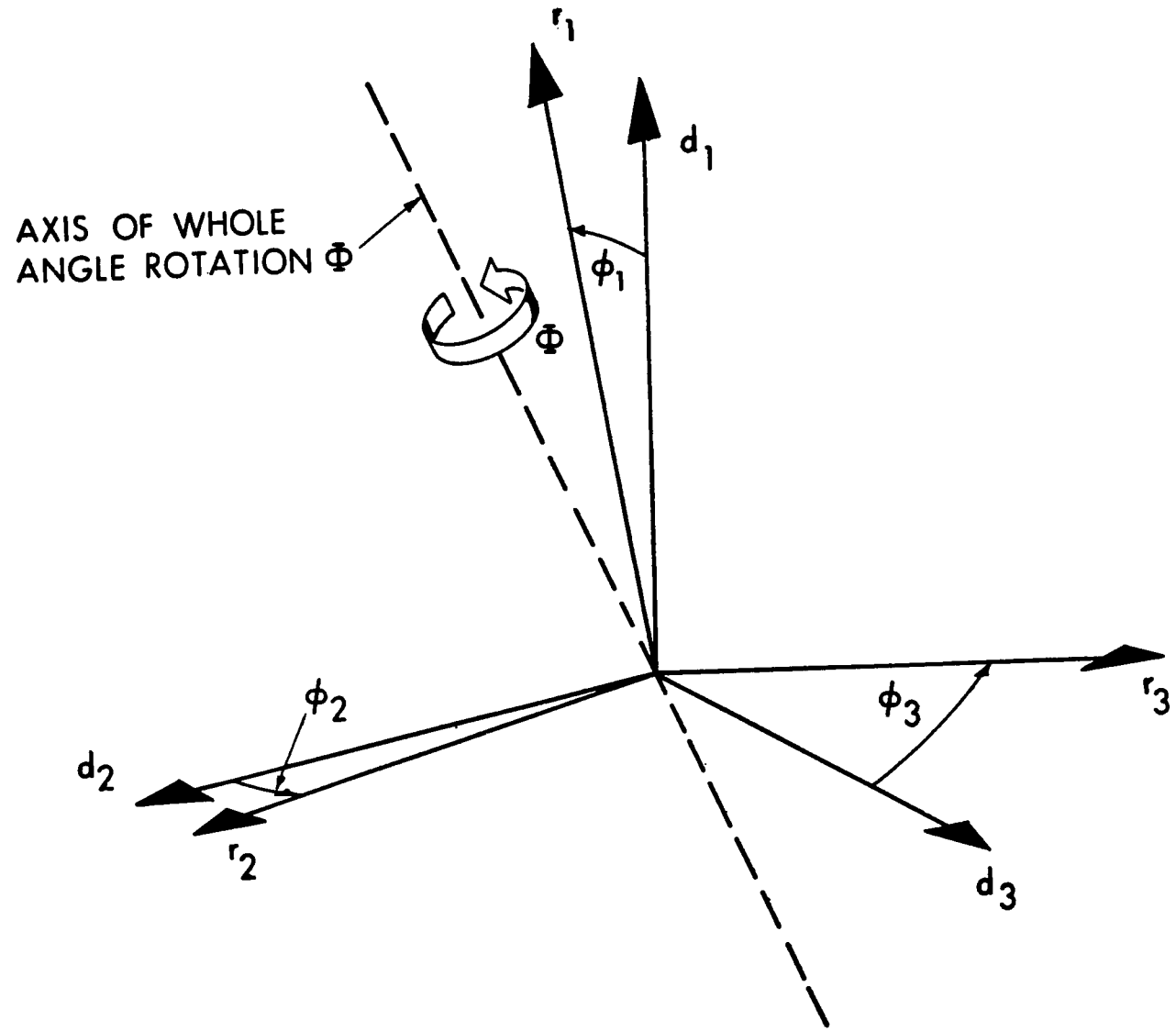


Figure 2-5 Definition of Angles Between Axes (ϕ_i) Equivalent to the Whole Angle Rotation Φ

orientation shown. Following, for example, the \bar{d}_1 and \bar{r}_1 axes, they are separated by the angle ϕ_1 as a result of rotating the entire d-coordinate frame by Φ relative to the r-frame. In general,

$$\phi_1 = \cos^{-1} (\bar{r}_i \cdot \bar{d}_i) \quad i = 1, 2, 3 \quad 2.4-1$$

The rotation of \bar{d}_1 is seen most easily by decomposing \bar{r}_1 (coinciding with the non-rotated \bar{d}_1) into a component perpendicular to the axis of rotation, $(\bar{r}_1)_\perp$, and a component parallel to the axis; $(\bar{r}_1)_\parallel$. When the d-coordinates undergo the rotation Φ , $(\bar{r}_1)_\perp$ rotates through the angle Φ to the position indicated by $(\bar{d}_1)_\perp$ while $(\bar{r}_1)_\parallel$ remains fixed. The displaced \bar{d}_1 axis is then constructed by the vector sum of $(\bar{r}_1)_\parallel$ and $(\bar{d}_1)_\perp$.

The geometry of Figure 2.6 can be used directly to establish that bounding Φ indeed sets an upper bound on ϕ_1 . The angles Φ and ϕ_1 are each apex angles of two isosceles triangles which have the common base b. These triangles are drawn in the same plane in Figure 2.7 for clarity. The triangles have sides $[\bar{r}_1, \bar{d}_1]$ and $[(\bar{r}_1)_\perp, (\bar{d}_1)_\perp]$ respectively. Since $|\bar{r}_1| = |\bar{d}_1| = 1$ and $|(\bar{r}_1)_\perp| = |(\bar{d}_1)_\perp| \leq 1$ we see immediately that

$$\Phi \geq \phi_1 \quad 2.4-2$$

where the equality holds when \bar{r}_1 is perpendicular to the axis of rotation.

To obtain an explicit relationship between Φ and ϕ , apply the law of sines to both triangles (Figure 2.7)

$$\frac{b}{\sin \Phi} = \frac{|(\bar{r}_1)_\perp|}{\sin \alpha} \quad 2.4-3a$$

$$\frac{b}{\sin \phi_1} = \frac{|\bar{r}_1|}{\sin \beta} \quad 2.4-3b$$

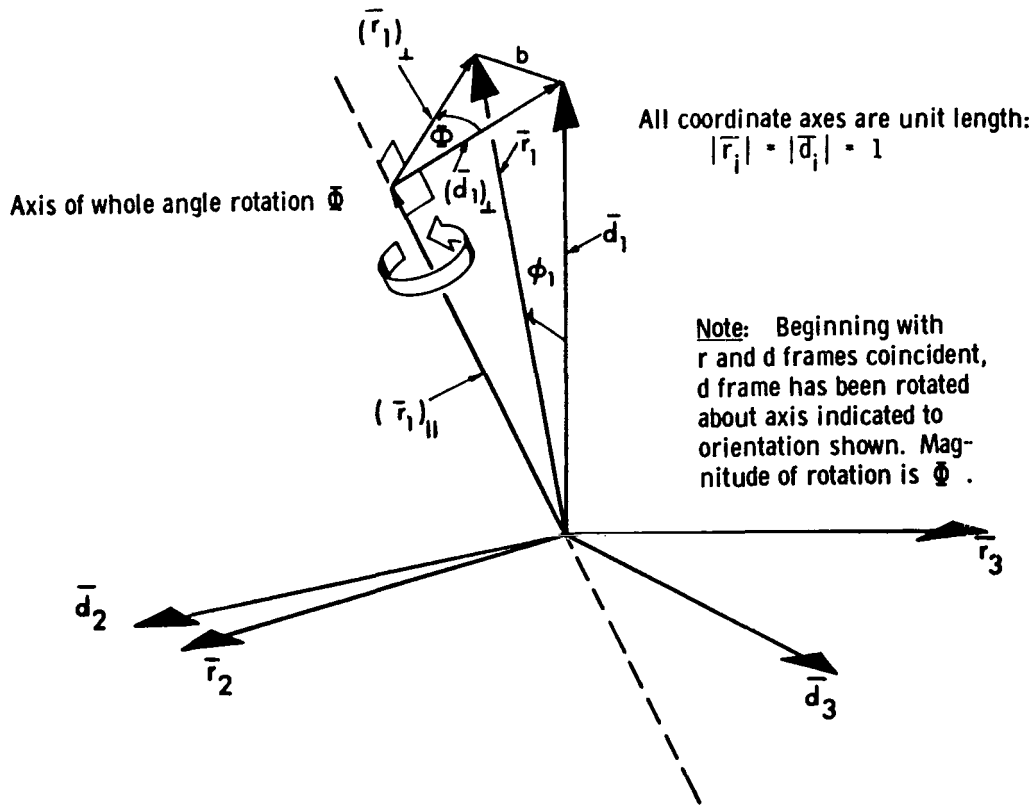


Figure 2-6 Geometry to Prove $\Phi \geq \phi$

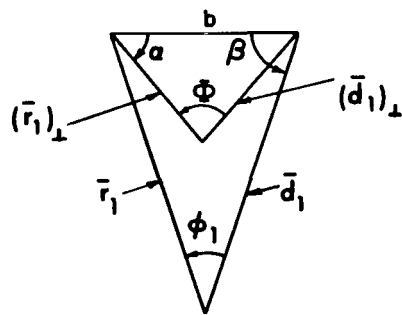


Figure 2-7 Isosceles Triangles of Figure 2-6 Drawn in Same Plane

Recognizing that

$$\sin \alpha = \sin \frac{1}{2} (\pi - \Phi) = \cos \frac{\Phi}{2} \quad 2.4-4a$$

$$\sin \beta = \sin \frac{1}{2} (\pi - \phi_1) = \cos \frac{\phi_1}{2} \quad 2.4-4b$$

yields

$$\sin \frac{\phi_1}{2} = \frac{|(\bar{r}_1)_\perp|}{|\bar{r}_1|} \sin \frac{\Phi}{2} \quad 2.4-5$$

If we define ψ_i as the angle between the axis of the whole angle rotation and the coordinate axis of interest (in this case \bar{d}_1), then

$$\frac{r_{1\perp}}{|\bar{r}_1|} = \sin \psi_1 \quad 2.4-6$$

Since the foregoing development holds independent of the coordinate considered, Equations 2.4-5 and 2.4-6 give the general result

$$\sin \frac{\phi_i}{2} = \sin \psi_i \sin \frac{\Phi}{2} \quad 2.4-7$$

Figure 2.8 shows ϕ_i as a function of Φ for fixed values of ψ_i . For very small ϕ_i and Φ the linear relationship 2.4-8 holds.

$$\phi_i = (\sin \psi_i) \Phi \quad 2.4-8$$

Φ as an exact function of the ϕ_i is obtained by squaring Equation 2.4-7 and summing over i

$$\sum_{i=1}^3 \sin^2 \frac{\phi_i}{2} = \sin^2 \frac{\Phi}{2} \sum_{i=1}^3 \sin^2 \psi_i$$

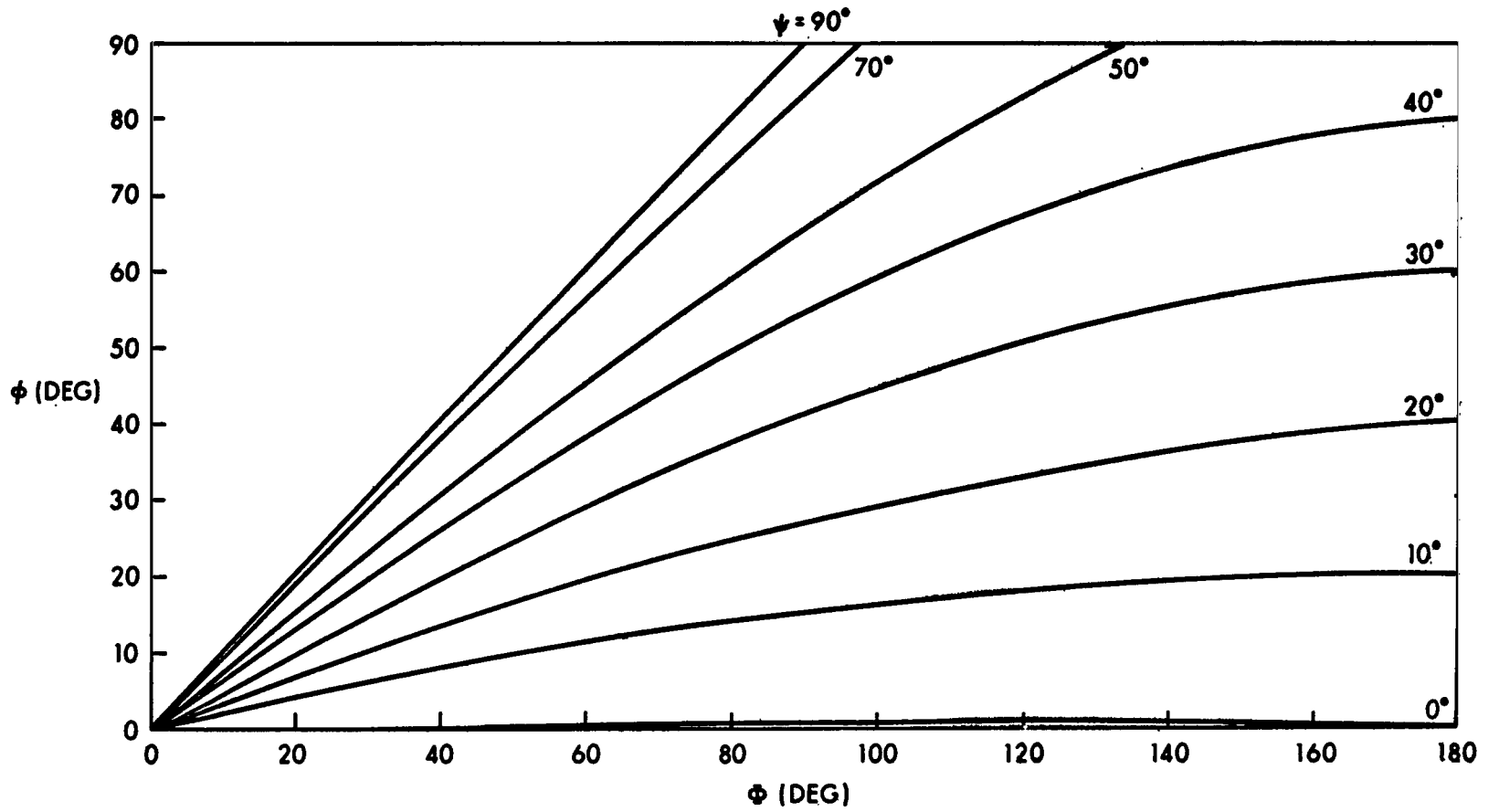


Figure 2-8 ϕ as a Function of Φ

Recognizing that $\sum_{i=1}^3 \sin^2 \psi_i = 2$ [derived from $\sum_{i=1}^3 \cos^2 \psi_i = 1$ and $\sum_{i=1}^3 (\cos^2 \psi_i + \sin^2 \psi_i) = 3$] gives the desired relationship

$$\sin^2 \frac{\Phi}{2} = \frac{1}{2} \sum_{i=1}^3 \sin^2 \frac{\phi_i}{2} \quad 2.4-9$$

When the small angle approximations are valid for Φ and ϕ_i , Equation 2.4-9 or Equation 2.4-8 yields

$$\Phi = \frac{1}{\sqrt{2}} \sqrt{\phi_1^2 + \phi_2^2 + \phi_3^2} \quad 2.4-10$$

The relationship 2.4-10 will be derived again further on in this section, without resort to the geometry of Figure 2.6. From the result 2.4-10 one may straightforwardly deduce Equation 2.4-2 but not the explicit relation 2.4-7. However, the forthcoming derivation demonstrates some important properties afforded by the use of the error angles ϕ_i .

First the relationship of the magnitude of the whole angle rotation to several coordinatized representations commonly used in the analysis of inertial navigation systems will be computed. This is most easily accomplished by using matrix representations for the rotations. A dependent coordinate set, d , and a reference coordinate set, r , may be related by

$$\begin{bmatrix} r_1 \\ r_2 \\ r_3 \end{bmatrix} = \begin{bmatrix} & & \\ & R & \\ & & \end{bmatrix} \begin{bmatrix} d_1 \\ d_2 \\ d_3 \end{bmatrix} \quad 2.4-11$$

where R is a three-by-three orthogonal matrix whose elements are functions of the angular changes required to rotate the d -frame into coincidence with the r -frame. The reduction of R to a form which relates the r and d frames by an equivalent whole

angle rotation proceeds by a similarity transformation^{12,16} using a derived matrix S and its inverse S^{-1}

$$R' = S R S^{-1} \quad 2.4-12$$

This equivalent rotation can be made of the form

$$R' = \begin{bmatrix} \cos \Phi & \sin \Phi & 0 \\ -\sin \Phi & \cos \Phi & 0 \\ 0 & 0 & 1 \end{bmatrix} \quad 2.4-13$$

permitting evaluation of the magnitude of the whole angle rotation, Φ , from knowledge of the trace of R'

$$\text{tr } R' = 1 + 2 \cos \Phi \quad 2.4-14$$

Because the trace of a matrix is invariant under a similarity transformation, $\text{tr } R = \text{tr } R'$ and therefore

$$\text{tr } R = 1 + 2 \cos \Phi \quad 2.4-15$$

By 2.4-15, the magnitude of the whole angle rotation, Φ , is evaluated from the trace of the matrix describing the desired rotation. This expression will be utilized frequently.

Consider now the set of Euler angles corresponding to the rotations of a typical three-gimbal inertial system. A particular set of rotation angles, θ_i , and an order of rotation are defined in Figure 2.9. Note that this set is the same as the traditional yaw, pitch and roll of aircraft axes if d_3 , d_2 and d_1 correspond to the aircraft's vertical, transverse and longitudinal axes respectively. The R matrix of Equation 2.4-11 is, for this order of rotation, the matrix product

$$R = L M N = \begin{bmatrix} 1 & 0 & 0 \\ 0 & C_1 & S_1 \\ 0 & -S_1 & C_1 \end{bmatrix} \begin{bmatrix} C_2 & 0 & S_2 \\ 0 & 1 & 0 \\ -S_2 & 0 & C_2 \end{bmatrix} \begin{bmatrix} C_3 & S_3 & 0 \\ -S_3 & C_3 & 0 \\ 0 & 0 & 1 \end{bmatrix} \quad 2.4-16$$

where the abbreviations employed are $S_i = \sin \theta_i$ and $C_i = \cos \theta_i$.

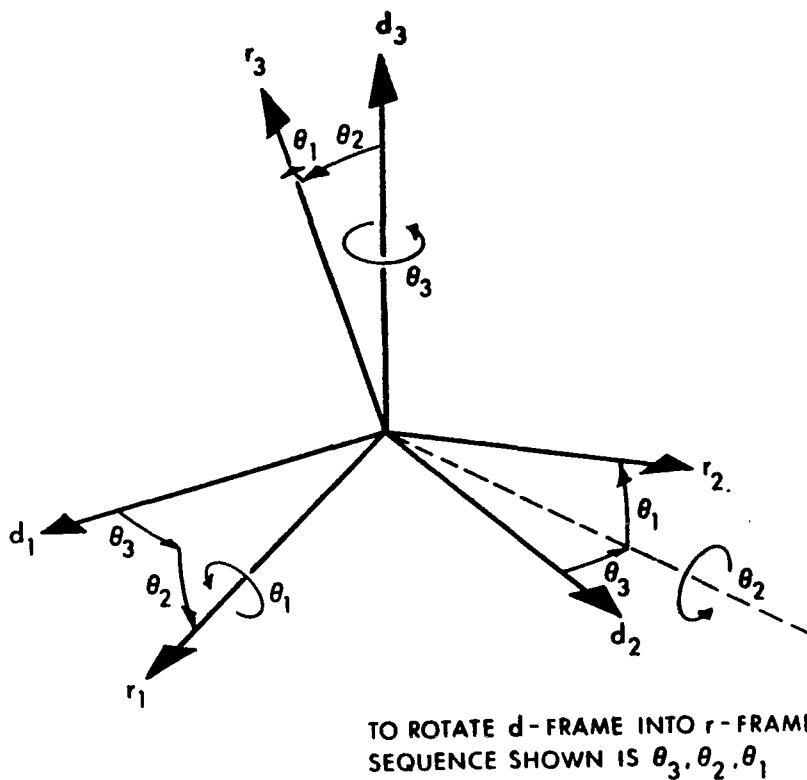


Figure 2-9 An Euler Angle Transformation Corresponding to A Set of Three Gimbals



Figure 2-10 Permutations of the Order of Rotations for Eulerian Transformation of Figure 2-9

For the same values of the angles θ_1 , θ_2 and θ_3 there are five orders of rotation different from that described by Equation 2.5-16 and Figure 2.9. The cyclical permutations of Figure 2.10 portray the entire selection of rotation sequences (Equation 2.4-16 is included in the cycle of Figure 2.10 a). Although the matrix products LMN, MNL and NLM are unequal in general, the traces of these products are equal. The trace of the triple matrix product LMN may be written in terms of matrix elements as

$$\text{tr LMN} = \sum_i \sum_j \sum_k l_{ij} m_{jk} n_{ki} \quad 2.4-17$$

that of MNL as

$$\begin{aligned} \text{tr MNL} &= \sum_i \sum_j \sum_k m_{ij} n_{jk} l_{ki} \\ &= \sum_i \sum_j \sum_k l_{ij} m_{jk} n_{ki} \end{aligned} \quad 2.4-18$$

and so forth, proving that

$$\text{tr LMN} = \text{tr MNL} = \text{tr NLM} \quad 2.4-19$$

It may similarly be shown that

$$\begin{aligned} \text{tr LNM} &= \text{tr NML} = \text{tr MLN} \\ &= \sum_i \sum_j \sum_k l_{ij} n_{jk} m_{ki} \end{aligned} \quad 2.4-20$$

and therefore

$$\text{tr LNM} \neq \text{tr LMN} \quad 2.4-21$$

By Equation 2.4-15, any matrices with equal traces describe equal magnitude rotations, Φ . We have thus shown that the magnitude of the whole angle rotation for any permutation within the same cycle of Figure 2.10 is identically the same. Only the sense of the permutation affects the magnitude of Φ , not the explicit order of rotation. This result is independent of the magnitudes of the θ_i .

The trace corresponding to the rotations of Figure 2.10a is (from Equation 2.4-16)

$$\begin{aligned} \text{tr } R &= \text{tr } L M N = \cos \theta_1 \cos \theta_2 + \cos \theta_2 \cos \theta_3 \\ &+ \cos \theta_3 \cos \theta_1 - \sin \theta_1 \sin \theta_2 \sin \theta_3 \end{aligned} \quad 2.4-22$$

while that corresponding to the rotations of Figure 2.10b is

$$\begin{aligned} \text{tr } R &= \text{tr } L N M = \cos \theta_1 \cos \theta_2 + \cos \theta_2 \cos \theta_3 \\ &+ \cos \theta_3 \cos \theta_1 + \sin \theta_1 \sin \theta_2 \sin \theta_3 \end{aligned} \quad 2.4-23$$

Equations 2.4-22 and 2.4-23 differ only by the sign of the $\sin \theta_1 \sin \theta_2 \sin \theta_3$ term. For the case of all θ_i small enough to neglect terms of order three and higher, the traces become equal and reduce to

$$\text{tr } L M N \approx \text{tr } L N M \approx 3 - \theta_1^2 - \theta_2^2 - \theta_3^2 \quad 2.4-24$$

which with Equation 2.4-15 gives

$$\Phi = \sqrt{\theta_1^2 + \theta_2^2 + \theta_3^2} \quad 2.4-25$$

The small angle result 2.4-25 is completely independent of the order of the Euler rotations about the d_1 , d_2 and d_3 axes. This agrees with the well known result that the angles commute when dealing with "small" rotations. Markey and Hovorka¹⁶ distinguish this situation by considering the "correction angles" C_x , C_y , C_z in their work. From 2.4-25 we immediately write

$$\Phi = \sqrt{C_x^2 + C_y^2 + C_z^2} \quad 2.4-26$$

For errors specified by an azimuth error angle, θ_a , and a vertical error angle θ_v ,

$$\Phi = \sqrt{2 \theta_v^2 + \theta_a^2} \quad 2.4-27$$

While the trace of the rotation matrix has been shown to be relatively independent of the order chosen for a given set of Euler angles, it is quite dependent on the combination of Euler angles selected. Figure 2.11 results from the following sequence of rotations: Beginning with the r and d frames coincident, rotate the d-frame first through θ_3 about d_3 , then through θ_2 about the displaced d_1 axis, and finally through θ_1 about the displaced d_3 axis. The R matrix for this rotation has the form

$$R = N(\theta_1) L(\theta_2) N(\theta_3) \quad 2.4-28$$

where the L and N matrices are those of Equation 2.4-16 with the appropriate substitution of trigonometric arguments indicated in Equation 2.4-28. The trace of this rotation happens to be the exact trace for every permutation of rotational order. It is given by

$$\begin{aligned} \text{tr } R &= \cos \theta_1 \cos \theta_3 + \cos \theta_2 + \cos \theta_1 \cos \theta_2 \cos \theta_3 \\ &\quad - \sin \theta_1 \sin \theta_3 \cos \theta_2 - \sin \theta_1 \sin \theta_3 \end{aligned} \quad 2.4-29$$

which for small angles results in

$$\Phi = \sqrt{\theta_1^2 + \theta_2^2 + \theta_3^2 + 2\theta_1 \theta_3} \quad 2.4-30$$

Relations between Φ and other Euler rotations can be evaluated similarly.

The previous result 2.4-10 can now be derived very easily. The arguments, ϕ_i , of the principal direction cosines were defined by Equation 2.4-1 as

$$\phi_i = \cos^{-1}(\bar{r}_i \cdot \bar{d}_i) \quad i = 1, 2, 3 \quad 2.4-1$$

Because the dot products $\bar{r}_i \cdot \bar{d}_i$ are precisely the diagonal terms of the R matrix relating the d and r frames, the trace of the R matrix is written directly (equation 2.4-31)

$$\text{tr } R = \cos \phi_1 + \cos \phi_2 + \cos \phi_3 \quad 2.4-31$$

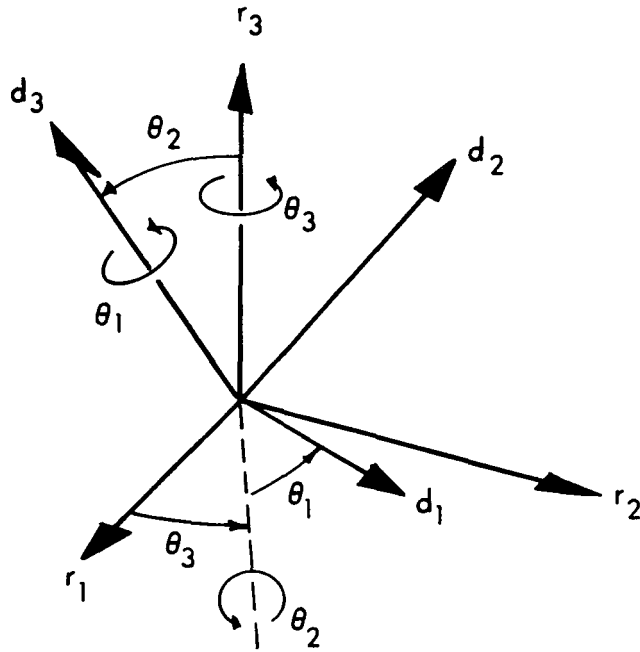


Figure 2-11 Another Sequence of Euler Rotations

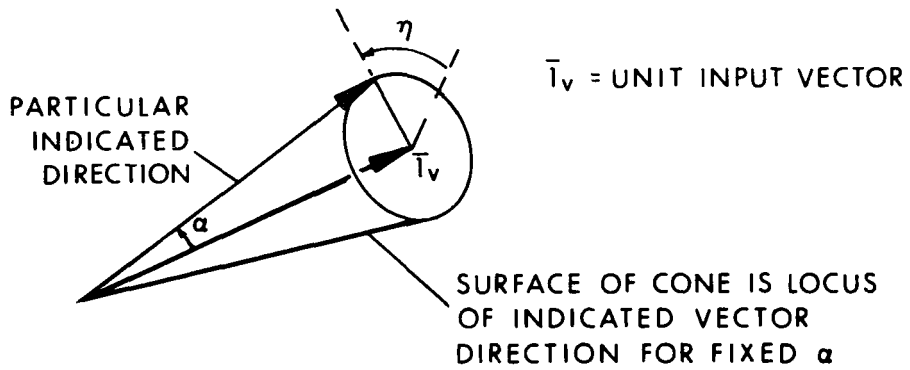


Figure 2-12 Description of Measurement Errors

The expression 2.4-31 is exact and has been obtained without regard for the rotations or order of rotations involved. Any set of ϕ_i describe a unique magnitude misalignment whose whole angle equivalent is given by

$$\cos \Phi = \frac{\cos \phi_1 + \cos \phi_2 + \cos \phi_3 - 1}{2} \quad 2.4-32$$

which reduces to Equation 2.4-10 for the small angle case.

$$\Phi = \frac{1}{\sqrt{2}} \sqrt{\phi_1^2 + \phi_2^2 + \phi_3^2} \quad 2.4-10$$

In addition to the ease with which Equation 2.4-31 is written when dealing with the ϕ_i , this choice of error angles is such that the results 2.4-32 and 2.4-10 hold exactly even when the coordinate systems under consideration are not orthogonal. This result is useful in relating misalignments to measurement capabilities, particularly when a non-orthogonal reference frame is established with two of its axes along the directions of the two non-collinear vectors measured for alignment. Since measurement capabilities are determined as the ability to locate the direction of a vector, the individual misalignment evaluations remain unchanged as the angle between the two vectors changes. In addition, if a d -frame is chosen coincident with instrument axes, the form of the error analysis is relatively insensitive to input axis misalignment when carried out in terms of the ϕ_i .

To prove the independence of Φ from orthogonality of coordinate frames, consider the rotation of a non-orthogonal frame (n) to an orientation (n') such that

$$n' = R^* n \quad 2.4-33$$

where the asterisk distinguishes R^* as a non-orthogonal matrix. This can be reduced to the equivalent rotation of an orthogonal coordinate set (o) defined by

$$\begin{aligned} o &= A n \\ o' &= A n' \end{aligned} \quad 2.4-34$$

The rotation between triads is

$$o' = (A R^* A^{-1}) o \quad 2.4-35$$

(A is guaranteed non-singular provided no two axes of n are collinear.) The similarity transformation and trace arguments of Equations 2.4-12 through 2.4-15, when applied to Equation 2.4-35 yield

$$\text{tr } S(A R^* A^{-1}) S^{-1} = \text{tr } A R^* A^{-1} = \text{tr } R^* = 1 + 2 \cos \Phi \quad 2.4-36$$

The trace of R^* is most easily expressed by choosing the angles between axes, ϕ_i , as the independent variables of R^* . Then

$$\text{tr } R^* = \sum_{i=1}^3 \cos \phi_i \quad 2.4-37$$

where the definition of Equation 2.4-1 must be modified to read

$$\phi_i = \cos^{-1} [\bar{n}_i \cdot \bar{n}'_i] \quad 2.4-38$$

The distinction is simply that the ϕ_i must be the angles between corresponding axes of two identical coordinate systems. If the d and r coordinate sets are defined alike, then Equation 2.4-37 is precisely Equation 2.4-31 and Equation 2.4-38 is the same as Equation 2.4-1.

To quantify this distinction, consider two coordinate sets (n) and (n_1) which are both non-orthogonal as well as non-identical. They are related by

$$n = B n_1 \quad 2.4-39$$

which establishes a coincident reference orientation of the n-frame and an n-equivalent n_1 -frame. Keeping the n-frame fixed, rotate the n_1 -frame to a new orientation n_1'

$$n_1' = R^* n \quad 2.4-40$$

where R^* is now the rotation matrix between non-orthogonal, non-identical frames. Using 2.4-39

$$n_1' = R^* B n_1 \quad 2.4-41$$

so that

$$1 + 2 \cos \Phi = \text{tr} (R^* B) \quad 2.4-42$$

The trace of $R^* B$ is a simple sum of the principal direction cosines only if B is diagonal, corresponding to the n and n_1 frame identical.

The ϕ_i will henceforth denote angles between axes of identical (but not necessarily orthogonal) coordinate frames to permit evaluation of Φ from

$$\cos \Phi = \frac{\cos \phi_1 + \cos \phi_2 + \cos \phi_3 - 1}{2} \quad 2.4-32$$

or

$$\Phi = \frac{1}{\sqrt{2}} \sqrt{\phi_1^2 + \phi_2^2 + \phi_3^2} \quad 2.4-10$$

as applicable.

The foregoing analysis of angular quantities which conveniently describe coordinate frame transformations concludes the first portion of the error analysis for this unified theory of alignment. As depicted in Figure 2-1, every alignment procedure involves the transfer of a reference frame's orientation to a dependent reference frame. The quantity of interest for an error analysis is the misalignment between coordinate frames resulting from this transfer. Because this alignment is mathematically indistinguishable from a general rotation, the whole angle description has been developed in detail as the simplest description for misalignments. The whole angle description is especially convenient for dealing with the series of transfers involved in certain alignment techniques.

2.4.2 System Measurement Capability

The actual transfer of coordinate frame orientation is accomplished by means of measurement processes. Errors made in these measurement processes are the fundamental source of the misalignments discussed in the previous section. In this section we establish the relationship between measurement errors and the resulting alignment errors.

Vectors are the quantities measured in order to transfer alignment. As stated in Section 2.3.1, the primary object of measurements made for alignment purposes is to determine the directions of these vector inputs. Although two non-collinear vectors are required to establish alignment unambiguously (Section 2.3.2), the measurement processes associated with these vectors are sufficiently independent of one another that the measurement of each vector may be considered separately. As a consequence of these facts, the basic measurement problem may be stated as a simple question: "With what accuracy can the measurements made with sensors integral to a particular inertial system indicate the direction of a vector?"

The phrasing of this question is such that the answer must be given in a particularly convenient form, namely as a single angular magnitude. This choice of an angular quantity as the interface between the measurement portion of the problem and the resultant alignment capability is a purposeful choice. While an angle is not necessarily the most natural means for specifying the measurement capability of all types of sensors, it is indeed the most mathematically convenient for alignment discussions. Additionally, it serves to highlight a logical cause and effect pattern. The "effect" is always angular (misalignment) in nature while the "causal" factor may well be a linear measurement error. This latter situation is to be considered in detail shortly. Finally, the angular tolerance within which an instrument or set of instruments can indicate the direction of an input

vector serves as a very natural "figure of merit" by which to compare various systems. The crux of any alignment technique is how well the direction of each of the required vectors can be indicated.

The problem of vector direction indication has an exceedingly simple, yet important, pictorial representation. This is given by Figure 2-12. There, $\bar{1}_V$ is the input vector normalized to unit magnitude. α is the angular uncertainty with which the measurement process indicates the direction of the unit vector, $\bar{1}_V$. In general, the plane defined by $\bar{1}_V$ and a unit vector along the direction of the misindication will have no preferred orientation about $\bar{1}_V$. This is an extension of the fact that even with perfect measurements, angular rotations about a vector cannot be detected by measurements of that vector alone. For the case of a non-zero measurement error, α is thus geometrically interpreted as the half-cone angle of the cone whose generatrix sweeps out the locus of possible incorrect indicated locations of the measured vector. The axis of the cone is along the true vector direction. The apex of the cone is at the center of measurement. The location of a particular incorrect indication is singled out by the azimuth angle, η . η is defined from an arbitrary (but fixed) reference and has any value on the interval $0 - 2\pi$, all of which are equally likely.

α is properly a random variable, not a deterministic parameter. This means that α actually describes a statistically distributed family of coaxial cones, rather than a single cone. In most cases, the distribution of α is functionally related to the distribution of several other random variables. However, it is a single parameter which has a significant geometric meaning and which may be considered as a fixed quantity for purely geometric considerations.

The uniform distribution of η is independent of the distribution of α . Yet it is recognized that the statistics of α may

vary according to the relative vector-sensor orientation. Statistical variations in both the magnitude and direction of α are logical. The magnitude variation of α is accounted for in this work. However, the fact that the misindication may be developed in a preferred direction relative to the sensor orientation is ignored here. Remember that our viewpoint is vector oriented, not system axis oriented. The preferred direction problem may be viewed as a second order refinement to be considered in the context of a detailed system analysis.

Before proceeding to relate α to specific types of measurement errors, its role as a figure of merit requires clarification. Because we consider only the errors introduced by uncertainties in the measurement process, α actually bounds the ultimate accuracy of alignment which may be achieved with a particular set of sensors. It represents the best one might hope to achieve given a basic uncertainty in knowledge of the sensors. Unaccounted for is any slight degradation in accuracy introduced by processing of the basic measurement within the system. However, this bound emphasizes the basic limitations on alignment accuracy implied by varying measurement capabilities.

2.4.2.1 Basic Sensor Errors and Their Equivalent Misalignments

Our discussion of measurements concerns only "black-box" single-degree-of-freedom sensors. This restriction is merely a conceptual aid which does not preclude the use of multi-degree-of-freedom sensors in an actual system. Two- or three-degree-of-freedom sensors are mathematically equivalent to two or three single-degree-of-freedom sensors appropriately mounted on a rigid structure.

There will follow shortly an examination of the ability of various groupings of these single-degree-of-freedom sensors to indicate the direction of a vector input.

First, however, we undertake a more abstract (but instructive) examination of the measurement problem by briefly considering a hypothetical instrument which aligns itself along a vector input (a "vector seeker", if you will). Every realistic sensor is characterized by two distinct quantities: 1) a sensitive axis (fixed relative to the sensor's case); and 2) a certain transducer behavior with respect to this axis. We will so characterize the "vector seeker".

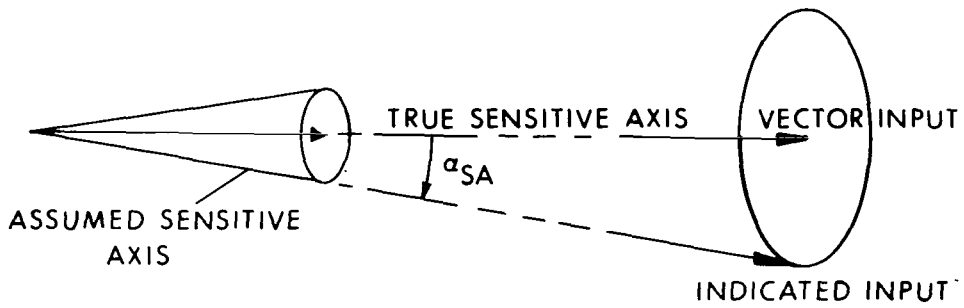
Due to errors in the construction and mounting of an instrument, its sensitive axis is typically not located with perfect precision. We call this imprecision, "sensitive axis uncertainty" and denote it by the angle α_{SA} ; so too for the vector seeker. Imperfect transducer behavior of an instrument also results in an angular indication error, α_T . This we denote transducer uncertainty. Again, this nomenclature is carried over for the vector seeker. For clarification of the meaning of the basic instrument uncertainties, the reader is referred to the more classical example of Appendix A.

The virtue of developing the vector seeker concept is that it reduces various mechanizations of the same basic problem to a common denominator. Our ability to evaluate and compare different sensor systems is thereby greatly enhanced. The development of the total indication uncertainty, α , of Figure 2-12 from α_T and α_{SA} now proceeds for the vector seeker. The "vector seeker" uncertainties equivalent to appropriate arrangements of single-degree-of-freedom sensors are calculated later in this section.

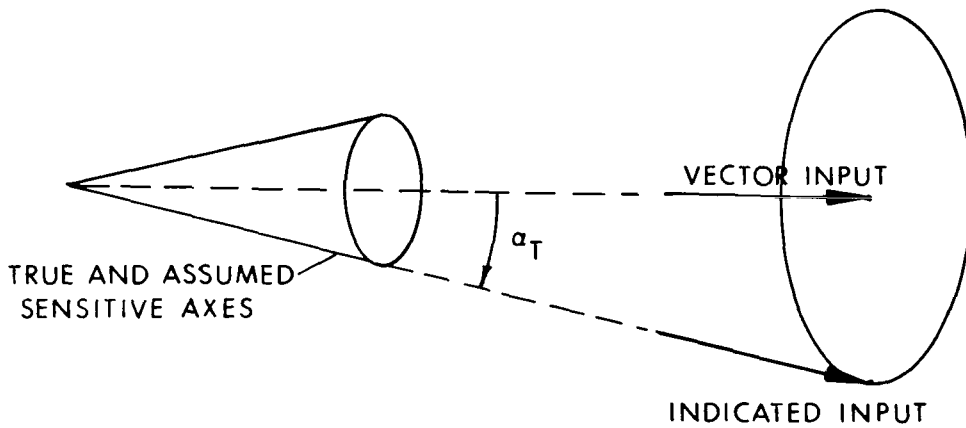
A vector seeker which is a perfect transducer indicates a signal null when its sensitive axis is collinear with a vector input. The geometry of such a situation is depicted in Figure 2-13a. As long as an observer knows the precise location of the sensitive axis, the vector's direction will be found without error. On the other hand, in spite of the fact that the



(a) PERFECT SENSOR

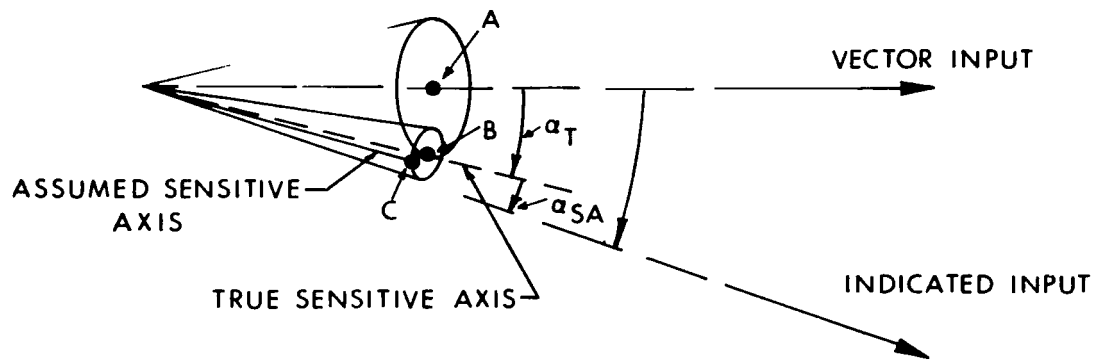


(b) SENSITIVE AXIS UNCERTAINTY
(LOCUS OF CONSTANT PROBABILITY DENSITY)

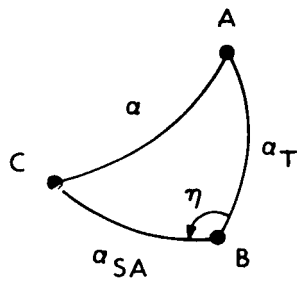


(c) TRANSDUCER UNCERTAINTY
(LOCUS OF CONSTANT PROBABILITY DENSITY)

Figure 2-13 The Geometry of Vector Direction Indication



(d) TRANSDUCER AND SENSITIVE AXIS UNCERTAINTY COMBINED



(e) SPHERICAL TRIANGLE FOR RELATING α , α_T , & α_{SA}

Figure 2-13, continued.

true instrument sensitive axis lies along the vector, any sensitive axis uncertainty (α_{SA} of Figure 2-13b) is directly reflected in an equal magnitude direction indication uncertainty. The constant probability density locus for misindications due to uncertainty in the location of a sensor's sensitive axis is a right circular cone whose axis is the true sensitive axis and whose half-cone angle is α_{SA} . Because the magnitude of α_{SA} is dependent merely on a defined quantity, it has no influence on the physics of the measurement itself. It is a random bias angle which cannot be calibrated out.

Figure 2-13c illustrates the situation where $\alpha_{SA} = 0$ but the transducer behavior of the "vector seeker" is imperfect. These errors affect the dynamics of the measurement process, resulting in the "seeker's" true sensitive axis coming to rest α_T from the vector's direction when a signal null is reached. The constant probability density locus for misindications due to imperfect transducer behavior is a cone whose axis is along the vector input, whose half-cone angle is α_T , and whose generatrix is the true sensitive axis of the sensor.

Combining the effects when both α_{SA} and α_T are non-zero results in Figure 2-13d. The total indication error, α , is the α of Figure 2-12. It is measured between the generatrix of the cone of half-angle α_{SA} and the direction of the vector input. The axis of the cone of half-angle α_{SA} is the generatrix of the cone of half-angle α_T . Note, therefore, that the surface of the cone of half-angle α_{SA} is the locus of misindicated directions only for the illustrated location of the true sensitive axis. The complete locus consists of the surfaces of all cones of half-angle α_{SA} drawn about the infinity of allowable positions of the generatrix of the cone of half-angle α_T .

In spite of the seeming complexity of this locus, the evaluation of α is straightforward. An exact relationship between the contribution of transducer uncertainty, α_T , and

the contribution of sensitive axis uncertainty, α_{SA} , to the total indication error, α , is obtained by analyzing the geometry of Figure 2-13d on a unit sphere. The center of the sphere is coincident with the center of measurement. The vertices of the spherical triangle (Figure 2-13e) of sides α_T , α_{SA} and α are found by the intersection of the following three radial directions with the surface of the sphere: the vector input direction (vertex A); the direction of the true sensitive axis (vertex B); and the direction of the assumed sensitive axis (vertex C). Defining the angle η between α_T and α_{SA} allows writing the law of cosines for spherical triangles

$$\cos \alpha = \cos \alpha_T \cos \alpha_{SA} + \sin \alpha_T \sin \alpha_{SA} \cos \eta \quad 2.4-43$$

For small values of α_T and α_{SA} , Equation 2.4-43 becomes

$$\alpha^2 = \alpha_T^2 + \alpha_{SA}^2 - 2 \alpha_T \alpha_{SA} \cos \eta \quad 2.4-44$$

η may be written in terms of the azimuth angles η_1 and η_2 of the cones of half angle α_T and α_{SA} , respectively

$$\eta = \pi - (\eta_1 - \eta_2) \quad 2.4-45$$

Substituting Equation 2.4-45 into Equation 2.4-44 yields

$$\alpha^2 = \alpha_T^2 + \alpha_{SA}^2 + 2\alpha_T\alpha_{SA} \cos(\eta_1 - \eta_2) \quad 2.4-46$$

η_1 and η_2 are statistically independent. Each is uniformly distributed on the interval $0 - 2\pi$.

Equation 2.4-46 is useful as written only when exact values of η_1 and η_2 are known. This corresponds to knowing the relative orientation of the true and assumed sensitive axes and is in violation of our basic error model. Meaningful quantities which may be readily evaluated from Equation 2.4-46 are the mean ($\bar{\alpha}$) and mean square ($\overline{\alpha^2}$) values of α .

The mathematics for this will be found in Appendix B, with the results

$$\bar{\alpha} = \frac{2}{\pi} (\alpha_T + \alpha_{SA}) \mathcal{E}(k^2) \quad 2.4-47$$

$$\overline{\alpha^2} = \alpha_T^2 + \alpha_{SA}^2 \quad 2.4-48$$

where \mathcal{E} is a complete elliptic integral¹⁸ of argument

$$k^2 = \frac{4\alpha_T\alpha_{SA}}{(\alpha_T + \alpha_{SA})^2}$$

Note that the results of 2.4-47 and 2.4-48 are purely geometric. They were obtained without knowledge of the statistical distributions of α_T and α_{SA} . The mean and mean square values of α as functions of the statistics of α_T and α_{SA} are obtainable from Equations 2.4-47 and 2.4-48 by further evaluation of the expectations indicated there. While $\bar{\alpha}$ cannot be evaluated without knowledge of the distribution of α_T and α_{SA} , $\overline{\alpha^2}$ is immediately given by

$$\overline{\alpha^2} = \overline{\alpha_T^2} + \overline{\alpha_{SA}^2} \quad 2.4-49$$

As stated at the outset of this section, the single-axis "vector-seeker" merely represents a system of from one to three single-degree-of-freedom sensors. In order to utilize this concept, we must derive the α_{SA} and α_T related to meaningful groups of sensors.

We first set α_{SA} to zero in order to investigate the relationship between α_T and various types of transducer inaccuracy. In certain cases, the basic output of the sensor is proportional to an angular quantity, one of whose rays is the measured vector. Optical instruments, such as star trackers and auto-collimators, fall into this category. In other cases, the sensor's output signal is proportional to the magnitude of the vector and this signal must be further processed to establish the vector's direction. Inertial sensors, such as gyroscopes and accelerometers, are in this category. In the former situation, error quantities are normally specified as angular deviations from a

nominal input direction. These specifications would determine α_T directly. In the latter situation, however, error quantities are related to magnitude uncertainties and these, in turn, must be converted to equivalent angular uncertainties. After conversion, the magnitude measurement errors determine α_T .

There are two distinct procedures for using magnitude sensitive instruments to determine a vector's direction. The first is to determine the direction directly from magnitude information. The second is to determine the null plane of the vector and infer the vector's direction from this. In the following, consider at first the measurements made by a single instrument and assume a priori knowledge of the magnitude of the vector or the significance of its null plane.

The cases of estimating the magnitude of a vector and estimating the null plane of the vector must be considered separately. Associated with these measurements are the magnitude estimation error quantities ϵ_m and ϵ_n respectively. ϵ_m is the error in the indicated measurement when the instrument's input axis is along the input vector and the input magnitude has been normalized to unity. ϵ_n is the indicated output when the input axis is in the null plane (the ideal output is zero) normalized against the magnitude of the vector quantity whose null is sought.

Figure 2-14 illustrates the case of attempting to measure the orientation of a normalized vector, $\bar{1}_V$, by measuring its magnitude. If the instrument is high reading (indicated input exceeds actual input by ϵ_m), it will indicate a unit magnitude when, in fact, there is only a projection of $(1 - \epsilon_m)$ along its input axis (Figure 2-13a). This corresponds to the angular error α_t indicated. If, on the other hand, the instrument is low reading, the relationship of Figure 2-13b holds. When the instrument is sensing an actual input magnitude $(1 + \epsilon_m)$ it indicates that it is along the unit magnitude vector $\bar{1}_V$ and the desired direction is removed from the indicated direction by α_b .

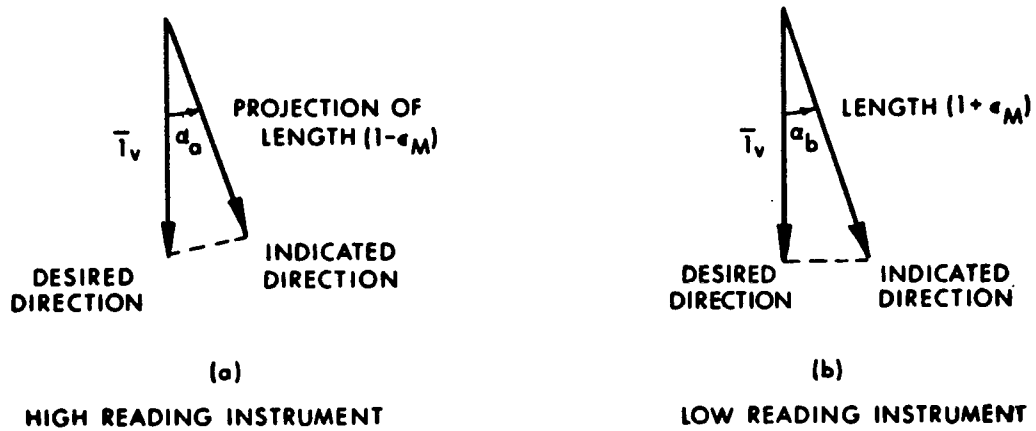


Figure 2-14 Vector Magnitude Measurement Errors

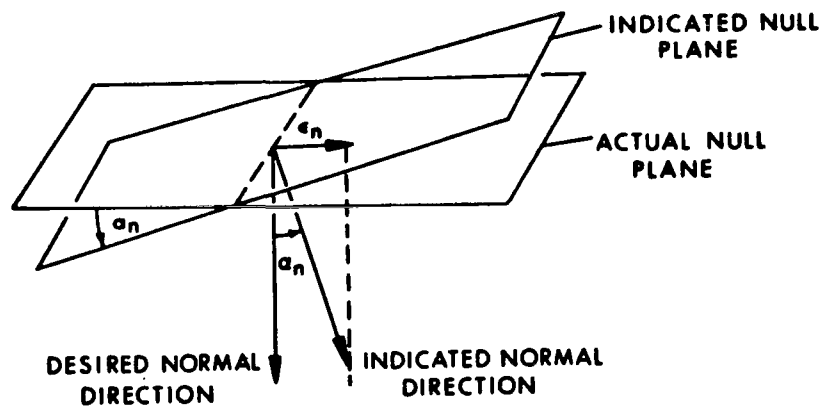


Figure 2-15 Vector Null Plane Measurement Errors

For the high reading case

$$\cos \alpha_a = 1 - \epsilon_m \quad 2.4-50a$$

while for the low reading case

$$\sec \alpha_b = 1 + \epsilon_m \quad 2.4-50b$$

Using the series expansion for the cosine and ignoring terms of order greater than two in α yields, respectively

$$\alpha_a = \sqrt{2 \epsilon_m} \quad 2.4-51a$$

and

$$\alpha_b = \sqrt{\frac{2 \epsilon_m}{1 + \epsilon_m}} \quad 2.4-51b$$

so that when $\epsilon_m \ll 1$ the error in indicating the direction of \bar{l}_V by measuring its magnitude becomes

$$\alpha_m = \alpha_a \approx \alpha_b$$

$$\alpha_m = \sqrt{2 \epsilon_m} \quad 2.4-52$$

The measurement of a vector's null plane is shown in Figure 2-15. The desired normal direction is \bar{l}_V , but due to the existence of ϵ_n normal to the unit vector \bar{l}_V , the indicated normal direction is rotated from the desired normal direction by an angle α_n . The null planes are therefore also α_n apart. Geometrically, $\tan \alpha_n = \epsilon_n$, which for small ϵ_n reduces to

$$\alpha_n = \epsilon_n \quad 2.4-53$$

The angles α_m and α_n are the α_T for each case. They represent the necessary conversion of magnitude errors to angular equivalents.

Equations 2.4-52 and 2.4-53, although derived for a restricted situation, contain an interesting fundamental result. For a fixed measurement capability ($\epsilon_m = \epsilon_n$ but $\epsilon < 2$) greater alignment accuracies can be achieved by mechanizations operating on a nulling principle (Equation 2.4-53) than by those operating on a magnitude measurement principle (Equation 2.4-52). For typical values of ϵ in the range of 10^{-1} to 10^{-6} , the alignment capabilities vary by one-half an order of magnitude to over three orders of magnitude. In many cases, $\epsilon_n < \epsilon_m$, widening the gap even further.

Unfortunately, the results 2.4-52 and 2.4-53 present a picture which is oversimplified on two counts. First of all, a single instrument will rarely suffice for either magnitude measurements or null-seeking measurements. It is more common in inertial systems to provide sufficient mutually orthogonal sensors to span the defined measurement space. Thus for null-seeking measurements, a minimum of two instruments is required to define the null plane. Except for special situations, magnitude measurements require three sensors. We must, therefore, determine the resultant direction indicating capability of appropriate groups of sensors rather than just that of single instruments. This will be calculated shortly.

The second oversimplification is in our error model for the inertial sensors. The quantities ϵ_m and ϵ_n imply that an instrument is defined by a fixed percentage error. This is not so for precision inertial sensors. Rather, the indicated output (V_{ind}) of a device is more commonly expressed as a weighted power series of the input (V) along its sensitive axis plus terms dependent on the sensor's environment (thermal, field, etc.) and terms related to inputs normal to its sensitive axis (See Equation 2.4-54).

$$V_{\text{ind}} = a_0 + a_1 V + a_2 V^2 + \dots$$

+ fcn of environment + cross axis coupling

2.4-54

There is a popular nomenclature associated with the coefficients a_i of Equation 2.4-54 which depends upon the instrument under consideration. Hence a_0 represents gyroscope drift equally as well as accelerometer bias (See Appendix A.) These distinctions are relatively unimportant in this paper as numerical alignment results are expressed in terms of non-dimensional quantities.

For convenience, all derivations will assume a normalized instrument whose ideal transfer from input to output is unity. Thus a perfect instrument is described by Equation 2.4-54 with $a_1 = 1$ and all other coefficients zero. In this work, imperfect sensors will be described by the truncated representation 2.4-55 rather than 2.4-54.

$$V_{\text{ind}} = a_0 + a_1 V \quad 2.4-55$$

The term "bias" will be synonymous with a_0 , "sensitivity" with a_1 . The uncertainty, or error, in a_1 is defined as $\Delta a_1 = (a - 1)$. Because the error coefficients a_0 and Δa_1 of an instrument are generally compensated to some degree in a system application, we take a_0 and Δa_1 to represent the uncompensated uncertainty existing in the sensor at the time of measurement. They are the residual error between the actual value of the coefficient and the best estimate of the coefficient available to the system at the time of alignment.

2.4.2.2 System Magnitude Measurements

Let us now reconsider the directional indication error associated with magnitude measurements of a vector \bar{V} ($|\bar{V}| = V$). Although we are most interested in measurements made with a triad of instruments, it is instructive

to rewrite the single instrument result (Equation 2.4-52) in terms of the description 2.4-55. When indicating the direction of a vector with a single instrument, the indicated vector magnitude (V_{ind}) is constrained to equal the true vector magnitude (V). In order to satisfy this constraint a directional error of

$$\alpha_T = \sqrt{2(a_0/V + \Delta a_1)} \quad 2.4-56$$

must exist. This error is physically realizable only if $(a_0/V) + \Delta a_1 \geq 0$; closed loop operation against an a priori magnitude is impossible to achieve with a low reading instrument. This is simply because the output of a low reading instrument can never be as large as the known magnitude of the measured vector. Only an open loop search for a maximum indicated magnitude is physically realizable on an unrestricted basis (It happens also to be free of transducer error in the steady state). Regardless of the restricted applicability of the expression 2.4-56, it demonstrates that the angular uncertainty resulting from locating a vector with a single instrument is an explicit function of V , a_0 and Δa_1 . Contrast this to the implicit form of Equation 2.4-52. The explicit form shows that ϵ_m (and thus the directional indicating capability) cannot be divorced from the magnitude of the input to the sensor and cannot therefore be generally described as a constant percentage. In fixed base alignment techniques, the viewpoint of the system designer is to take the magnitude of the measured vector (e.g., $|\bar{g}|$ or $|\bar{\omega}_{ie}|$) as a fixed quantity and adjust his alignment capability, α_T , primarily through the choice of instrument parameters. In this context, once his choice of instrument is made ϵ_m may be properly thought of as a fixed percentage error. By contrast, the designer faced with a moving base alignment problem must often consider the magnitude, V , of the vector as another variable over which he exercises considerable choice. In fact, by specifying the carrying vehicle's motion during alignment he chooses the dimensions, direction and magnitude of \bar{V} . His choice is bounded only by the operational restrictions on movements of the carrying vehicle. The

accuracy α_T achieved at any given time depends on just how closely \bar{V} approaches a desired nominal value. Because V may not be considered fixed in moving base alignment, ϵ_m may not properly be considered a fixed percentage.

We proceed now with the more realistic problem of indicating the direction of a vector, \bar{V} , with an orthogonal triad of instruments characterized by

a_{0i} = Bias uncertainty of i^{th} instrument.

a_{1i} = Scale factor of i^{th} instrument.

Δa_{1i} = Scale factor uncertainty of i^{th} instrument.

$$= a_{1i} - 1$$

\bar{V} is described in instrument coordinates by

$$\bar{V} = V (\cos \psi_1 \bar{i} + \cos \psi_2 \bar{j} + \cos \psi_3 \bar{k}) \quad 2.4-57$$

while the vector indicated by the instruments, \bar{V}_{ind} , is described in the same coordinates by

$$\begin{aligned} \bar{V}_{\text{ind}} = & [(a_{01} + a_{11} V \cos \psi_1) \bar{i} \\ & + (a_{02} + a_{12} V \cos \psi_2) \bar{j} \\ & + (a_{03} + a_{13} V \cos \psi_3) \bar{k}] \end{aligned} \quad 2.4-58$$

(See Figure 2-16) Equation 2.4-58 may also be written

$$\bar{V}_{\text{ind}} = \bar{V} + \bar{\epsilon} \quad 2.4-59$$

where

$$\begin{aligned} \bar{\epsilon} = & [(a_{01} + \Delta a_{11} V \cos \psi_1) \bar{i} \\ & + (a_{02} + \Delta a_{12} V \cos \psi_2) \bar{j} \\ & + (a_{03} + \Delta a_{13} V \cos \psi_3) \bar{k}] \end{aligned} \quad 2.4-60$$

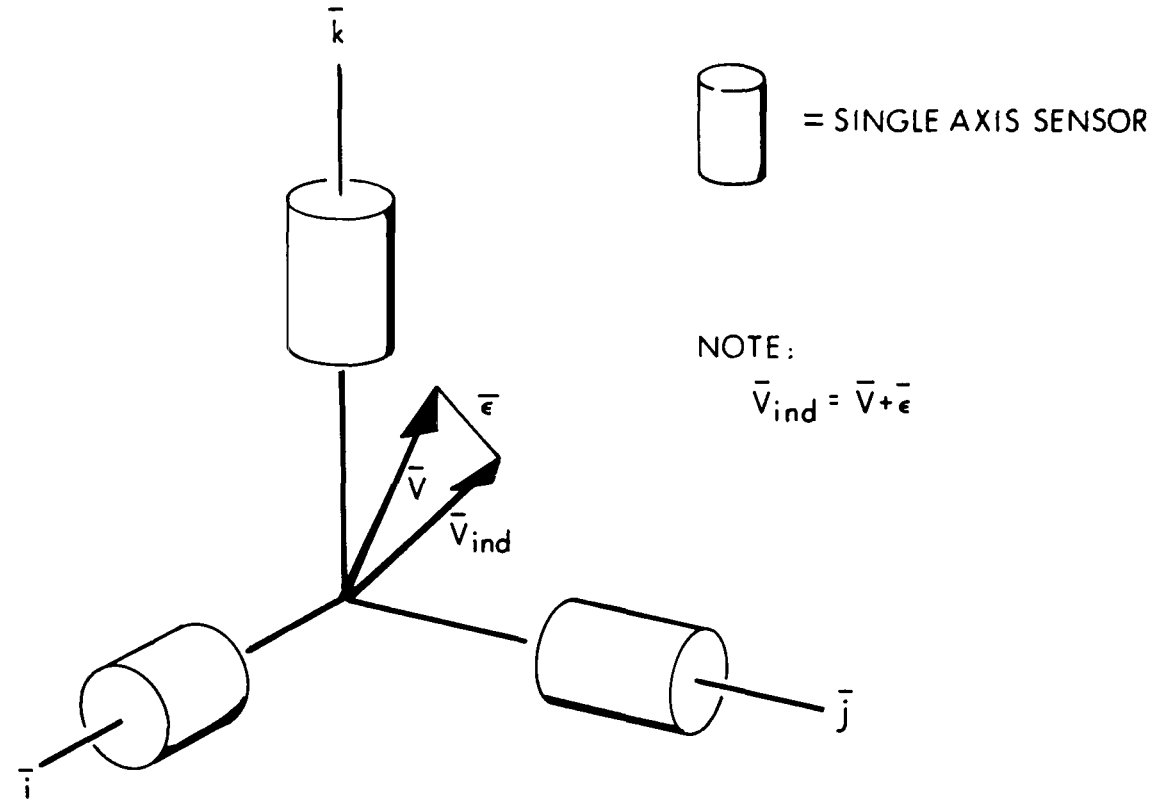


Figure 2-16 Vector Direction Indication With A Triad of Sensors

It is reasonable to expect that on the average any worthwhile system of sensors will indicate \bar{V} perfectly. That is, the mathematical expectation of \bar{V}_{ind} is \bar{V}

$$E(\bar{V}_{ind}) = \bar{V} \quad 2.4-61$$

and consequently

$$E(\bar{\epsilon}) = 0 \quad 2.4-62$$

Equation 2.4-62 may be guaranteed independent of the magnitude or direction of \bar{V} provided

$$E(a_{0i}) = E(\Delta a_{1i}) = 0 \quad 2.4-63$$

The techniques for establishing a zero mean-value for sensor coefficients (via instrument design and calibration) are sufficiently well established¹⁹ that this paper takes the statement of Equation 2.4-63 as a basic assumption rather than as a requirement.

The reader is cautioned that Equation 2.4-61 must be interpreted literally. It is a vector equality stating that the vector \bar{V}_{ind} equals the vector \bar{V} on the average. This does not imply that, for instance, the magnitude of \bar{V}_{ind} equals the magnitude of \bar{V} on the average. Nor does it imply that the average direction of \bar{V}_{ind} is that of \bar{V} . In spite of our intuition that the average measured magnitude and direction are correct it merely states that the average total measurement of \bar{V} is correct. This point is often missed in optimization studies²⁰ which concentrate on trajectory endpoint miss-distance minimization. The distinction will be quantified shortly.

For alignment, of course, the direction indicating capability of the triad is of greatest interest. An error in directional indication is expressed as the angle α_T between \bar{V} and \bar{V}_{ind} . Because the triad is insensitive to rotations about \bar{V} , we ignore the triad-referenced direction in which α_T is developed and concentrate on evaluating the magnitude of α_T .

This is an approximation which merits closer attention only when the platform rotation about \bar{V} is precisely constrained.

The magnitude of α_T may be calculated from

$$\cos \alpha_T = \frac{\bar{V} \cdot \bar{V}_{ind}}{|\bar{V}| |\bar{V}_{ind}|} = \frac{1 + \frac{\bar{V} \cdot \bar{\epsilon}}{V^2}}{\left(1 + 2 \frac{\bar{V} \cdot \bar{\epsilon}}{V^2} + \frac{\bar{\epsilon} \cdot \bar{\epsilon}}{V^2}\right)^{1/2}}$$

2.4-64

which may be expanded to

$$\begin{aligned} \alpha_T^2 &= \left(\frac{\bar{\epsilon} \cdot \bar{\epsilon}}{V^2}\right) - \left(\frac{\bar{V} \cdot \bar{\epsilon}}{V^2}\right)^2 - 2\left(\frac{\bar{V} \cdot \bar{\epsilon}}{V^2}\right)\left(\frac{\bar{\epsilon} \cdot \bar{\epsilon}}{V^2}\right) - \frac{3}{4}\left(\frac{\bar{\epsilon} \cdot \bar{\epsilon}}{V^2}\right)^2 \\ &\quad - 3\left(\frac{\bar{V} \cdot \bar{\epsilon}}{V^2}\right)^3 - 3\left(\frac{\bar{V} \cdot \bar{\epsilon}}{V^2}\right)^2\left(\frac{\bar{\epsilon} \cdot \bar{\epsilon}}{V^2}\right) - \frac{3}{4}\left(\frac{\bar{V} \cdot \bar{\epsilon}}{V^2}\right)\left(\frac{\bar{\epsilon} \cdot \bar{\epsilon}}{V^2}\right)^2 - \dots \end{aligned}$$

2.4-65

Note that although $|\bar{\epsilon}| \ll |\bar{V}|$, terms of $\bar{\epsilon} \cdot \bar{\epsilon}$ may not be ignored in comparison with terms of $\bar{\epsilon} \cdot \bar{V}$ because orthogonality is sufficient to cause $\bar{\epsilon} \cdot \bar{V} = 0$.

For three instruments of equal quality with symmetrically distributed coefficients (e. g., normal, uniform) and assuming (1) that each instrument is independent of every other instrument and (2) that the bias and scale factor uncertainty of any one instrument are also independent, it is a straightforward procedure to compute the mean-square value of α_T as

$$E(\alpha_T^2) = 2 \left(\frac{\sigma_{a_0}}{V} \right)^2 + \sigma_{\Delta a_1}^2 \left(1 - \sum_{i=1}^3 \cos^4 \psi_i \right) \quad 2.4-66$$

where terms of fourth- and higher-order smallness have been dropped from the result 2.4-66. σ_{a_0} and $\sigma_{\Delta a_1}$ are the standard deviations of instrument bias and scale factor respectively.

Equation 2.4-66 provides a good deal of insight to the direction indication problem. First of all, it is possible to minimize the mean-square value of α_T by adjusting the orientation of the triad with respect to \bar{V} . Referring to

Figure 2-17, the function $\left(1 - \sum_{i=1}^3 \cos^4 \psi_i \right)$ is zero when \bar{V} is

parallel (or anti-parallel) to any one of the instruments' sensitive axes. Not only does this physical orientation correspond to null seeking with two instruments but also the mean-square $E(\alpha_T^2) = 2 (\sigma_{a_0}/V)^2$ is identically that derived for the null seeking case (See Equation 2.4-78). This is interesting because the result appears to be independent of whether or not the instrument along \bar{V} is operative or inoperative. Why, in fact, does the factor 2 appear in Equation 2.4-66 when three instruments are active? In answering this, remember that we are only considering direction indication. The probability density for bias is spherically symmetric (for equal instruments), but only components of bias in the plane perpendicular to \bar{V} contribute to α_T . The very important contribution of spherical symmetry is that the tangential component of bias always appears due to two instruments while the radial component appears due to the third. The radial component affects only the magnitude of \bar{V}_{ind} (See Equation 2.4-67).

From these considerations we draw the important conclusion: On the basis of minimum mean-square error, it is optimum to indicate the direction of a vector by

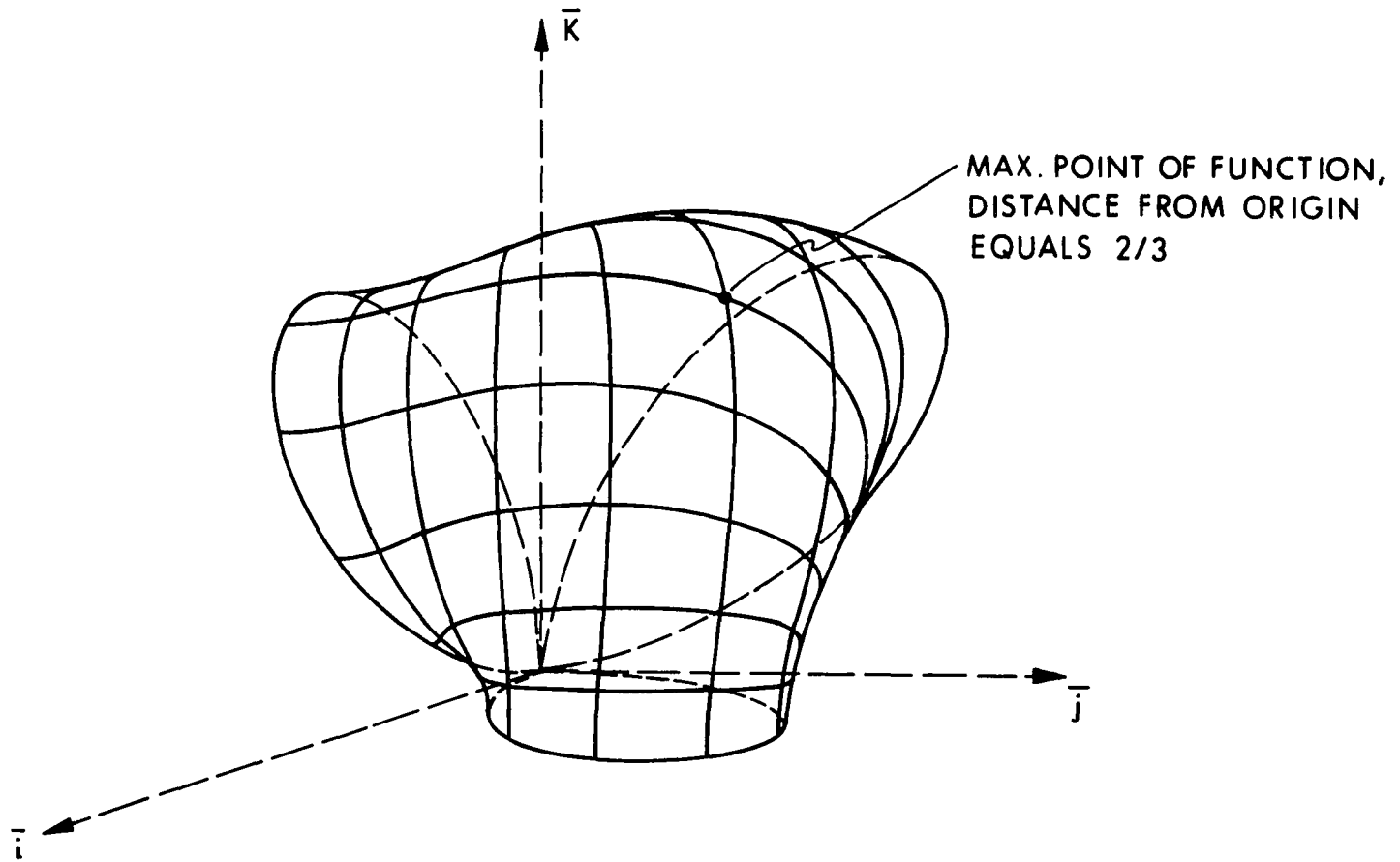


Figure 2-17 The Surface Described by a Radius of Magnitude $(1 - \sum_{i=1}^3 \cos^4 \psi_i)$.

seeking its null plane with two instruments. This result strongly supports the practical reasons usually advanced¹⁷ for placing the accelerometer input axes of a terrestrial navigator in local geographic coordinates.

The maximum value of $E(\alpha_T^2)$ occurs when \bar{V} is symmetrically located with respect to the sensors, i. e., in the center of the triad. It is relatively easy to show the importance of orientation on the error α_T . As an example, evaluating Equation 2.4-66 with constant σ_{a_0} , $\sigma_{\Delta a_1}$, and V demonstrates that merely by adjusting the location of the vector relative to the triad there is at least a 10% reduction of $E(\alpha_T^2)$ available provided

$$\frac{\sigma_{a_0}}{V} \leq \sqrt{3} \sigma_{\Delta a_1} \quad \text{For} \quad \frac{\sigma_{a_0}}{V} \geq \sqrt{3} \sigma_{\Delta a_1} \quad \text{the reduction}$$

available by choice of orientation is less than 10 percent. In situations where the bias uncertainty predominates, therefore, the orientation of \bar{V} with respect to a triad of sensors becomes less significant.

We turn for a moment to examine the accuracy with which the preceding triad measures the magnitude of \bar{V} . The mean-square magnitude measurement error may be calculated as

$$E[(|\bar{V}_{ind}| - |\bar{V}|)^2] = \sigma_{a_0}^2 + V^2 \sigma_{\Delta a_1}^2 \sum_{i=1}^3 \cos^4 \psi_i$$

2.4-67

As with Equation 2.4-66, Equation 2.4-67 ignores terms of fourth- and higher-order smallness. From Figure 2-18 it is evident that the minimum value of Equation 2.4-67 occurs when \bar{V} is in the center of the triad and the maximum occurs when \bar{V} is along any one of the instrument axes. This is clearly opposite to the results for direction indication. See Table 2-1. The

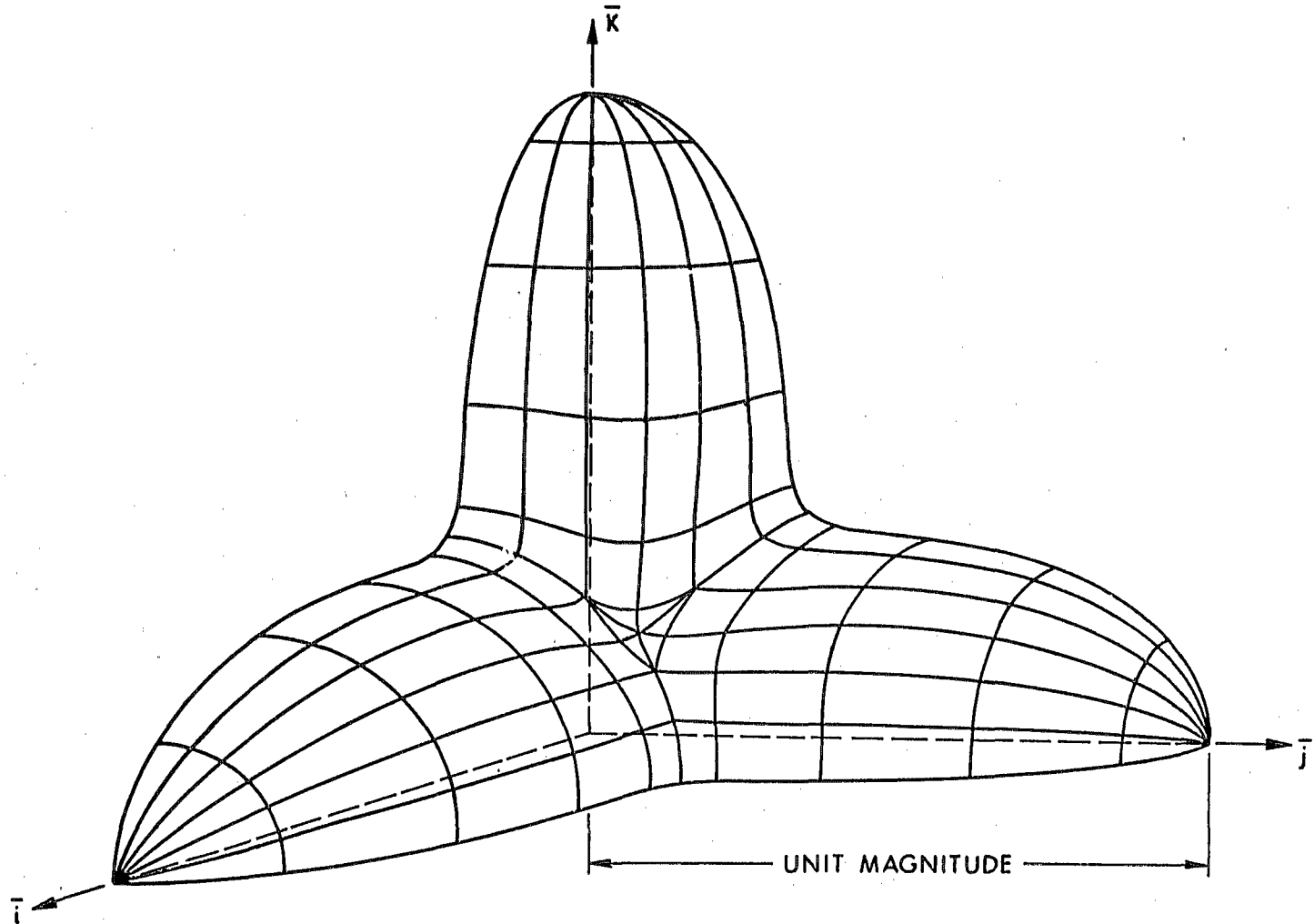


Figure 2-18 The Surface Described by a Radius of Magnitude $\sum_{i=1}^3 \cos^4 \psi_i$

applicable statement here is: On the basis of minimum mean-square error, it is optimum to measure the magnitude of a vector with a triad of instruments by placing the vector at the center of the triad.

<u>Vector Orientation</u>	<u>Magnitude Error</u>	<u>Direction Error</u>
Along any instrument axis	Maximum	Minimum
Center of Triad	Minimum	Maximum

Table 2-1

Demonstrating the Difference Between
Magnitude and Direction Measurement
Errors with a Triad of Instruments

For any situation simultaneously requiring accurate measurements of the direction and magnitude of a vector, the choice of vector orientation with respect to the triad is obviously a compromise. For example, the thrust vector is an attractive vector for alignment purposes but accurate knowledge of magnitude of this vector is simultaneously important for guidance.

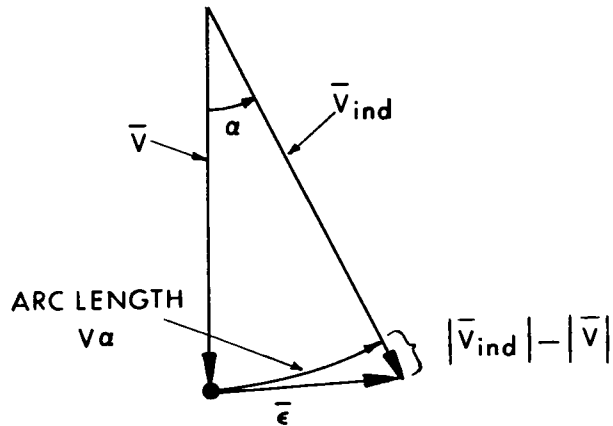
An interesting constraint exists between mean-square magnitude and direction errors. It derives from the fact that the mean-square value of the error vector $\bar{\epsilon}$ is independent of the vector's orientation. See Equation 2.4-68.

$$E(\bar{\epsilon}^2) = 3\sigma_{a_0}^2 + V^2\sigma_{\Delta a_1}^2 \quad 2.4-68$$

Equations 2.4-66 through 2.4-68 may be combined to show

$$E(\bar{\epsilon}^2) = V^2 E(\alpha_T^2) + E[(|\bar{V}_{ind}| - |\bar{V}|)^2]$$

$$2.4-69$$



For small α , $|\bar{\epsilon}|^2 \approx (V\alpha)^2 + (|\bar{V}_{ind}| - |\bar{V}|)^2$

- $\bar{\epsilon}$ = total indication error vector
- α = direction indication error
- $|\bar{V}_{ind}| - |\bar{V}|$ = magnitude indication error

Figure 2-19 Relationship Between Magnitude and Direction Measurement Errors for a Given Triad

Figure 2-19 presents a graphical interpretation of this equation. It is accurate to the extent that the chord length subtended by the arc $V\alpha_T$ numerically equals $V\alpha_T$. The available tradeoff between magnitude and direction errors is thus seen to be simply described (Equation 2.4-69) as a linear constraint. In a situation such as this, the discretion of the designer in choosing an appropriate compromise is extremely important.

It is also interesting here to compare the quality of magnitude estimation attainable with a triad of instruments and that attainable with a single instrument whose input axis is perfectly aligned with the vector. On the basis of mean-square errors, this ratio is written as

$$\frac{\text{Magnitude Estimation Error of Triad}}{\text{Magnitude Estimation Error of Single Instrument}} = \frac{1 + r^2 \sum_{i=1}^3 \cos^4 \psi_i}{1 + r^2} \quad 2.4-70$$

where

$$r = \frac{\sigma_{\Delta a_1}}{\sigma_{a_0}/V}$$

The upper and lower bounds of 2.4-70 are plotted in Figure 2-20 as a function of r . With any one instrument of the triad along the vector, the ratio is unity independent of the value of r . In other words, the triad is then no better than a single instrument. When the vector is in the center of the triad, however, there is an improvement with the triad of up to a factor of three (for predominant scale factor error). In between these extremes of no improvement and a factor of three improvement in magnitude estimation, the parametric variation is dependent upon both the value of r and the relative location of the vector with respect to the triad. As with the direction indication problem, the

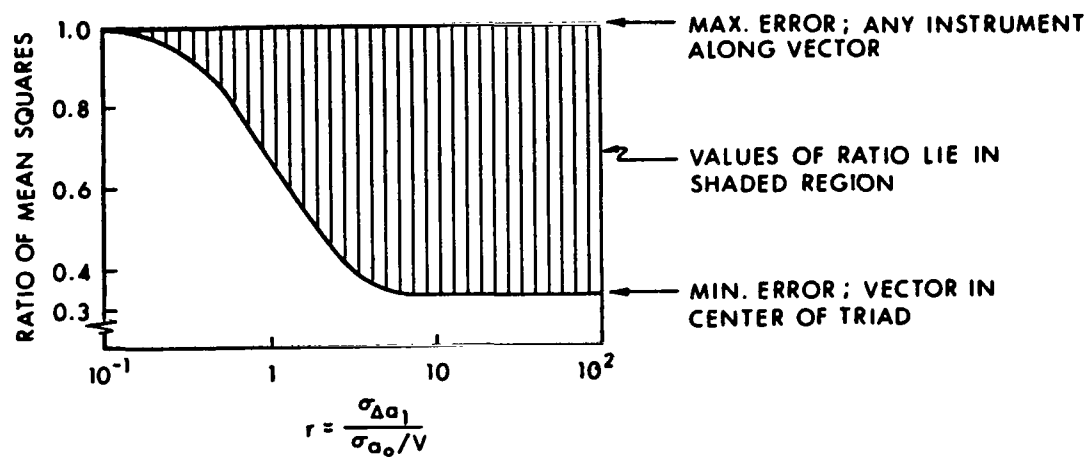


Figure 2-20 Comparing Magnitude Estimation Error of a Triad to That of a Single Instrument

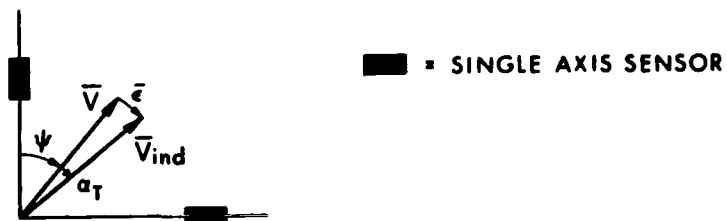


Figure 2-21 Relative to Vector Direction Indication by Means of Two Magnitude Sensitive Instruments

orientation of the triad is least significant when bias uncertainty predominates.

One additional situation is relevant to direction indication via magnitude measurements. This entails indicating the direction of a vector by use of two orthogonal instruments and is germane to azimuth alignment by a vector matching procedure (see Chapter III). Using the geometric definition of Figure 2-21 and assumptions similar to those employed in the derivation of Equation 2.4-66, we obtain the result

$$E(\alpha_T^2) = \left(\frac{\sigma_{a_0}}{V} \right)^2 + \sigma_{\Delta a_1}^2 \left(1 - (\cos^4 \psi + \sin^4 \psi) \right) \quad 2.4-71$$

This is rigorously correct for situations where \bar{V} is out of the plane of the instruments provided V represents the magnitude projection onto the instrument plane. The error 2.4-71 is minimum when either instrument is along the vector ($\psi = 0^\circ, 90^\circ, 180^\circ, 270^\circ$). In these orientations the scale factor uncertainty makes no contribution to the mean-square direction indication error. At $\psi = 45^\circ, 135^\circ, \dots$ the maximum error of $\left[\left(\frac{\sigma_{a_0}}{V} \right)^2 + 1/2 \sigma_{\Delta a_1}^2 \right]$ occurs. There is at least a 10% reduction of $E(\alpha_T^2)$ available by orientation provided $\left(\frac{\sigma_{a_0}}{V} \right) \leq 2.12 \sigma_{\Delta a_1}$.

Results have been derived in this section concerning the errors resulting from indicating the direction of a vector with various groups of magnitude sensitive instruments. The mean-square results are combined with those of the next section concerning null-plane seeking with the same instruments and are presented in Table 2-3.

2.4.2.3 System Null-Seeking Measurements

We turn now to the problem of direction indication by null-seeking measurements. The explicit object of null-seeking mechanizations is to determine the null-plane of a vector. Implicit in this determination is the knowledge that the

normal to the null-plane is parallel (or anti-parallel) to the direction of the vector. If it is necessary to determine the signed direction of the vector, the sign ambiguity inherent in null-seeking must be resolved by other measurements.

The principle of null-seeking measurements is to control the orientation of a sensor's axis in order to achieve an indicated output of zero. For a perfect sensor, the null indication is achieved when the sensitive axis is normal to the vector input. This is independent of the vector's magnitude. A sensor with zero bias error but with a sensitivity error will likewise have zero output when its sensitive axis is in the null plane. Directional indication errors can arise only in the presence of an instrument bias. In order to obtain a net sensor output of zero when bias is present, the sensitive axis must be tipped out of the null plane an amount sufficient to cancel the bias term with a small projection of \bar{V} along the sensitive axis. From Equation 2.4-55 the constraint is

$$a_0 + a_1 V \sin \alpha_t = 0 \quad 2.4-72$$

where α_t is the angle between the sensor's sensitive axis and the normal projection of the sensitive axis on the null plane (i. e., the complement of the angle from the sensitive axis to \bar{V}). for small α_t

$$\alpha_t \approx - \frac{a_0/V}{a_1} \quad 2.4-73$$

By comparison with 2.4-53, the magnitude of the parameter ϵ_n is seen to be $|\epsilon_n| = \frac{(a_0/V)}{a_1}$. The fixed percentage error description

of inertial instruments is thus invalid for nulling mechanizations as well as magnitude measurements.

The complete indication of a vector's null plane requires two instruments, each of whose capability is described by Equation 2.4-73. We calculate now the net transducer inaccuracy, α_T , of Equations 2.4-48 and 2.4-49 for the complete null-seeking mechanization. In Figure 2-22 the instruments are distinguished by the subscripts a or b. $\bar{1}_V$ is a unit vector along the input vector direction. $\bar{1}_a$ and $\bar{1}_b$ are unit vectors along the sensitive axes, separated by the angle θ ($\theta = 90^\circ$ nominally) in the plane of the sensitive axes. The indicated direction of $\bar{1}_V$ is the direction of the cross product $\bar{1}_a \times \bar{1}_b$, shown by the unit vector $\bar{1}_{ab}$. α_a and α_b represent the α_t of Equation 2.4-73 for each of the instruments.

α_T is derived by writing $\bar{1}_V$ as components along $\bar{1}_a$, $\bar{1}_b$ and $\bar{1}_{ab}$

$$\begin{aligned}\bar{1}_V &= \bar{1}_a (\bar{1}_V \cdot \bar{1}_a) + \bar{1}_b (\bar{1}_V \cdot \bar{1}_b) + \bar{1}_{ab} (\bar{1}_V \cdot \bar{1}_{ab}) \\ &= \bar{1}_a \sin \alpha_a + \bar{1}_b \sin \alpha_b + \bar{1}_{ab} \cos \alpha_T\end{aligned}\quad 2.4-74$$

Taking the inner product of $\bar{1}_V$ with itself and solving for $\cos \alpha_T$ gives the result

$$\cos \alpha_T = \sqrt{1 - \sin^2 \alpha_a - \sin^2 \alpha_b - 2 \sin \alpha_a \sin \alpha_b \cos \theta}\quad 2.4-76$$

For small error angles this reduces to

$$\alpha_T = \sqrt{\alpha_a^2 + \alpha_b^2 + 2 \alpha_a \alpha_b \cos \theta}\quad 2.4-77$$

Both 2.4-76 and 2.4-77 emphasize the sign ambiguity inherent in null-seeking mechanizations. In fact, the α_t of Equation 2.4-73 does not have to be carried as a signed quantity. Only its magnitude is important.

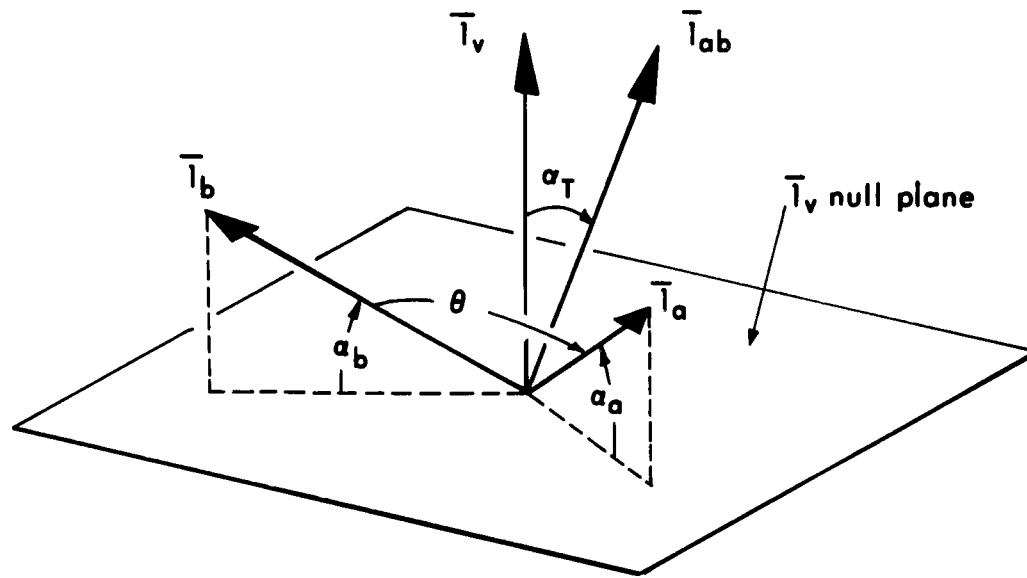


Figure 2-22 Geometry for determination of α_T for Null Seeking Mechanization

By 2.4-77 a null-seeking mechanization with two orthogonal instruments of equal quality is found to have a resultant mean-square transducer error of

$$\overline{\alpha_T^2} \cong 2 (\sigma_{a_0}/V)^2 \quad 2.4-78$$

This expression recognizes that the error contribution of scale factor uncertainty in nulling mechanizations is of secondary importance compared to the bias contribution. α_T^2 represents one of the statistical parameters of a "vector seeker" operating on the nulling principle. There is no spatial dependence of α_T^2 as with the triad of magnitude sensitive instruments, but this does independently check the results obtained for a triad (Equation 2.4-66) when any instrument is along the vector. Since 2.4-78 was calculated on the basis of two instruments and 2.4-66 on the basis of three instruments, it is indeed interesting that the results are identical.

It is instructive to investigate the relative importance of matching instrument quality versus maintaining precise orthogonality. For orthogonal but unequal instruments, Equation 2.4-77 may be written as

$$\alpha_T = \sqrt{n^2 + 1} \alpha_t \quad 2.4-79$$

where n is chosen from either $n = \frac{\alpha_a}{\alpha_b}$ or $n = \frac{\alpha_b}{\alpha_a}$ in order to constrain $n \geq 1$. For equal but non-orthogonal instruments

$$\alpha_T = \sqrt{2 + 2 \cos \theta} \alpha_t = (2 \cos \frac{\theta}{2}) \alpha_t \quad 2.4-80$$

The points where instrument mismatch and non-orthogonality make equal contributions to the misalignment α_T are obtained by equating 2.4-79 and 2.4-80. The percentage mismatch between instruments is given by $100(n-1)$ while the percentage orthogonality error is given by $100(1 - \frac{\theta}{\pi/2})$. The curve of equal

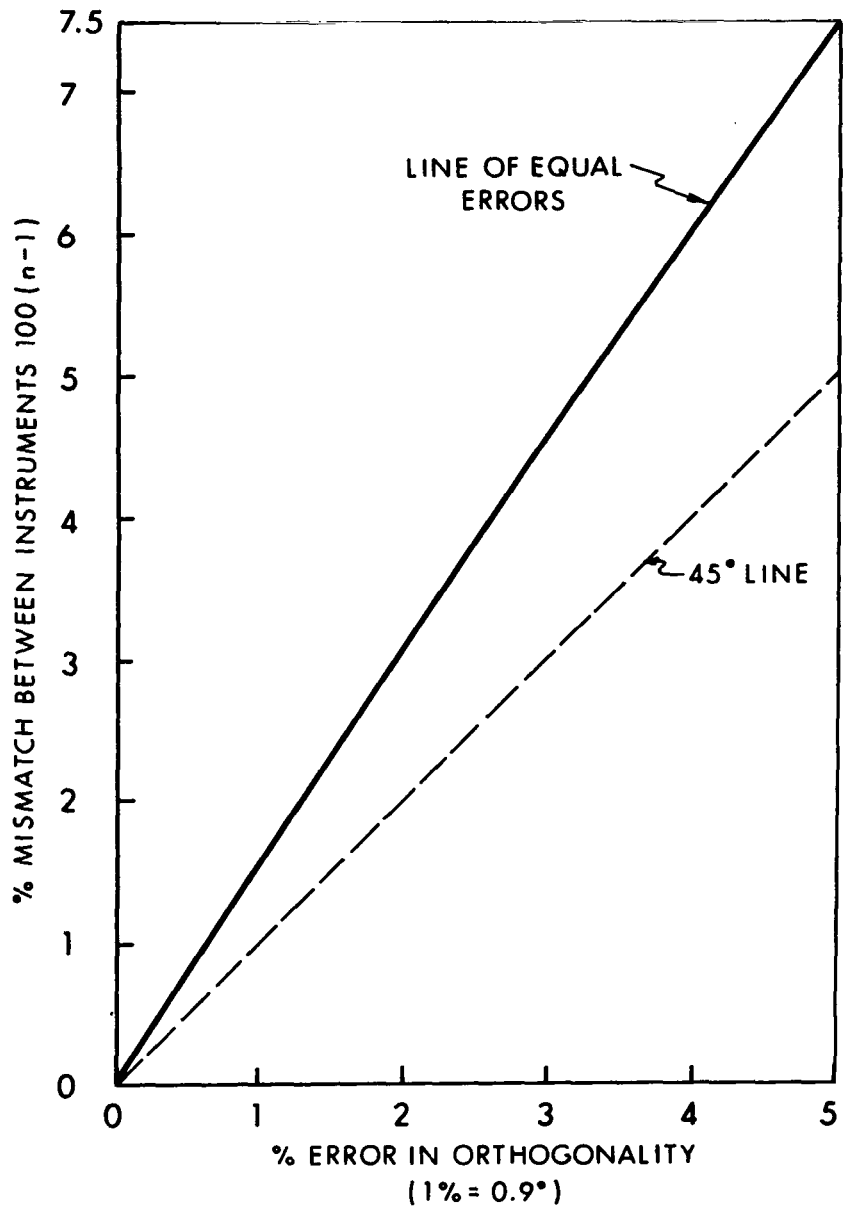


Figure 2-23 Curve Relating Orthogonality and Instrument Mismatch Errors which Cause Equal Misalignments

misalignment contributions is plotted in Figure 2-23. This shows that on a percentage basis the total null-seeking capability is more dependent on maintaining orthogonality than on matching instruments. For example, an error caused by a 3% instrument mismatch is the same as that caused by a 2% orthogonality error.

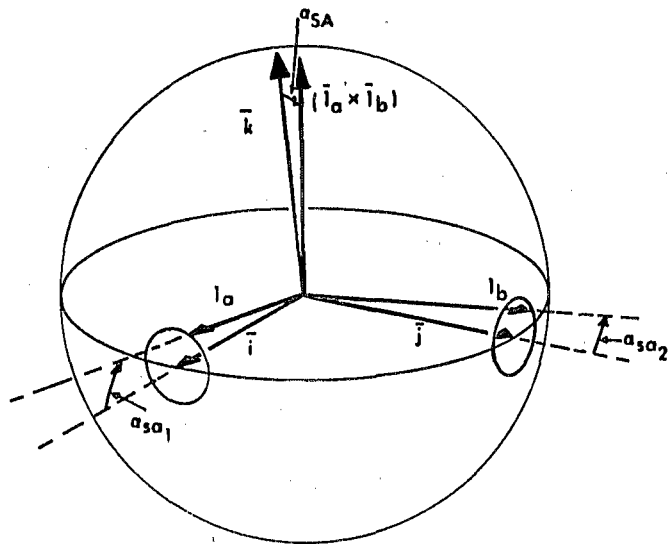
The results of this section concerning the errors resulting from seeking the null-plane of a vector with magnitude-sensitive instruments are tabulated in Section 2.4.2.5, Table 2-4.

2.4.2.4 System Sensitive Axis Uncertainty

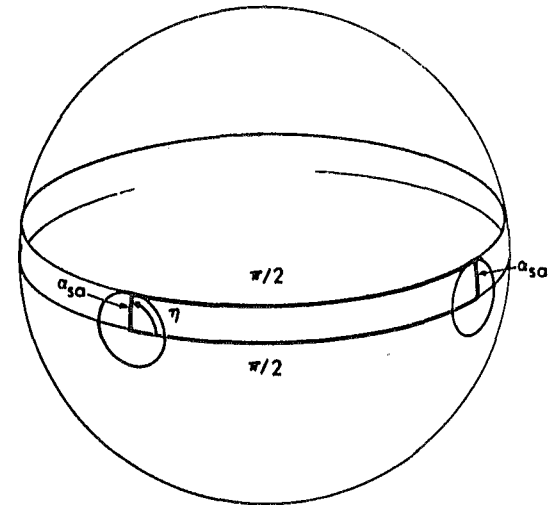
In this section the equivalent sensitive axis uncertainty, α_{SA} , for systems of sensors is calculated. The measurement principles considered correspond to those discussed in the preceding two sections. In keeping with the earlier assumption of equal quality sensors for each system, the instruments are all assumed to have the same sensitive axis uncertainty, α_{sa} . Additionally, the sensitive axes of multiple sensor systems are assumed orthogonal. α_T is temporarily set to zero.

Both magnitude and nulling measurements with single instruments are trivial cases for which the equivalent uncertainty and instrument uncertainty are identical ($\alpha_{SA} = \alpha_{sa}$).

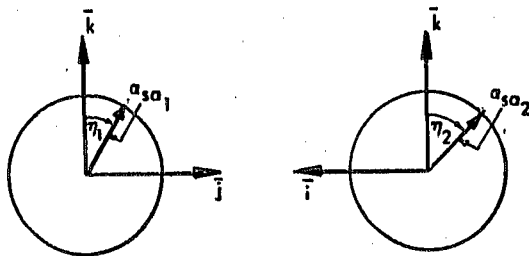
Two sensors employed in a nulling mechanism, however, present a much more difficult situation. With multiple sensor operation, we revert once again to the "vector seeker" concept in order to define the equivalent α_{SA} for the system. The angle between the assumed and actual sensitive axes of a system's equivalent "vector seeker" is the desired angle α_{SA} . For the nulling system, therefore, α_{SA} is the angle between the normal to the plane containing the actual sensitive axes and the normal to the plane defined by the assumed sensitive axes. Figure 2-24 a shows this situation. The unit vectors \bar{i} and \bar{j} lie along the instruments' actual sensitive axes while the unit vectors $\bar{1}_a$ and $\bar{1}_b$ lie along the assumed sensitive axes



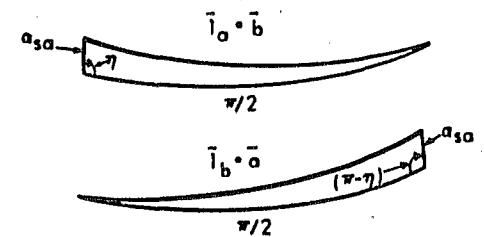
(a) GENERAL GEOMETRY



(c) "FOUR-BAR LINKAGE"



(b) PROJECTED VIEWS FROM (a)



(d) SPHERICAL TRIANGLES FOR DIAGONAL EVALUATION

Figure 2-24 Geometry for Determination of α_{SA} for Null Seeking Mechanization

(coinciding with the "scribed line"). The axes are related by the constraints

$$\bar{l}_a \cdot \bar{i} = \cos \alpha_{sa_1} \quad (2.4-81)$$

$$\bar{l}_b \cdot \bar{j} = \cos \alpha_{sa_2}$$

The actual sensitive axis of the equivalent vector seeker is determined by $\bar{k} = \bar{i} \times \bar{j}$ whereas the assumed sensitive axis is coincident with $\bar{l}_a \times \bar{l}_b$. The deviation between these axes is evaluated from

$$\cos \alpha_{SA} = \frac{(\bar{l}_a \times \bar{l}_b) \cdot \bar{k}}{|\bar{l}_a \times \bar{l}_b|} \quad (2.4-82)$$

From the projected views of Figure 2-24b it is simple to write

$$\begin{aligned} \bar{l}_a &= \quad 1 \quad \quad \quad \bar{i} + \alpha_{sa_1} \sin \eta_1 \quad \quad \bar{j} + \alpha_{sa_1} \cos \eta_1 \bar{k} \\ \bar{l}_b &= -\alpha_{sa_2} \sin \eta_2 \quad \bar{i} + \quad 1 \quad \quad \quad \bar{j} + \alpha_{sa_2} \cos \eta_2 \bar{k} \end{aligned} \quad (2.4-83)$$

The angles η_1 and η_2 are independent random variables, each uniformly distributed on the interval 0 to 2π . This recognizes that sensitive axis uncertainty for a single instrument is specified merely as an angular uncertainty from a nominal scribed line.

If terms of second order smallness are retained when evaluating 2.4-82 by use of 2.4-83, the following results

$$\alpha_{SA}^2 = 2 \left\{ \alpha_{sa_1}^2 \cos^2 \eta_1 + \alpha_{sa_2}^2 \cos^2 \eta_2 - \alpha_{sa_1} \alpha_{sa_2} \sin \eta_1 \sin \eta_2 \right\} \quad (2.84)$$

In terms of mean square values, $\overline{\alpha_{SA}^2} = \overline{\alpha_{sa_1}^2} + \overline{\alpha_{sa_2}^2}$

which leads to the simple result for equal quality instruments in a null seeking arrangement.

$$\overline{\alpha_{SA}^2} = 2\overline{\alpha_{sa}^2} \quad (2.4-85)$$

Before proceeding to derive α_{SA} for other situations, let us examine an important distinction between the problems represented by Figures 2-22 and 2-24a. If α_t is considered on a deterministic basis, the value of α_T is uniquely determined. In contrast, for a fixed value of α_{sa} there is an indeterminacy in the evaluation of α_{SA} . This may be explained graphically as well as by writing the mathematical expressions for α_{SA} .

Consider \bar{i} , \bar{j} and \bar{k} in Figure 2-24a as a fixed reference coordinate set. The \bar{l}_a , \bar{l}_b and $(\bar{l}_a \times \bar{l}_b)$ triad is considered as a rigid member free to pivot about its origin and, therefore, rotate with respect to the fixed triad. This motion is subject only to the constraint that the tips of \bar{l}_a and \bar{l}_b remain in contact with the edges of the unit-height cones of half-angles α_{sa} . If we assume the half-cone angles are identical, each vector \bar{l}_a and \bar{l}_b may traverse a full conical locus while satisfying this constraint. One of the possible motions results in the line $(\bar{l}_b - \bar{l}_a)$ always remaining parallel to $(\bar{j} - \bar{i})$ but varying in separation from zero to α_{sa} . The angle α_{SA} takes on corresponding values between zero and some maximum. The fact that α_{SA} has a range of values for a fixed value of α_{sa} is the indeterminacy mentioned earlier.

For an explicit solution of this deterministic problem, one must solve a three-dimensional geometry which might be described as a four-bar linkage mapped onto a sphere. The four links are arc-lengths subtending the angles

α_{sa} , $\pi/2$, α_{sa} and $\pi/2$ in sequence (See Figure 2-24c). The angle η is the independent variable required to make the problem completely deterministic. The reader is cautioned at this point that an explicit solution is afforded by the introduction of η only because the half cone angles α_{sa} are assumed identical.

The mathematical expression for α_{SA} is

$$\begin{aligned}\cos \alpha_{SA} &= (\bar{\mathbf{i}}_a \times \bar{\mathbf{i}}_b) \cdot (\bar{\mathbf{i}} \times \bar{\mathbf{j}}) \\ &= (\bar{\mathbf{i}}_a \cdot \bar{\mathbf{i}})(\bar{\mathbf{i}}_b \cdot \bar{\mathbf{j}}) - (\bar{\mathbf{i}}_a \cdot \bar{\mathbf{j}})(\bar{\mathbf{i}}_b \cdot \bar{\mathbf{i}})\end{aligned}\quad 2.4-86$$

Using 2.4-81 with

$$\cos \alpha_{SA} = \cos^2 \alpha_{sa} - (\bar{\mathbf{i}}_a \cdot \bar{\mathbf{j}})(\bar{\mathbf{i}}_b \cdot \bar{\mathbf{i}})\quad 2.4-87$$

The unevaluated dot products of 2.4-87 are geometrically interpreted as the diagonals of the four-bar linkage mentioned above. These diagonals separate the four-bar linkage into the two spherical triangles of Figure 2-24d. Application of the law of cosines yields the results

$$\bar{\mathbf{i}}_a \cdot \bar{\mathbf{j}} = \sin \alpha_{sa} \cos \eta\quad 2.4-88$$

$$\bar{\mathbf{i}}_b \cdot \bar{\mathbf{i}} = -\sin \alpha_{sa} \cos \eta$$

Substituting 2.4-88 into 2.4-87 and reducing for the case of small α_{sa}

$$\alpha_{SA} \approx \sqrt{2} \alpha_{sa} \sin \eta\quad 2.4-89$$

which has a maximum value of $\alpha_{SA} = \sqrt{2} \alpha_{sa}$.

There is another locus which satisfies the constraints 2.4-81. In this case the lines $(\bar{\mathbf{i}}_b - \bar{\mathbf{i}}_a)$ and $(\bar{\mathbf{j}} - \bar{\mathbf{i}})$ do not remain parallel but intersect. It happens that this results in the same maximum value for α_{SA} . Therefore, for a nulling measurement with two sensors of deterministically equal

uncertainty, the equivalent sensitive axis uncertainty is given by

$$0 \leq \alpha_{SA} \leq \sqrt{2} \alpha_{sa} \quad 2.4-90$$

The foregoing discussion relates to an admittedly restricted situation. Yet it is important to recognize the indeterminacies which may result from considering single-axis conical error loci. The concept of evaluating parameters of an equivalent "vector seeker" suppresses these indeterminacies effectively.

For a two-instrument magnitude measurement, an orthogonality constraint is required to describe the sensitive axis uncertainty as an equivalent rotation. In this case, the equivalent sensitive axis uncertainty is precisely the uncertainty in the best estimate of the individual sensors' axis locations. For identical instruments $\alpha_{SA} = \alpha_{sa}$.

The equivalent "vector seeker" for a three-instrument magnitude measurement has its sensitive axis in the geometrical center of the triad. As in the earlier null-seeking situation, a triple constraint of the form 2.4-81 does not yield a unique value of α_{SA} even in a deterministic situation. Yet we know from Equation 2.4-10 that these three constraints do fix a unique value for the magnitude of the whole angle rotation between the two triads. The discrepancy involves the location of the axis about which the whole angle rotation develops. If the rotation happens to occur about the sensitive axis of the "vector seeker," then $\alpha_{SA} = 0$. However, if it develops about any axis normal to the sensitive axis, α_{SA} takes on its maximum value. On a mean square basis, the equivalent sensitive axis uncertainty for a magnitude measurement with three sensors is given by

$$\overline{\alpha_{SA}^2} = \frac{3}{2} \overline{\alpha_{sa}^2} \quad 2.4-91$$

The reader is reminded that the result 2.4-91 is valid whether or not the sensitive axes are mutually orthogonal. We have, assumed, however, that they are.

2.4.2.5 Summary of System Measurement Capability

At the beginning of Section 2.4, the following question was posed: "With what accuracy can the measurements made with sensors integral to a particular inertial system indicate the direction of a vector?" We review now the key results obtained in response to this question.

The evaluation of the measurement capability of a system depends upon computation of the statistics of the parameter α . Figure 2-12 shows the simple geometric interpretation of α as the angle between the indicated and actual vector directions. This single parameter serves for quantitative comparison of various systems regardless of the instruments or measurement technique under consideration. It has been shown (Equations 2.4-48 and 2.4-49) how α is related to uncertainties of the instruments employed by a system and, further, that the values of α are a useful means for comparing the self-contained measurement portion of various alignment schemes.*

The instrument uncertainties which affect alignment measurements fall into two classes, namely those related to knowledge of sensitive axis locations (α_{SA}) and those related to knowledge of transducer behavior (α_T). In addition to depending on the magnitude of individual instrument uncertainties, uncertainties for systems of sensors depend upon both the instrument configuration and the technique of measurement. The determination of α from α_{SA} and α_T , however, is independent of the instrument configuration and measurement technique.

The mean-square error contribution of sensitive axis uncertainty, α_{SA}^2 , is presented in Table 2-2. Entries in this table were analyzed in Section 2.4.2.4. Because our definition of α_{sa} does not admit negative values, α_{sa} will have an asymmetric probability density function with mean value other than zero. This is why α_{SA}^2 is written in terms of mean-

* The reader is reminded that α , therefore, relates to the maximum achievable accuracy, not the minimum.

square values rather than variances.

The mean-square error contribution of transducer uncertainty, $\overline{\alpha_T^2}$, is presented in Table 2-3. The transducer-limited ability of an inherently angle sensitive device to measure the direction angle of a vector is obtained directly from its specifications. α_t denotes this uncertainty. It is measured in a plane containing the vector and the instrument's sensitive axis. The complete specification of a vector's direction only requires the measurement of two direction angles. The corresponding measurement planes intersect in the vector and it is assumed they are orthogonal. The angular uncertainty, α_T , within which two such sensors indicate the vector's direction is given by $\sqrt{\alpha_{t_1}^2 + \alpha_{t_2}^2}$. (In Table 2-3 $\overline{\alpha_{t_1}^2} = \overline{\alpha_{t_2}^2} = \overline{\alpha_t^2}$.) The entries in Table 2-3 pertinent to sensors whose output is proportional to the magnitude of the vector measured, summarize the efforts of Section 2.4.2.2 and 2.4.2.3 in converting magnitude uncertainties into equivalent angular uncertainties.

Tables 2-2 and 2-3 are meant primarily to help evaluate the mean-square direction-indicating error of a system. Knowing the measurement technique to be employed, the value of $\overline{\alpha_{SA}^2}$ obtained with the help of Table 2-2 and the value of $\overline{\alpha_T^2}$ obtained with the help of Table 2-3 are combined by the simple sum of Equation 2.4-48 to yield $\overline{\alpha^2}$. This sort of procedure is the essence of the "vector seeker" concept. All measurement techniques and sensor descriptions are reduced to an ability to seek the direction of a vector. An evaluation of other statistics of the vector seeker, as for example the mean value of α (See Equation 2.4-48), requires further reduction of the equations for α derived in the text.

As a somewhat trivial example of the use of the tables, we calculate the maximum accuracy to be expected in finding the direction of \bar{g} with particular accelerometers. From a standard catalog, we chose at random an accelerometer with specifications (as interpreted by this author)

$$\begin{aligned}\alpha_{sa} &= 0.1 \text{ mr} \\ \sigma_{a_0} &= 5 \times 10^{-5} \text{ g} \\ \sigma_{\Delta a_1} &= 1 \times 10^{-4} \text{ g/g}\end{aligned}$$

By simple algebraic manipulation we find

$$\begin{aligned}\alpha_{\text{rms}} &= 0.158 \text{ mr for null-seeking} \\ \alpha_{\text{rms}} &= \left\{ \begin{array}{l} 0.163 \text{ mr max} \\ 0.141 \text{ mr min} \end{array} \right\} \text{ for a triad}\end{aligned}$$

In addition to providing a calculational aid, Tables 2-2 and 2-3 yield certain fundamental comparisons between various measurement methods. The results of Table 2-3 have been largely discussed in Section 2.4.2.2. One remaining comparison is that for measurements made with angle-sensitive instruments to be equivalent to those made with magnitude-sensitive instruments, then either

$$\overline{\alpha_t^2} = \left(\sigma_{a_0/V} \right)^2 \quad 2.4-91a$$

or

$$\overline{\alpha_t^2} = \left(\sigma_{a_0/V} \right)^2 + \frac{1}{2} \sigma_{\Delta a_1}^2 \left(1 - \sum_{i=1}^3 \cos^4 \psi_i \right) \quad 2.4-91b$$

NUMBER OF SENSORS	MAGNITUDE SENSITIVE INSTRUMENTS		ANGLE SENSITIVE INSTRUMENT
	NULL SEEKING	MAGNITUDE MEASUREMENT	
1	$\overline{\alpha_{sa}^2}$	$\overline{\alpha_{sa}^2}$	$\overline{\alpha_{sa}^2}$
2	$2 \overline{\alpha_{sa}^2}$	$\overline{\alpha_{sa}^2}$	$2 \overline{\alpha_{sa}^2}$
3	—————	$\frac{3}{2} \overline{\alpha_{sa}^2}$	—————

Mean-Square Error Contribution, $\overline{\alpha_{SA}^2}$, of Sensitive Axis Uncertainty for Various Combinations of Measurement Methods and Equal Quality Sensors.

Table 2-2

NUMBER OF SENSORS	MAGNITUDE SENSITIVE INSTRUMENTS		ANGLE SENSITIVE INSTRUMENTS
	NULL SEEKING	MAGNITUDE MEASUREMENT	
1	$(\sigma_{a_0}/V)^2$	Indeterminate	$\overline{\alpha_t^2}$
2	$2(\sigma_{a_0}/V)^2$	$\left(\frac{\sigma_{a_0}}{V}\right)^2 + \sigma_{\Delta a_1}^2 \left(1 - (\cos^4 \psi + \sin^4 \psi)\right)$	$2 \overline{\alpha_t^2}$
3	————	$2\left(\frac{\sigma_{a_0}}{V}\right)^2 + \sigma_{\Delta a_1}^2 \left(1 - \sum_{i=1}^3 \cos^4 \psi_i\right)$	————

Mean-Square Error Contribution, $\overline{\alpha_T^2}$, of Transducer Uncertainty for Various Combinations of Measurement Methods and Equal Quality Sensors

Table 2-3

depending upon whether null-seeking or direction-seeking are employed respectively.

Equation 2.4-48 shows that on a mean-square basis the contribution of sensitive axis uncertainty to a system's vector indicating capability is every bit as important as the contribution of transducer uncertainty. Reduction of the magnitude of α_{SA} is, thereby, an important objective. Table 2.3 shows that a reduction of 25% in a α_{SA}^2 may be had by using two instruments rather than three. An alternative means of reducing α_{SA}^2 is by minimization of α_{sa}^2 .

The ultimate goal of alignment is to orient the guidance sensors (gyros and accelerometers). Yet frequently this is achieved indirectly by aligning a set of fiducial axes scribed in the IMU's stable member. In any situation where a set of scribe-marks define the prime reference frame of a system, the relative orientation between the sensitive axes of the inertial sensors and reference coordinates must be established by a carefully controlled instrument mounting procedure and/or a calibration procedure. Knowledge of this relative orientation is necessary in order to transform data from the measurement frame defined by the sensitive axes to the scribed reference frame. It is precisely such a data transformation requirement which introduces sensitive axis uncertainty problems. Let us pursue this by assuming the role of an observer standing on the platform. If an inertial vector is measured for alignment, the inertial sensors can determine their orientation relative to the vector (e. g., the accelerometers locating \bar{g}). But unless we know our orientation (i. e. the scribe-mark locations) relative to the instruments, this information is useless in establishing our orientation relative to the vector. α_{SA} describes the uncertainty in knowledge of our orientation with respect to the instruments. But of what importance is our orientation (scribe-marks) to the guidance function? In a word, none. When measurements of the inertial sensors are used for alignment as well as for guidance, the system's

prime reference frame should be affixed to the sensitive axes of a set of inertial sensors. The location of the reference frame with respect to the structure is no longer of interest, except to know that it is described by a fixed rotation. In just a very few words, by defining our reference coordinate frame coincident with a set of instrument axes we set the sensitive axis uncertainty for those instruments to zero.

Lest anyone promote the setting of a reference frame according to an instrument frame as a cure-all for sensitive axis uncertainty problems, there are many limitations. First, it requires a triad of sensors to do a job of which a pair of sensors may be capable. Second, unless one triad of instruments can be used for all alignment measurements (at least two required), the problem of relating two sets of sensors to one another is very similar to relating each set to an arbitrary reference frame. Third, external information supplied to the system must be coordinatized via the platform axes seen by the external sensor. This requires the sensitive axes to be calibrated in platform reference coordinates once again. More particularly, when non-inertial inputs are used for alignment, the use of scribe-mark coordinates are necessary to relate the sensitive axes of inertial and non-inertial sensors.

In view of these drawbacks, it is best stated here only that sensitive axis uncertainty 1) is a significant source of error, 2) can be reduced by careful mounting and calibration procedures, and 3) can be eliminated for one set of sensors by the proper choice of reference coordinates.

2.4.3 Composite Misalignment For Two Vector Measurement

Thus far the ability of an IMU to independently indicate the direction of each of two non-collinear vectors has been established. This ability is expressed for each vector by the uncertainty angle α . It remains to develop the magnitude of the total IMU misalignment resulting from imperfect measurement of the vectors.

The directions of the two vectors $(\overline{V}_1, \overline{V}_2)$ being measured and the loci of possible independently indicated directions are shown in Figure 2-25. θ is the angle between the measured vectors, corresponding for example to the co-latitude angle in a gyrocompassing system. The dependent reference frame being aligned is essentially fixed to the unit vectors $(\overline{I}_{V_1})_{ind}$

and $(\overline{I}_{V_2})_{ind}$. It may be represented by the non-orthogonal coordinate set composed of $(\overline{I}_{V_1})_{ind}$, $(\overline{I}_{V_2})_{ind}$, and the unit normal to them, $(\overline{I}_n)_{ind}$. The frame being aligned to is similarly fixed to the coordinate set \overline{I}_{V_1} , \overline{I}_{V_2} , \overline{I}_n .

It is shown at the end of Section 2.4.1 that, provided

$$\left| (\overline{I}_{V_1})_{ind} \times (\overline{I}_{V_2})_{ind} \right| = \left| (\overline{I}_{V_1} \times \overline{I}_{V_2}) \right| = \sin \theta,$$

the evaluation of the magnitude of the whole angle rotation, Φ , for the non-orthogonal coordinate set is the same as the evaluation for an orthogonal set. The provision that the angle between $(\overline{I}_{V_1})_{ind}$ and $(\overline{I}_{V_2})_{ind}$ be θ is more a natural than an artificial constraint. As noted recently, θ is the co-latitude angle in gyrocompassing system.. In master-slave configurations, θ is effectively measured by the master and supplied to the slave for control purposes (θ is implicitly $\pi/2$ for vertical-azimuth situations). Lack of any constraint between the allowed indications merely renders the concept of a total misalignment meaningless. In that case the realizable platform misalignment angles assume the infinity of values related to all combinations of points on the indicated loci.

The angles α_1 and α_2 will be recognized as equivalent to the ϕ_i of Equation 2.4-1 so that Φ is obtained from

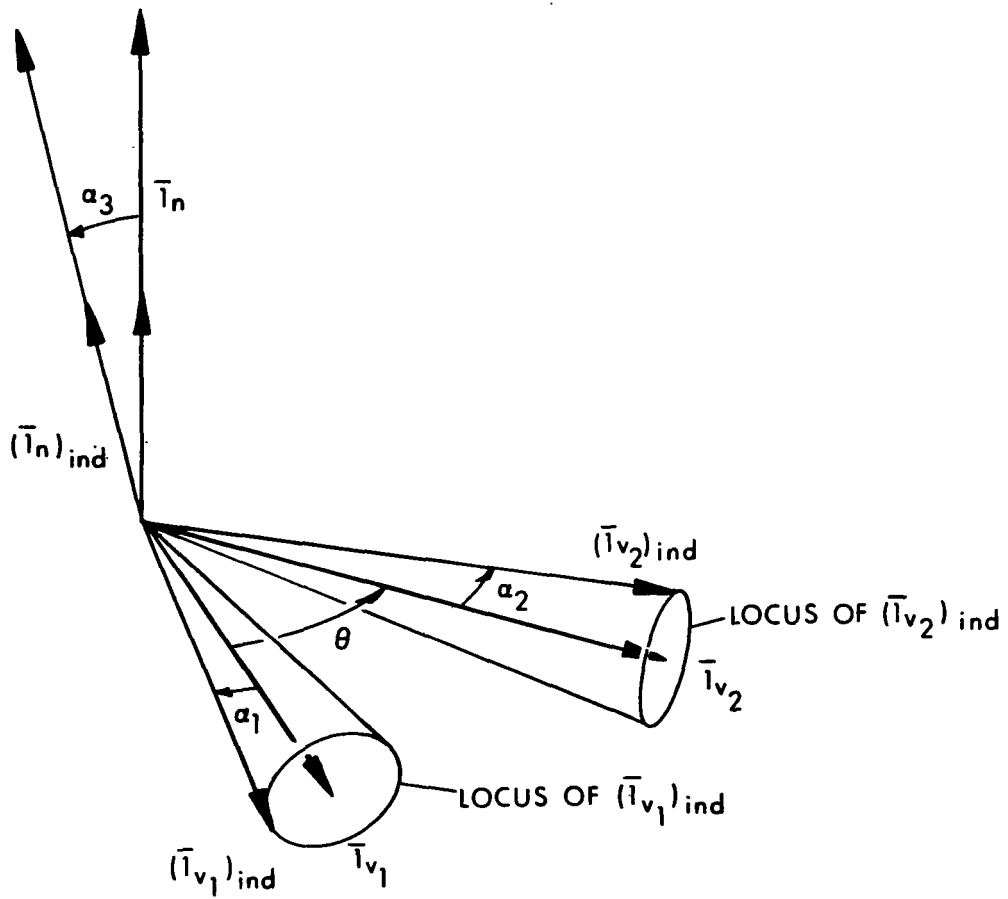


Figure 2-25 Geometry of Two-Vector Composite Misalignment

$$\Phi = \frac{1}{\sqrt{2}} \sqrt{\alpha_1^2 + \alpha_2^2 + \alpha_3^2} \quad 2.4-10$$

where α_3 is defined by Figure 2-25. To calculate α_3

$$\begin{aligned} \cos \alpha_3 &= (\bar{1}_n) \cdot (\bar{1}_n)_{\text{ind}} \\ &= \frac{[\bar{1}_{V_1} \times \bar{1}_{V_2}]}{\sin \theta} \cdot \frac{[(\bar{1}_{V_1})_{\text{ind}} \times (\bar{1}_{V_2})_{\text{ind}}]}{\sin \theta} \\ &= \frac{1}{\sin^2 \theta} \left\{ \cos \alpha_1 \cos \alpha_2 - [\bar{1}_{V_1} \cdot (\bar{1}_{V_2})_{\text{ind}}] \cdot \right. \\ &\quad \left. [\bar{1}_{V_2} \cdot (\bar{1}_{V_1})_{\text{ind}}] \right\} \end{aligned}$$

from which

$$\alpha_3^2 = \frac{1}{\sin^2 \theta} \left\{ \alpha_1^2 + \alpha_2^2 - 2 \cos^2 \theta + 2 [\bar{1}_{V_1} \cdot (\bar{1}_{V_2})_{\text{ind}}] [\bar{1}_{V_2} \cdot (\bar{1}_{V_1})_{\text{ind}}] \right\} \quad 2.4-93$$

Except in the vicinity of $\theta = 0^\circ$ or $\theta = 90^\circ$ the approximation

$$\bar{1}_{V_1} \cdot (\bar{1}_{V_2})_{\text{ind}} \simeq \bar{1}_{V_2} \cdot (\bar{1}_{V_1})_{\text{ind}} \simeq \cos \theta \quad 2.4-94$$

is reasonable. Cases of θ near zero are uninteresting but cases of θ near 90° are important. Figure 2-24 and its associated mathematics substantiate that the value of α_3 resulting from use of the approximation 2.4-94 at $\theta = 90^\circ$ is the correct upper bound on α_3 and therefore also on Φ . (The value of α_3 is only bounded for fixed α_1 , α_2 and θ ; it is not unique.)

Introducing Equation 2.4-94 into 2.4-93 and introducing that result into Equation 2.4-10, the following is obtained:

$$\Phi^2 = \frac{1}{2} (\alpha_1^2 + \alpha_2^2) (1 + \csc^2 \theta) \quad 2.4-95$$

The mean-square angular uncertainties, $\overline{\alpha_1^2}$ and $\overline{\alpha_2^2}$, are not generally equal. For cases where they may be related by a simple numerical factor n, ascribe the literal $\overline{\alpha^2}$ to the smaller of $\overline{\alpha_1^2}$ and $\overline{\alpha_2^2}$ such that in the expression 2.4-96

$$\overline{\Phi^2} = \left[\frac{1}{2} (n^2 + 1)(1 + \csc^2 \theta) \right] \overline{\alpha^2} \quad 2.4-96$$

the quality factor n is always greater than unity. The square-root of this equation is plotted in Figure 2-26 as a function of n and θ .

A word regarding the "quality factor" n is in order. It is admittedly a shaky proposition to relate complex systems by simple numerics, but only from the viewpoint of mathematical rigor. From the viewpoint of practical utility, the use of simple numerics for comparative purposes is commonplace. That we have chosen the ratio of root-mean-square direction-indication errors as a figure-of-merit is a natural result of the preceding developments.

It may be seen from Figure 2-26 that at $\theta = 90^\circ$ the total rms misalignment is approximately 98 per cent attributable to the poorer measurement when $n = 5$. In fact, when one measurement is only twice as good as the other at $\theta = 90^\circ$, the poorer measurement accounts for almost 90 per cent of the total error. Only when θ is significantly less than 90° does the total error reflect a meaningful component from the more accurate measurement.

2.4.4 Information Transferred From An External Sensor or System

Section 2.4.2 was concerned with the ability of a set of sensors to indicate the direction of a vector input. One of the characteristics of moving base phenomena is that frequently the measured vector differs in direction and/or magnitude from the desired vector. If disturbances causing changes

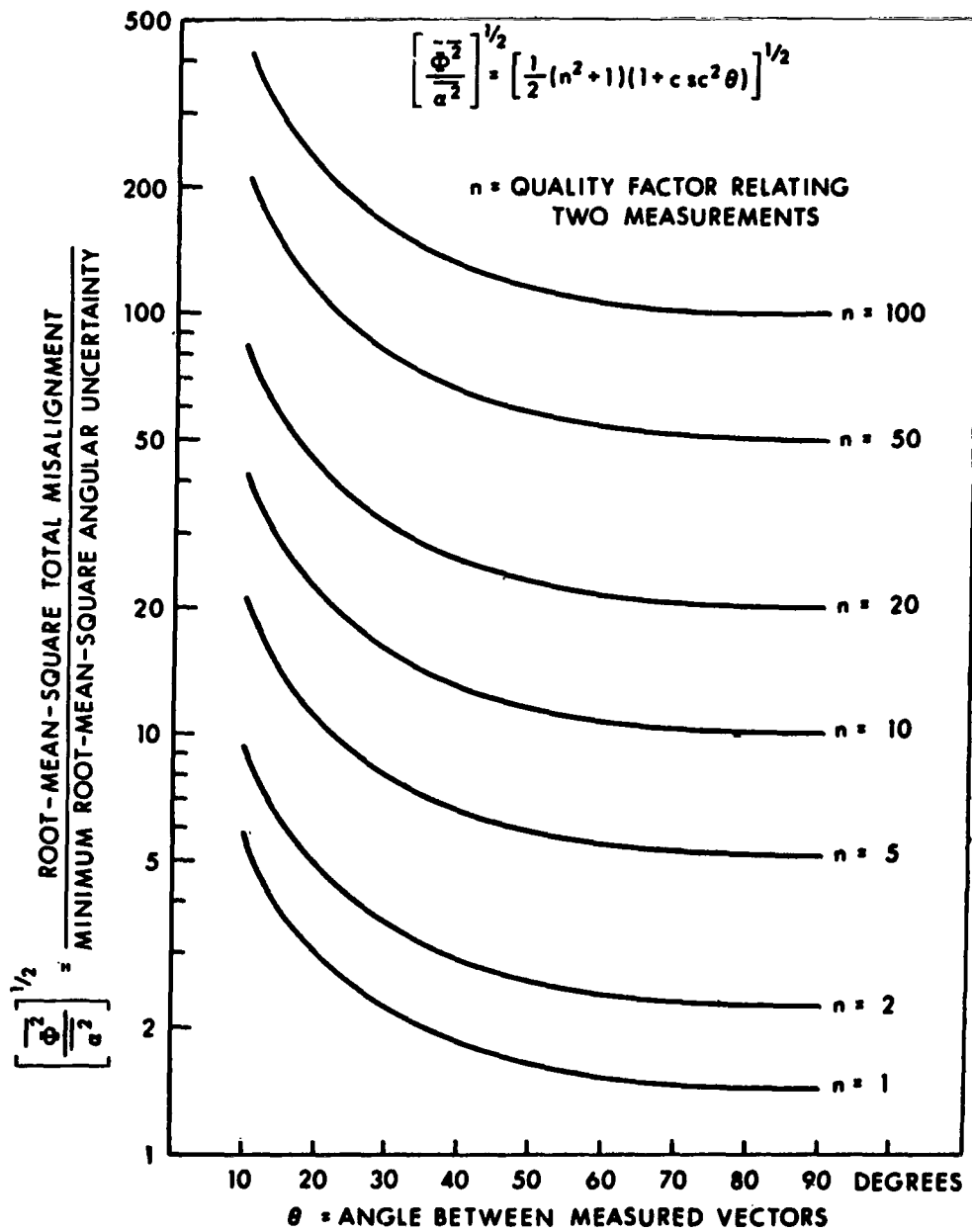


Figure 2-26 Composite Misalignment for Two-Vector Measurement

in the desired vector's direction are of sufficient intensity, compensatory information may be supplied in an attempt to reduce the discrepancy. Considering that compensation procedures are rarely perfect, a residual angular uncertainty (β) between the direction of the desired and compensated actual vectors (See Figure 2-27) must be accounted for. The resulting total uncertainty in finding the direction of a desired vector input is assigned as γ .

From Figure 2-25,

$$\gamma^2 = \alpha^2 + \beta^2 - 2\alpha\beta \cos \eta \quad 2.4-97$$

where η is uniformly distributed. Using the results of Appendix B, Equation B-13 and B-16,

$$\overline{\gamma} = \frac{2}{\pi} (\alpha + \beta) \mathcal{E}(k^2) ; \quad k^2 = \frac{4\alpha\beta}{(\alpha + \beta)^2} \quad 2.4-98$$

$$\overline{\gamma^2} = \overline{\alpha^2} + \overline{\beta^2} \quad 2.4-99$$

α was the subject of Section 2.4.2. The evaluation of β , since it is strongly related to specific schemes applicable to the moving base alignment problem, is deferred to Chapter III. If β is non-zero when the results of Section 2.4.3 are used, a simple substitution of γ for α is rigorously correct.

2.5 Summary

This chapter has attempted to develop a unified theory of alignment whose purpose is to lend coherence to the analysis of numerous techniques proposed as solutions of the moving base alignment problem. It is founded on the two considerations common to all alignment procedures: coordinate frames and measurements. This serves to adequately bound expected alignment accuracies. All alignment procedures are viewed as the transfer of orientation between two coordinate frames by the measurement of at least two non-collinear vectors. Separate techniques vary only in the mechanization of particular measurements.

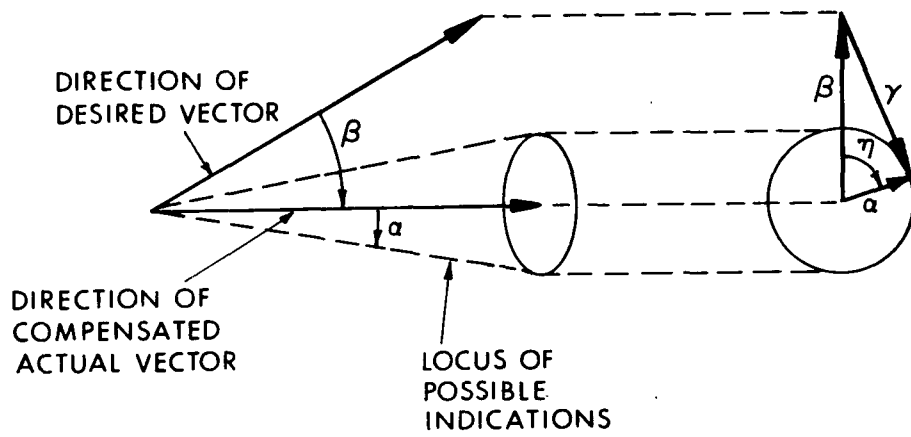


Figure 2-27 Geometry Relating γ to α and β

Coordinate frame rotations are handled as whole-angle rotations, the latter being developed in terms of all the more usual rotational parameters. Certain interesting results are derived concerning the magnitude of the whole-angle rotation in the case of Euler angles and principal direction cosines. The latter angles are also shown to be an especially convenient representation for problems involving non-orthogonal coordinate sets.

Measurements are discussed from the viewpoint of a system of single-degree-of-freedom sensors attempting to locate the direction of a vector input. Both magnitude-sensitive and angle sensitive instruments are considered. In the former case, bias and scale factor uncertainties are the assumed errors. In the latter case, the uncertainties are inherently angular. Sensitive axis location uncertainties are included for both cases. The measurement error of any system is reduced to an angular uncertainty in indicating the direction of a vector by converting the uncertainties of magnitude sensitive instruments to their angular equivalents. This conversion is carried out for all practical combinations of sensor-to-vector orientation. An important result of this conversion is the establishment of definite guidelines to minimize magnitude and direction indication errors as a function of instrument uncertainties and the orientation of the vector with respect to the sensors.

Deviation of a vector input from a desired nominal direction due to base motion is expressed in angular terms and included with the basic measurement error. The magnitude of the total platform misalignment resulting from independent measurements of two non-collinear vectors is calculated as a function of the angular uncertainties about the nominal positions of each of the vectors.

Application of the unified analysis to specific alignment techniques is accomplished in Chapter III.



CHAPTER III

ANALYSIS OF ALIGNMENT TECHNIQUES

3.1 Introduction

The preceding chapter considers all approaches to the solution of the moving base alignment problem as a class of non-dimensional vector direction indication problems. In contrast to this, the majority of the literature concerned with aligning inertial systems on a moving base is an exposition of distinct "techniques." The abstractness of the former approach is reconciled with the latter approach in this chapter. This is accomplished by individually discussing several techniques within the analytical framework of Chapter II.

The most significant techniques appearing in the literature (and those considered in this chapter) are:

- 1) Vertical Indication
- 2) Gyrocompassing
- 3) Star Tracking
- 4) Fix Monitored Azimuth
- 5) Vector Matching
- 6) Gimbal Angle Matching
- 7) Optical Comparison

Each of the foregoing techniques makes measurements on a different vector quantity. This is perhaps the clearest distinction among them. Once the vector associated with a given technique is identified and the measurement sensors are defined, the limiting ability of the sensors to indicate the direction of the vector is obtained from the results of Chapter II (as a quantitative evaluation of the angle α). We also establish the significance of the vector

relative to a coordinate frame of interest and express the degree to which it maintains its significance in the face of perturbing environmental influences by evaluating the angle β . The total vector direction indication error, γ , follows directly from Equation 2.4-97

The techniques by which alignment is effected fall into two distinct categories: Direct Measurement Techniques and Transfer Techniques. Recalling the definition of alignment, angular coincidence is sought between the dependent reference frame (Section 2.2.2) and the independent reference frame (Section 2.2.1) of Figure 2-1. This is accomplished by measurements on at least two non-collinear vectors. In direct measurement techniques, equipment associated with the dependent reference frame measures vector quantities which have a unique geometrical relationship to the independent reference frame. This geometrical relationship constitutes a priori information which must be available to the dependent reference frame. A simple example is the measurement of \bar{g} coupled with the knowledge that it lies along one axis of a local geographic coordinate frame.

In transfer techniques, equipment associated with the dependent reference frame measures vector quantities which do not necessarily have an a priori geometrical relationship to the independent reference frame. Rather, an intermediate (Section 2.2.3) or transfer (Section 2.2.4) reference frame simultaneously measures the same vector quantity as the dependent reference frame. This second measurement serves to establish the geometrical significance of the vector with respect to a mechanized representation of the independent reference frame. Once determined, of course, this information must be communicated to the dependent system. The vector, as a common sensory input to both systems, is serving only as an information transfer medium. Of the measurement techniques listed earlier, the first four are in the direct measurement category; the remainder are in the transfer category.

Prior to examining individual techniques, we call attention

to one further distinction. Indicating the particular direction known as the vertical is well enough solved in both theory and application as to be the most widely acceptable measurement for moving base alignment. In fact, because of the tendency to rely upon the vertical to provide one of the two required vector inputs, the moving base literature is largely oriented to the single vector problem of azimuth determination. For this reason, many of the techniques discussed later in this chapter are intended only for azimuth alignment of a system which is already correctly oriented with respect to the vertical.

3.2 Vertical Indication

We consider here the fundamental limitations in locating the vertical direction by means of specific force measurements. The specific force sensor employed for vertical indication on a moving base is the accelerometer. Devices such as a spirit level are often employed in a more benign environment but do not possess the combined dynamic range and accuracy of which accelerometers are capable. We are interested in quantifying how well the accelerometer can measure a specific force vector and how well this vector's direction represents the vertical direction.

The independent reference frame for vertical indication is an earth fixed reference frame. This reflects the unique geometrical relationship between the vertical direction at a point and the earth. According to Wrigley¹³

"The Vertical at a point on the Earth's surface is defined as the local direction of the force of gravity as indicated by a plumb bob hanging from a base that is stationary relative to the Earth. The horizontal plane is defined as the plane perpendicular to the vertical, or as the surface of a free liquid under the influence of gravity alone."

Note that although the vertical is intimately related to a physical vector, it is not itself a vector. It is merely a signed direction. This is as stated in Section 2.3.1: when a vector is the input to the alignment problem, only its direction is of ultimate interest. There is no requirement to explicitly compute the

magnitude of the gravity vector and, therefore, no requirement to perform a complete vector measurement.

In considering vertical indication from a carrier operating above or below the earth's surface, the local vertical is understood to imply the direction of the extended plumb bob vertical passing through the center of measurement of an inertial system. Additionally, we assume that deviations in the direction and magnitude of gravity (\bar{g}) are generally negligible within the volume of space occupied by a carrying vehicle. For an analytic gravity field non-parallelism is only on the order of 0.01 arc second per foot of separation in the horizontal plane. By comparison, gravity anomalies may cause parallel gravity vectors to appear at points on the earth's surface within a subtended angle of 15 arc seconds.¹⁷

Of far greater significance to the vertical indication problem is the difference between the "dynamic" (or apparent) vertical and the "static" (or true) vertical. The true and apparent verticals are defined respectively by the directions of gravity (\bar{g}) and total specific force (\bar{f}). Depending upon one's point of view, either the apparent vertical is an imperfect representation of the true vertical or the true vertical is a special case of the apparent vertical occurring when the measuring system is at rest with respect to the earth. Since only the true vertical has a unique geometrical meaning with respect to the earth, we adopt the former point of view. That is, by severing the connection between the system and the earth, we invite base motion to destroy the uniqueness of the quantity we are able to measure. Error-free accelerometers are only capable of indicating the direction of \bar{f} ; they require additional intelligence to deduce the direction of \bar{g} from that of \bar{f} . In essence, we must now process the moving base measurements in order to obtain an equivalent fixed-base indication.

Relative to the format of Chapter II, the angular discrepancy between \bar{g} and \bar{f} is geometrically defined by β . (See Figure 2-27 reproduced here as Figure 3-1, but with the vector designations

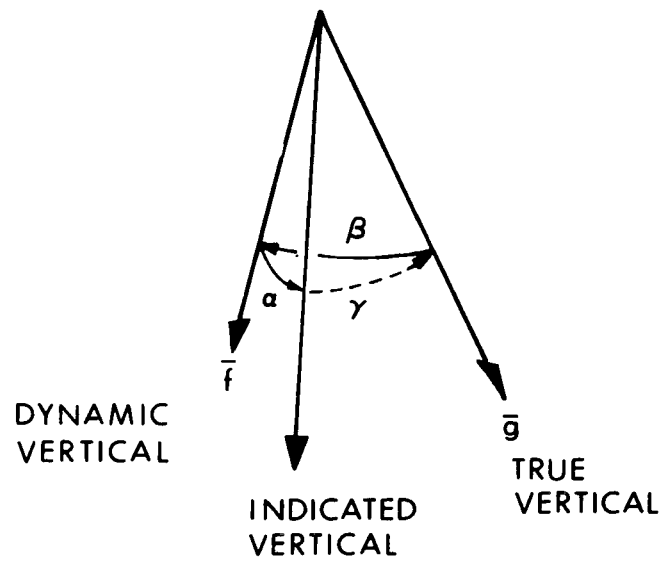


Figure 3-1 Geometric Quantities Relevant to Vertical Indication

appropriate for vertical indication.) The problem of deducing the direction of \bar{g} from \bar{f} is equivalent to forcing β to zero. The limited instrument capability to accurately indicate the direction of \bar{f} is given by the appropriate angle α (relative to the instrument configuration employed)

3.2.1 Evaluation of β for Vertical Indication

A small angular difference (β) between the true and apparent verticals is described by

$$\beta = \frac{|\bar{g} \times \bar{f}|}{|\bar{g}| |\bar{f}|}$$

For most conditions of interest,

$$|\bar{f}| \approx |\bar{g}|$$

and

$$\beta \approx \frac{|\bar{g} \times \bar{f}|}{g}$$

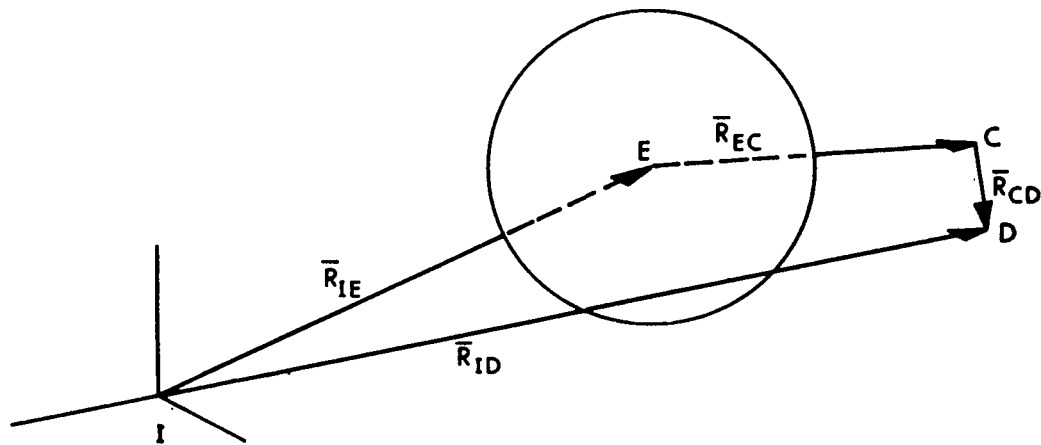
3.2-1

from which it is seen that the horizontal component of \bar{f} deflects the vertical at the rate of 1 minute of arc for each 290 micro-g.

A mathematical relationship between \bar{g} and \bar{f} is obtained in convenient form by expressing the inertially referred acceleration of a point as the vector sum of component accelerations referred to several coordinate systems. * Using the four coordinate frames and position vectors defined by Figure 3-2, \bar{f} at point D may be written as

$$\begin{aligned} \bar{f} &= \bar{G} - p_I^2 \bar{R}_{ID} \\ \bar{f} &= \bar{G} - \left[p_I^2 \bar{R}_{IE} + p_E \bar{\omega}_{IE} \times \bar{R}_{ED} \right] \\ &\quad - \left[p_E^2 \bar{R}_{EC} + p_E \bar{\omega}_{EC} \times \bar{R}_{CD} + 2\bar{\omega}_{EC} \times p_C \bar{R}_{CD} + \bar{\omega}_{EC} \times (\bar{\omega}_{EC} \times \bar{R}_{CD}) \right] \\ &\quad - \left[2\bar{\omega}_{IE} \times p_E \bar{R}_{ED} + \bar{\omega}_{IE} \times (\bar{\omega}_{IE} \times \bar{R}_{ED}) \right] - p_C^2 \bar{R}_{CD} \end{aligned} \quad 3.2-2$$

* See Appendix D, Reference 13 for a detailed mathematical development.



- I is center of an inertial system - no acceleration relative to fixed space
- E is center of the earth; origin of axes fixed in the earth
- C is center of gravity of the carrying vehicle; origin of axes fixed in the vehicle
- D is center of dependent reference frame; origin of axes fixed in the inertial measuring unit

$$\bar{R}_{ID} = \bar{R}_{IE} + \bar{R}_{EC} + \bar{R}_{CD}$$

Figure 3-2 Vector Representation by Components of the Position of the Center of Measurement of an Inertial Measuring Unit in Motion with Respect to the Earth

where

- p_i is the time derivative operator in the subscripted coordinate frame
- $\bar{\omega}_{EC}$ is the angular velocity of the vehicle about its center of gravity measured with respect to the earth
- $\bar{\omega}_{IE}$ is the angular velocity of the earth with respect to an inertial frame
- \bar{G} is the gravitation at point D

Equation 3.2-2 is equally valid for vehicles operating below, on or above the surface of the earth. Figure 3-2 merely depicts an extra-terrestrial vehicle for convenience.

In assuming that \bar{f} is the specific force measured by the IMU's accelerometers, we ignore a slight refinement occasioned by the required pendulosity of the instruments. A more complete characterization only results in additional terms of negligible magnitude.

As an initial simplification of Equation 3.2-2, the terms included in the first bracket make no significant contribution to \bar{f} . They will, therefore, be dropped. Furthermore, the definition of the observed local acceleration of gravity, \bar{g} , at point D

$$\bar{g} = \bar{G} - \bar{\omega}_{IE} \times (\bar{\omega}_{IE} \times \bar{R}_{ED}) \quad 3.2-3$$

allows two terms to be combined. These simplifications result in the following expression for \bar{f}

$$\bar{f} = \bar{g} - \left[p_E^2 \bar{R}_{EC} + p_E \bar{\omega}_{EC} \times \bar{R}_{CD} + 2\bar{\omega}_{EC} \times p_C \bar{R}_{CD} + \bar{\omega}_{EC} \times (\bar{\omega}_{EC} \times \bar{R}_{CD}) + p_C^2 \bar{R}_{CD} + 2\bar{\omega}_{IE} \times p_E \bar{R}_{ED} \right] \quad 3.2-4$$

Bracketed in Equation 3.2-4 are the terms which corrupt the physical observable representing the vertical. We are interested in their horizontal components. The physical sources of the interference are motions of the vehicle relative to the earth and

dynamic behavior of the vehicle as a non-rigid base. Notice that static alignment accuracies between the C and D frames are not important. In the absence of system motion with respect to the earth, $\bar{f} = \bar{g}$, whereas, in the face of significant base motion, the magnitude of β (Equation 3.2-1) is sufficient to require compensatory modification of the accelerometer's raw outputs. Certain terms of Equation 3.2-4 are known, in fact, as "acceleration compensation terms."¹⁷ When compensation is employed, Figure 3-1 is still accurate for error determination provided β now represents the residual uncertainties for the compensation process.

The compensation requirements for individual applications are derived in a straightforward manner from Equations 3.2-1 and 3.2-4. However, the requirements are too strongly related to parameters such as desired accuracy, vehicle configuration, vehicle speed and expected maneuvers to permit general quantitative conclusions here. We can discuss, however, the alternate means of compensation.

Compensation of the output of a sensor (or some deterministically derived function thereof) is basically of two types: 1) signal modification by filtering; and 2) signal modification by the addition of an externally derived signal. Depending on the character of the base motion, these techniques may be employed separately or simultaneously. The attraction of signal filtering is that it may be mechanized on a self-contained basis without additional sensory requirements. Unfortunately, it is limited in its ability to discriminate between signal components on any basis other than frequency. Externally derived compensation signals, while imposing the requirement for additional sensory equipment, are capable of accurately discriminating between like frequency signals on an amplitude basis. Filtering also may be applied directly to the output of external sensors in order to reduce the noise associated with these measurements.

The frequency at which \bar{g} is observed depends only on the relative motion between the dependent reference frame and

\bar{g} . By Equation 3.2-4, angular motion of the dependent frame does not affect \bar{f} . Therefore, the frequency modulation of \bar{g} by platform motion is reflected in the same fashion by all terms of \bar{f} . This permits us to arbitrarily choose to examine base motion interference from a frame in which \bar{g} is a zero frequency quantity. (Note that this restricts only two degrees of freedom of the platform.)

As to motion of the carrying vehicle relative to the earth, Brock¹ states that the filtering problem is greatly aided if the vehicle is controlled so that the velocity (vector) between maneuvers fluctuates only slightly from some nominal value. An examination of Equation 3.2-4 shows that this is indeed a help in reducing bias accelerations. Yet for the very condition of constant velocity, a bias Coriolis acceleration ($2 \bar{\omega}_{IE} \times p_E \bar{R}_{ED}$) deflects the vertical at the rate of $2.29 \times 10^{-2} \sin \lambda$ minutes of arc per mile per hour of horizontal speed ($\lambda =$ latitude). For a ship at high latitudes this might approach a value as high as one arc minute. For a subsonic airplane it might easily approach 10 arc minutes. This term will generally have to be compensated, requiring thereby sensors capable of providing a measure of the vehicle velocity $p_E \bar{R}_{ED}$.

A measure of the high bias accelerations generated by vehicle maneuvers is given by the term $p_E^2 \bar{R}_{EC}$ evaluated at constant speed. The radial accelerations at constant speed are plotted in Figure 3-3. Note that a man walking at 5 miles per hour around a circular path of one mile radius experiences a constant vertical deflection of one arc minute. While these high maneuver accelerations make vertical indication difficult, they are indispensable to the vector matching technique of Section 3.5.

An example of an easily filterable horizontal acceleration is that due to vibrational modes of the vehicle. Given a suitable period of observation, physical constraints prohibit $p_C^2 \bar{R}_{CD}$ from making any net contribution to \bar{f} . This is true even in a

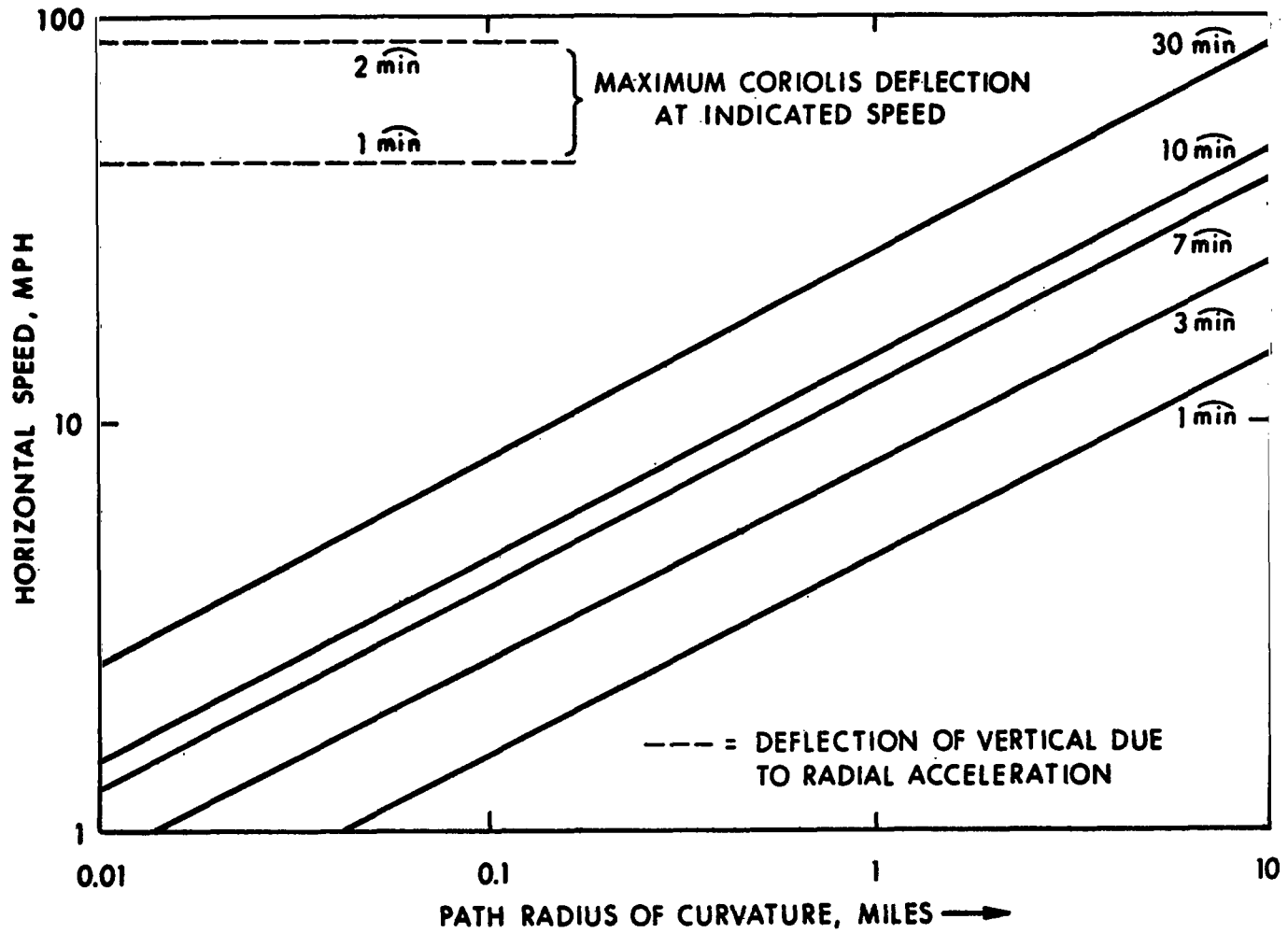


Figure 3-3 Deflection of the Vertical, β , as a Function of Horizontal Speed and Path Radius of Curvature

violent environment such as a missile under the wing of an airplane. The time required to discriminate against this (and any filterable quantity) is determined by the vibrational spectral characteristics, the nature of the filter, and the amount of noise suppression required.

Schuler tuning is, of course, a unique form of filtering whereby the vehicle's tangential acceleration becomes an aid in tracking the vertical rather than a quantity to be discriminated against. This concept and the attendant damping problems are thoroughly considered in the literature.

3.2.2 Evaluation of α for Vertical Indication

Measurement of the specific force vector's direction using single-degree-of-freedom accelerometers requires either two or three instruments. With two accelerometers, they must be servo-controlled to enable orientation of their sensitive axes in the null plane. This represents by far the most common mechanization of vertical indication. From Tables 2-2 and 2-3 (with $|\bar{f}| \simeq |\bar{g}|$)

$$\overline{\alpha_{SA}^2} = 2\overline{\alpha_{sa}^2}$$

$$\overline{\alpha_T^2} = 2\left(\sigma_{a_0/g}\right)^2$$

so that

$$\overline{\alpha^2} = \left[2\overline{\alpha_{sa}^2} + \left(\sigma_{a_0/g}\right)^2 \right] \quad 3.2-5$$

by Equation 2.4-48.

For three accelerometers, it is beneficial but not required to specially orient the sensitive axes. The tables yield

$$\overline{\alpha^2} = \frac{3}{2}\overline{\alpha_{sa}^2} + 2\left(\sigma_{a_0/g}\right)^2 + \sigma_{\Delta a_1}^2 \left(\frac{3}{1 - \sum_{i=1}^3 \cos^4 \psi_i} \right) \quad 3.2-6$$

In Equations 3.2-5 and 3.2-6, $\overline{\alpha_{sa}^2}$ is the mean-square sensitive axis uncertainty of each instrument expressed in radian measure to the second power, σ_{a_0} is the standard deviation of accelerometer bias expressed in equivalent "g's," and $\sigma_{\Delta a_1}$ is the standard deviation of accelerometer scale factor (a dimensionless quantity sometimes expressed in units of g/g). Notice that with either two or three accelerometers, vertical indication accuracy is inherently bias limited.

3.3 Gyrocompassing

The interpretation of the term "gyrocompass"¹⁷ (the precursor of gyrocompassing) has remained unambiguous, that being a pendulous gyroscopic element arranged to track the horizontal component of the earth's daily rotation ($\overline{\omega}_{IE}$). The term "gyrocompassing," on the other hand, has become subject to much looser interpretation, to the point that it more connotes the general process of aligning by means of an angular velocity vector than it does the specific process of aligning to $\overline{\omega}_{IE}$ by a particular mechanization. We restrict our attention here to the vector $\overline{\omega}_{IE}$ and investigate the fundamental limitations in establishing its direction with gyroscopic sensors mounted on a moving base.

The unique geometrical relationship between the direction of $\overline{\omega}_{IE}$ and the earth's polar axis dictates that the independent reference frame be an earth-fixed reference frame. This is the same frame employed for vertical indication. Base motion relative to this frame, it will be shown, generally can cause severe bias deflections of the measured angular velocity relative to $\overline{\omega}_{IE}$.

Prior to evaluating α and β , let us briefly consider a practical example of the importance of determining system alignment accuracy relative to instrument performance. The majority of operational situations requiring alignment of a dependent frame in a mobile environment will employ the dependent frame, once aligned, for a relatively short period of time. In such situations, gyros with only moderate drift performance may be capable of maintaining the

dependent reference frame with sufficient accuracy. The practical advantages inherent in the use of such gyros are numerous. It is desirable, in such situations, that the alignment scheme not require a level of gyro performance better than that required for guidance. Thus, although gyros of sufficient performance to permit gyroscopic alignment may be within the current technological capability, such alignment methods must often be ruled out. The uniform presentation of performance parameters developed in this thesis is an aid in making such a decision.

3.3.1 Evaluation of β for Gyrocompassing

Referring to Figure 3-2 the angular velocity relative to inertial space sensed by the dependent frame gyros, $\bar{\omega}_{ID}$, is expressed as the simple vector sum

$$\bar{\omega}_{ID} = \bar{\omega}_{IE} + \bar{\omega}_{EC} + \bar{\omega}_{CD} \quad 3.3-1$$

An angular difference (β) between the direction of $\bar{\omega}_{ID}$ and the earth's polar axis is described by

$$\sin \beta = \frac{|\bar{\omega}_{IE} \times \bar{\omega}_{ID}|}{|\bar{\omega}_{IE}| |\bar{\omega}_{ID}|} \quad 3.3-2$$

We must defer temporarily an explicit solution of 3.3-2 for β . As mentioned earlier, the possible base motion influence here is much more severe than that found in vertical indication. Gravity is a field force; its influence is felt even when removed from stable contact with non-force motion-parameters such as $\bar{\omega}_{IE}$. One of the better advertised "problems" of angular rate sensing is that a westward speed of approximately $1040 \cos \lambda$ mph ($\lambda =$ latitude) cancels $\bar{\omega}_{IE}$ completely (Equation 3.3-2 is then indeterminate.) Rather than fearing the lack of a quantity to sense, one should be more concerned that a reduced magnitude vector input always increases the indication error (See Table 2-3). Hovorka² concludes from the masking of earth rate by vehicle speed that gyrocompassing

is a slow-vehicle process. Independent of the rationale, this is a widely held viewpoint.

To the extent that the dependent frame is caged to the vehicle, $\bar{\omega}_{CD}$ represents structural angular vibrations of the vehicle. If the structure cannot assume quasi-static deflections, $\bar{\omega}_{CD}$ must have zero-average value; if the structure does assume quasi-static deflections, the average value of $\bar{\omega}_{CD}$ tends to zero over an extended period of observation. It appears, therefore, that $\bar{\omega}_{CD}$ can be successfully filtered from the gyro's output. This we will assume, with the understanding that it may only be a first approximation. Even if $\bar{\omega}_{CD}$ has a zero average value, the gyro output may well have a non-zero average indication of $\bar{\omega}_{CD}$ due to "kinematic rectification" ²¹ or "coning." ^{22, 23} The magnitude of a problem such as this is strongly related to design details and its examination is beyond the scope of this thesis.

If we set $\bar{\omega}_{CD}$ to zero in 3.3-1 and assume that the carrying vehicle is restricted to motion in the local horizontal plane, Eq 3.3-2 may be evaluated with the result

$$\sin \beta = \frac{V_N}{R \left(\omega_{IE}^2 + V^2/R^2 \right)^{1/2}} \quad 3.3-3$$

where V is the vehicle groundspeed, V_N is the northerly component of groundspeed and R is the distance of the vehicle from the center of the earth. Notice that even at constant speed and constant heading, β may have a bias value which is non-filterable.

The problem of forcing β to zero is equivalent to forcing V_N to zero. This may be accomplished obviously by heading due east or west, or, in fact, by stopping the vehicle. It may also be accomplished by an external source of velocity information (such as Doppler radar, airspeed indicator or pitometer log) which provides a signal to compensate the gyro output. Any one of these situations serves to place the measured vector collinear with its

meaningful orientation. The compensation process effectively re-couples the gyros to the earth.

It is recognized that errors will exist in any auxiliary reference and that their nature will vary. Let us assume that the reference is subject to bias errors (a_0) and sensitivity errors (Δa_1). Bias errors may exist simply because speed is measured relative to a medium (air, water) which itself is in motion relative to the earth. Sensitivity errors will be sensor related but may correlate with the environment, as in the gain shift of Doppler radar with varying terrain reflectivity.

When such a compensating reference is used, Equation 3.3-4 becomes

$$\beta \cong \frac{(a_0 + \Delta a_1 V_N)}{R(\omega_{IE}^2 + (a_0 + \Delta a_1 V)^2 / R^2)^{1/2}} \quad 3.3-4$$

which, if the reference error coefficients have zero mean value and we neglect the second order effect of an error in the total velocity measurement, has a mean square value

$$\overline{\beta^2} = \frac{\sigma_{a_0}^2 + \sigma_{\Delta a_1}^2 V_N^2}{R^2 \omega_{IE}^2} \quad 3.3-5$$

It is noted that in developing this expression we have neglected an additional second order correction due to imperfect resolution of total measured velocity into north and east components. Details such as this must be considered at the design stage.

In Equation 3.3-5, σ_{a_0} is the standard deviation of velocity bias expressed in the same units as V_N (feet per second, miles per hour, etc.) and $\sigma_{\Delta a_1}$, is the standard deviation of velocity scale factor (a dimensionless quantity). As an indication of the order of magnitude of these standard deviations, Reference 24 states that

the accuracy of modern Doppler radar approaches 0.1%; $\sigma_{\Delta a_1}$ is thereby implied of the order of 0.001. Uncompensated northerly groundspeed deflects $\bar{\omega}_{IE}$ at the rate of 1 arc-minute per 0.3 miles per hour. In a 300 mph plane using 0.1% speed measurement, β has at least a one arc-minute value for northerly flight.

3.3.2 Evaluation of α for Gyrocompassing

Measurement of the direction of the angular velocity vector, $\bar{\omega}_{ID}$, requires two or three single-degree-of-freedom gyros. With two gyros, they must be servo-controlled to enable orientation of their sensitive axes in the null plane. From Tables 2-2 and 2-3 (with $|\bar{\omega}_{ID}| \approx |\bar{\omega}_{IE}|$)

$$\begin{aligned}\overline{\alpha}_{SA}^2 &= 2\overline{\alpha}_{sa}^2 \\ \overline{\alpha}_T^2 &= 2\left(\sigma_{a_0/\omega_{IE}}\right)^2\end{aligned}$$

so that

$$\overline{\alpha}^2 = 2\left[\overline{\alpha}_{sa}^2 + \left(\sigma_{a_0/\omega_{IE}}\right)^2\right] \quad 3.3-6$$

With three gyros, the tables yield

$$\overline{\alpha}^2 = \frac{3}{2}\overline{\alpha}_{sa}^2 + 2\left(\sigma_{a_0/\omega_{IE}}\right)^2 + \sigma_{\Delta a_1}^2\left(1 - \sum_{i=1}^3 \cos^4 \psi_i\right) \quad 3.3-7$$

One of the more common system mechanizations places one gyro east, one north, and one either parallel or anti-parallel to the gravity vector. In this case, 3.3-7 becomes

$$\overline{\alpha}^2 = \frac{3}{2}\overline{\alpha}_{sa}^2 + 2\left(\sigma_{a_0/\omega_{IE}}\right)^2 + \sigma_{\Delta a_1}^2(1 - \cos^4 \lambda - \sin^4 \lambda) \quad 3.3-8$$

where $\lambda =$ latitude.

In these equations, $\overline{\alpha_{sa}^2}$ is the mean square sensitive axis uncertainty of each instrument expressed in radian measure to the second power, σ_{a_0} is the standard deviation of bias gyro drift expressed in the same units as $\overline{\omega_{IE}}$, and $\sigma_{\Delta a_1}$ is the standard deviation of gyro scale factor (a dimensionless quantity). Notice that with either two or three gyros, the directional indication is bias limited.

The total error, γ , in indicating the direction of $\overline{\omega_{IE}}$ is described geometrically by Figure 3-4 (See also Figures 3-1 and 2-27) and the mean square value is given analytically as

$$\overline{\gamma^2} = \overline{\alpha^2} + \overline{\beta^2} \quad 2.4-9$$

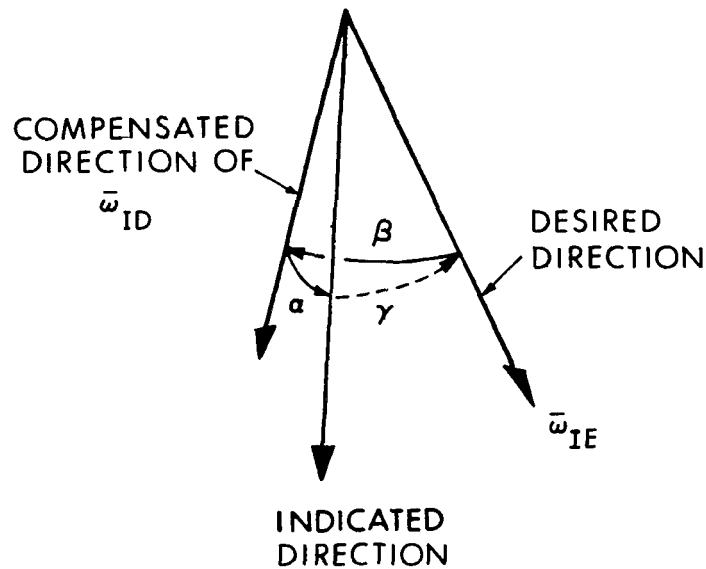


Figure 3-4 Geometric Quantities Relevant to Gyrocompassing

3.3.3 A Special One-Gyro Situation

An important gyrocompassing system mechanization^{1, 2, 17} relies upon accelerometer measurements to place the sensitive axis of a single gyroscope in the horizontal plane. The gyro axis is also adjusted in the plane until it detects no component of earth rate's horizontal component. By this process, the gyro's input axis indicates an azimuth line precisely 90° from true north.

In the context of Chapter II, this is a single instrument nulling on a vector component of magnitude $(\omega_{IE} \cos \lambda)$. From Table 2-3, the transducer error is described by

$$\overline{\alpha_T^2} = \left(\sigma_{a_0} / \omega_{IE} \cos \lambda \right)^2 \quad 3.3-9$$

This, however, is not the complete story. Whereas a sensor is insensitive to rotations about a vector, it is certainly sensitive to rotations about a component of a vector. A vertical error of θ_{Vn} about a north-south axis causes the gyro to sense a component of earth rate's vertical component of magnitude $(\theta_{Vn} \omega_{IE} \sin \lambda)$. Equation 3.3-9 is corrected to read

$$\overline{\alpha_T^2} = \left(\sigma_{a_0} / \omega_{IE} \cos \lambda \right)^2 + \theta_{Vn}^2 \tan^2 \lambda \quad 3.3-10$$

The total mean-square error in azimuth indication is given by

$$\overline{\theta_a^2} = \overline{\alpha_{sa}^2} + \overline{\alpha_T^2} + \overline{\beta^2} \quad 3.3-11$$

where $\overline{\alpha_{sa}^2}$ is the gyro's mean-square input axis uncertainty, $\overline{\alpha_T^2}$ is given by 3.3-10, and $\overline{\beta^2}$ is given by 3.3-5.

3.4 Star Tracking

Unless a star tracker is a necessary part of the carrying vehicle's navigation equipment, it represents equipment provided solely for alignment. This implies that measurements of the

dependent frame's inertial sensors are unable to provide a suitable alignment. The usual military application of star tracker alignment relates to aligning a pre-leveled inertial system in azimuth; this requires one star sighting. Full three axis alignment is possible with two star sights.

In spite of the numerous design options available in the system application of star trackers²⁵, the basic problem remains one of accurately determining the line of sight (LOS) to a star. The vector input to the star tracking process is electromagnetic in nature, coincident with the position vector from the star to the system. The line of sight is concerned only with this vector's direction. It is possible, with an appropriate star and tracker, to determine an LOS within several arc seconds, even in daylight.

The independent reference frame for star tracker alignment is the inertial frame. A star tracker can measure directly in this frame, thereby not requiring a master inertial system. With accurate time and position information, it is possible to translate the inertial frame measurements to an earth fixed reference frame.

Figure 3-5 (See also Figure 2-27) casts the star tracking problem in the context of Chapter II. The angle α is measured from the star line-of-sight to the tracker-indicated LOS. The angle β accounts for those situations (See Section 3.4.1 below) where the transfer of star LOS information to the inertial sensor package produces an apparent deflection in the indicated line-of-sight. The total error, γ , in measuring the star LOS is measured from the star LOS to the platform indicated LOS.

3.4.1 Discussion of β for Star Tracking

Reference 25 informs us that military-type applications usually do not allow star trackers to be platform mounted. This is normally a mission oriented constraint required to provide the

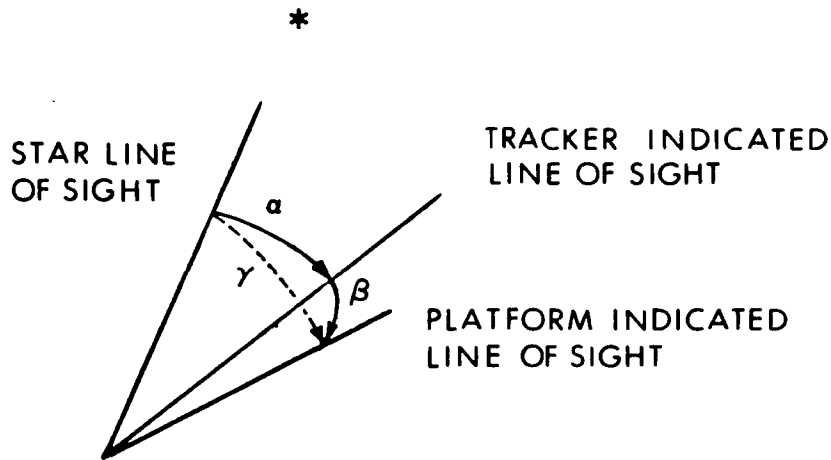


Figure 3-5 Error Geometry Appropriate to Star Tracking

tracker with an unobstructed view of the celestial sphere. As mentioned earlier, the technology is available (when the situation warrants) to provide values of α on the order of a few seconds of arc. Unless β is restrained to this same order of magnitude, it represents the limiting factor on star tracker azimuth.

A simple way to visualize β is to consider the whole angle description of the rotation between the dependent frame and a coordinate frame fixed in the case of the tracker. The projection of this angle along the indicated line of sight is of no consequence; the perpendicular component is the angle β . This presents us with a simple rule of thumb: when employing star trackers physically separated from the inertial sensors, the error due to this separation is reduced by placing the line of sight as nearly coincident with the principal flexure axis as possible.

β may contain significant static, quasi-static and dynamic portions. The static portion is a result of inaccurate installation of the tracker and system. It exists when, say, an aircraft is on the ground or a ship is in port. Quasi-static contributions to β arise from approximately constant angular deflections of the carrying vehicle related to the average stress condition changes induced by motion of the vehicle (e.g., aerodynamic loading of wings and pylons) and by environmental changes (e.g., thermal gradient loading). The dynamic portion of β is caused by excitation of the angular vibration modes of the craft. Total relative angular excursions between two points in the same vehicle may well be as large as 10^0 (Reference 3).

Since β is strictly an angle transfer problem, it is theoretically possible to compensate the non-rigid transfer medium by means of optical comparison between the tracker and inertial system. This compensation is attractive but is not without its practical problems (See Section 3.8).

In the absence of data which conclusively prove for a given application that β is either negligible or compensable by non-optical means, proposals to use a physically separate star tracker without optical compensation of flexural base motion should be viewed skeptically. When mission and economic constraints permit, alignment accuracies will be enhanced by mounting the star tracker integral with the inertial sensors. It is wasteful to measure quantities better than you can transfer the information about those quantities

3.4.2 Comment on β for Star Tracking

The basic optics and detector of a star tracker are the fundamental physical limitations on determining a line-of-sight. A frequently used figure of merit which describes this limitation²⁶ is called the "tracking accuracy." This accuracy number is identical with the parameter α .

Rotations about a starline cannot be distinguished by the combination of optics and detector. On this basis, the conical, constant probability density locus interpretations used in deriving α (Section 2.4.2.1) are a valid interpretation of fundamental star tracking limitations. The reader is cautioned, however, that the uniform statistics afforded by a vector viewpoint, when processed through angle transformations to obtain a component viewpoint, may lose the interpretation used in this thesis.

3.5 Fix Monitored Azimuth

Fix monitored azimuth is a method of employing checkpoint data to align a pre-leveled platform in azimuth. In common with all usages of checkpoint information* (position reference) to reduce the effects of system and component error sources, fix monitored azimuth (FMA) is completely dependent on the accuracy of a model. The fundamental premise of FMA is that azimuth misalignment is not only the dominant source of position error during the time interval considered but is also nearly constant in this period. Given this model, the principle of FMA is exceedingly simple.

A pre-leveled system, free from error in every respect except a fixed azimuth misalignment (θ_a), begins to navigate at station A (Figure 3-6) with the expectation of arriving at Station B.

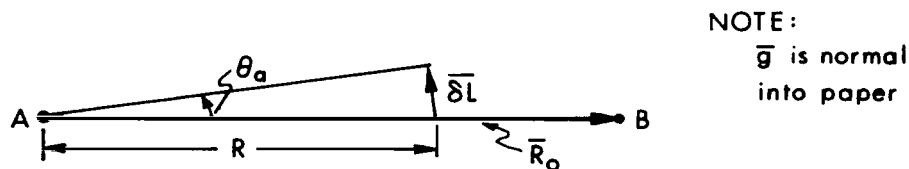


Figure 3-6 Lateral Error Propagation for Fixed Azimuth Misalignment

*Reference 5, pp 312 ff, presents a concise description of several uses of position references.

The range from A to B is R_0 . Due to θ_a , lateral position error propagates approximately as

$$\delta L = R\theta_a \quad 3.5-1$$

so that after navigating a distance R_0 the lateral error magnitude at station B is $R_0\theta_a$. By measuring $\overline{\delta L}$ at B and knowing the range vector \overline{R}_0 , the azimuth error existing at A is calibrated and may be corrected.

In the context of Chapter II, the lateral error vector $\overline{\delta L}$ is the input to the alignment process. From $\overline{\delta L}$ we infer the discrepancy between the nominal and actual navigation paths. The magnitude of $\overline{\delta L}_i$ specifies the magnitude of θ_a (equivalent to the general error parameter α) while the direction of $\overline{\delta L}_i$ relative to the range vector determines the sense of the required azimuth correction. The reference coordinate frame is that in which the checkpoints are known. For direct azimuth alignment with respect to the earth, the checkpoints are physical observables (e.g., terrain features, radio or radar beacons) of known location. There is no reason, however, why any point in space where the vehicle's position can be calibrated should not suffice for the FMA method.

Measurements of $\overline{\delta L}_i$ generally will be imperfect. This leaves a residual uncertainty in the corrected azimuth at each checkpoint. A powerful means of reducing certain measurement errors is to use multiple checkpoints. Let us now examine this.

Allow errors in the measurement of $\overline{\delta L}_i$ to be of the bias (a_0) and proportional (Δa_1) types. The residual azimuth error $(\Delta\theta_a)_i$ at the i^{th} checkpoint due to these error sources may be expressed as

$$(\Delta\theta_a)_i = \frac{a_0 + \Delta a_1 \overline{\delta L}_i}{R_{i-1,i}} \quad 3.5-2$$

Assuming that an azimuth misalignment estimate has been made at the previous (i-1) checkpoint, $(\Delta\theta_a)_i$ is actually the uncertainty in estimating the previous error $(\Delta\theta_a)_{i-1}$. δL_i may in fact, be expressed as

$$\delta L_i = R_{i-1, i} (\Delta\theta_a)_{i-1} \quad 3.5-3$$

As long as the proportional measurement error is dominant ($\Delta a_1 \delta L_i \gg a_0$) the azimuth uncertainty at the i^{th} checkpoint is written (from Equation 3.5-2).

$$(\Delta\theta_a)_i = \frac{\Delta a_1 \delta L_i}{R_{i-1, i}} \quad 3.5-4$$

Substituting 3.5-3 into 3.5-4 yields the simple recursion relationship

$$(\Delta\theta_a)_i = \Delta a_1 (\Delta\theta_a)_{i-1} \quad 3.5-5$$

Equation 3.5-5 is very significant. It implies that every time we make a misalignment estimate, we obtain a fixed percentage reduction in the error in our previous best estimate ($\Delta a_1 \ll 1$). Iterating 3.5-5 from the first checkpoint [initial azimuth error $(\theta_a)_1$] to the n^{th} checkpoint, the error in estimating $(\theta_a)_1$ depends only on $(\theta_a)_1$ and the number of checkpoints (See Equation 3.5-6).

$$(\Delta\theta_a)_n = (\Delta a_1)^{n-1} (\theta_a)_1 \quad 3.5-6$$

The reader is reminded that in going from the first to the n^{th} point we have only estimated azimuth (n-1) times.

The natural lower limit of this rapid convergence of the azimuth error is provided by the bias error (a_0) existing in the measurement of δL_i . When the lateral error is small enough so that bias becomes dominant, we see from Equation 3.5-2 that the

lower limit on azimuth correction is expressed as

$$(\Delta\theta_a)_i = \frac{a_0}{R_{i-1,i}} \quad 3.5-7$$

Note that this is a function only of the bias measurement error and the range between the last two checkpoints.

The convergence of the FMA process is so rapid that two or three inter-checkpoint legs suffice under most conditions to reach the bias limitation of 3.5-7. In the face of a 10% proportional measurement error, a 10^0 initial azimuth error is reduced to 6 arc-minutes after only two estimates. But on a 100 mile final leg, the bias error must be no greater than 150 feet to ensure azimuth alignment of 1 arc-minute. An arbitrary increase in $R_{i-1,i}$ would seem to reduce $(\Delta\theta_a)_i$ to an arbitrarily small level. The penalties here are two-fold. First, it is a severe operational restriction to require large inter-checkpoint distances. Second, as the time to complete the FMA process increases, the validity of the model deteriorates rapidly.

Let us examine this latter point briefly. If a constant, uncalibrated platform drift (D_v o/hr) exists about the vertical, the lateral error due to this drift propagates as

$$\delta L_i = 1/2 D_v t^2 \quad 3.5-8$$

If a small constant platform drift (D_R) exists about the range vector \overline{R}_O , the lateral error propagates as

$$\delta L_i = 1/6 D_R g t^3 \quad 3.5-9$$

For demonstration purposes, we sum the contributions of 3.5-3, 3.5-8, and 3.5-9 to δL_i .

$$\delta L_i \approx R_{i-1,i} (\Delta \theta_a)_{i-1} + 1/2 D_v t^2 + 1/6 D_R g t^3 \quad 3.5-10$$

If the vehicle maintains a roughly constant speed, V , the lateral error propagation due to azimuth error is proportional to the time elapsed between points (i-1) and (i). It should be clear that the model postulated for a system using FMA is valid for a restricted time interval; from 3.5-10, azimuth error is dominant over the drift sources only if

$$V(\Delta \theta_a)_{i-1} t_{i-1,i} > 1/2 D_v t^2 + 1/6 g D_R t^3 .$$

The higher the speed of the vehicle, the more applicable the technique. Fix monitored azimuth is basically a fast vehicle technique suggested for airborne missile applications.

Error sources other than system drift conspire to destroy the validity of the FMA model (e. g., a steady state vertical error about \overline{R}_O will cause an azimuth error to be introduced even if none existed previously). The foregoing examples were merely by way of illustration.

In this author's opinion the major deterrents to more widespread application of the fix monitored azimuth concept are

- 1) The severe operational requirements imposed by navigating a required course
- 2) The inherently long reaction time
- 3) The restricted validity of the model on which FMA is based

Mitigation of the first objection would be obtained by provision of a master inertial system whose continuous navigation outputs serve for checkpoint comparison at chosen intervals. This does not evade the other objections, however, leaving other master-slave configurations more desirable.

We present here for the sake of completeness a variation on the FMA procedure. It is a proposed means for the azimuth alignment of a pre-leveled aircraft navigator. Referring to Figure 3-6,

checkpoints A and B are at opposite ends of a calibrated runway. In other words, the direction of \bar{R}_O is calibrated relative to true north. If the pilot holds the course of the plane very close to \bar{R}_O during takeoff, then the average direction of the plane's horizontal acceleration is well-known. This is sensed by the navigator's accelerometers and used for alignment.

There are three basic error sources in this scheme. First, if the pilot misses the takeoff point (B) by an amount δL , the azimuth calibration is in error by

$$\theta_a = \delta L / R_O .$$

On a 10,000 foot runway this amounts to approximately 20 $\overset{\circ}{\text{sec}}$ per foot of lateral error. Secondly, even if the pilot passes directly over B, any lateral velocity is an indication that the average acceleration vector does not lie along \bar{R}_O . Thirdly, there is the limited ability of the navigator's accelerometers to locate the average acceleration vector (given by the angle α of Chapter II). It is relatively easy to measure and compensate for the first two errors but we do not wish to consider this scheme in further detail here. As with the basic FMA technique, it suffers from limited applicability

3.6 Vector Matching

3.6.1 "Memory" in Transfer Alignments

Vector matching is the first transfer alignment technique (See Section 3.1) we will consider. All transfer techniques are concerned with aligning a dependent reference frame to a pre-aligned intermediate frame. The inertial system associated with the dependent frame is often called a "slave", that associated with the intermediate frame a "master".

The analysis of transfer alignment errors relates to errors developed between the master and slave only. The master system is assumed perfectly pre-aligned to an independent

reference frame. Any error existing in the master's "memory" of the independent frame is necessarily transferred to the slave system. The total error in mechanizing a copy of the independent reference frame in a slave system is a linear superposition of the error in the master's memory and the error in aligning the slave to the master (See the functional diagram 2-1). A simple means of evaluating the total error for specific cases is by superposing the whole angle rotations representing master system drift and master-slave misalignment.

3.6.2 Vector Matching Theory and Mechanizations

The concept of vector matching is to constrain each of two systems to have an identical attitude relative to a common vector. Since the vector acts only as an intermediate variable, its orientation in the independent reference frame is not constrained (and β is automatically zero). In the case of inertial vectors this means we can utilize "any" acceleration vector, not just \bar{g} ; we can use "any" angular velocity vector, not just $\bar{\omega}_{ie}$. Gross motions of the carrying vehicle are turned to good advantage as generators of vector quantities measurable by the system's inertial sensors*; they are no longer interfering motions. Nominally horizontal acceleration or velocity change vectors can be generated for azimuth alignment purposes by simple vehicle heading changes.

Although the concept and basic mathematics of vector matching apply to every measurable vector (inertial, magnetic, electromagnetic) we restrict our attention to those measurable by inertial sensors**. Earlier analyses distinguish

* Sutherland²⁷ applies optimal linear estimation to maneuver determination for an airborne problem.

** The special case of "vector matching" by means of a light beam is discussed in Section 3.8.

between acceleration matching and velocity matching in a manner which implies the existence of fundamental differences. These differences are neither conceptual nor mathematical. The vector \bar{V} discussed in the following development represents any vector, be it acceleration (linear or angular) or velocity (linear or angular). Any and all differences must lie in

- 1) the ability to generate a particular vector
- 2) the instruments available to measure vector quantities
- 3) the resolution of the instruments.

The mechanization of vector matching takes several forms. These are well illustrated by the two-dimensional problem of Figure 3-7, corresponding to the historically important case of two platforms which have already been erected to the vertical (i. e., Z axes coincident) by some prior operation and which are to be accurately aligned in azimuth by means of a vector matching procedure. If the two equivalent coordinate frames X_1-Y_1 and X_2-Y_2 are identically aligned to the vector \bar{V} (but not necessarily about the vector*), the magnitudes of the components of the vector measured along corresponding instrument axes will be equal. Conversely, when the coordinate frames are misaligned (by the angle $\phi_x = \phi_y = \phi$) the measured components will be different. Constraining the measured magnitude components to be equal by slewing the slave system results in proper alignment. This mechanization seeks to zero the orthogonal magnitude differences:

$$\Delta V_x = V_{x1} - V_{x2} = V \left[\cos \psi - \cos (\psi + \phi) \right] \quad 3.6-1a$$

or

$$\Delta V_y = V_{y1} - V_{y2} = V \left[\sin \psi - \sin (\psi + \phi) \right] \quad 3.6-1b$$

*Alignment about \bar{V} is achieved by vertical erection.

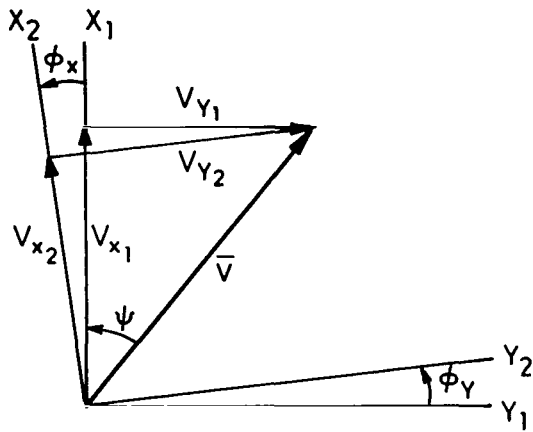


Figure 3-7 Geometry for Azimuth Alignment by Vector Matching.

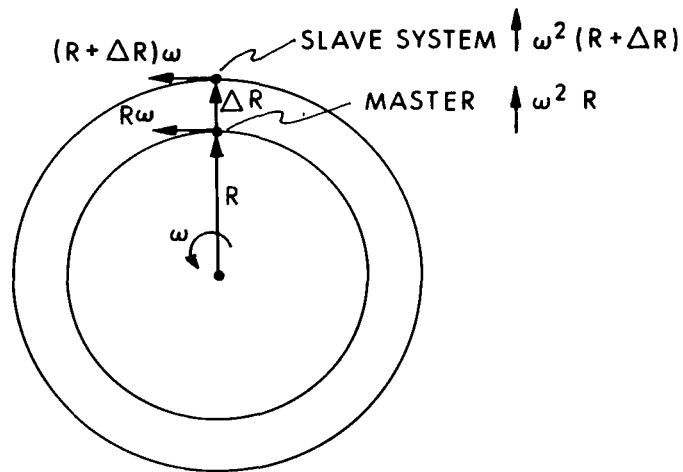


Figure 3-8 Different Magnitude, Parallel Direction Accelerations and Velocities Sensed by Two Systems on a Common Base

where $V \equiv |\bar{V}|$. Applying Taylor's series expansions about ψ to Equation 3.6-1 yields to first order in ϕ

$$\phi \simeq \frac{\Delta V_x / V}{\sin \psi} = \frac{\Delta V_x}{V_{y_1}} \quad 3.6-2a$$

or

$$\phi \simeq \frac{\Delta V_y / V}{\cos \psi} = \frac{\Delta V_y}{V_{x_1}} \quad 3.6-2b$$

Due to measurement errors, ΔV_x and ΔV_y will generally have non-zero minima with a corresponding residual misalignment. To the extent that there are equal irreducible minima in the x and y channel measurements (i. e. $\Delta V_x = \Delta V_y = \Delta V$), it becomes obvious that a judicious choice of the mechanized difference quantity guarantees a maximum azimuth misalignment of

$$\phi_{\max} = \sqrt{2} \frac{\Delta V}{V} \quad 3.6-3$$

This occurs at $\psi = 45^\circ$ and agrees with a basic result of Chapter II. Equation 2.4-71 shows that independent of the vector matching mechanization, the error of each system in determining the direction of \bar{V} is maximum at $\psi = 45^\circ$.

There may be situations where it is more advantageous to numerically evaluate the misalignment angle rather than eliminate it by a continuous difference technique. The computed angle may then either be (1) stored within the system computer and accounted for in all subsequent computations or (2) torqued out by a precision torquing procedure. Equation 3.6-4 evaluates ϕ in terms of measured magnitude components.

$$\phi = \left[\psi + \phi_x \right] - \psi = \tan^{-1} \frac{V_{y_2}}{V_{x_2}} - \tan^{-1} \frac{V_{y_1}}{V_{x_1}} \quad 3.6-4$$

3.6.3 Compensation for Platform Separation

It has been shown in Chapter II that alignment requires finding vector directions; magnitude measurements may be a means to that end (e. g., Equations 3.6-1 and 3.6-4). A physical separation of two inertial systems attached to the same vehicle can cause both magnitude and direction differences in the maneuver-generated vector as sensed by each system.

Consider as an example a vehicle traveling in a perfect circle (Figure 3-2). The magnitude of the centripetal acceleration sensed by two systems separated a radial distance ΔR differs by an amount $\Delta R\omega^2$ even though the sensed vectors are collinear. Similarly, the tangential velocity vectors differ in magnitude by $\Delta R\omega$ even though the sensed vectors are parallel. If the separation were tangential rather than radial, and both systems were equidistant from the center of rotation, then the magnitudes of the sensed vectors would be identical but their directions would differ.

Directional differences must always be compensated; magnitude differences, when employing schemes such as 3.6-1 and 3.6-4, must also be compensated. This is readily accomplished by measurements of the master system together with information on relative system locations.

3.6.4 The Vector Match Vertical - A Fallacy

The existence of a pre-aligned master system which can calibrate horizontal accelerations of a vehicle presents a strong temptation to establish vertical alignment by vector matching in the horizontal plane. The following statement should therefore be read carefully: It is impossible to achieve accurate vertical alignment by acceleration matching in the horizontal plane unless an accurate azimuth alignment has been established first. This is simply because a component of \bar{g} projected on an axis due to vertical error is indistinguishable from a projected component of horizontal acceleration. Yet both are subject to the same

interpretation, namely vertical error. Only if azimuth alignment is perfect will the horizontal acceleration components sensed by the master and slave be equal and cancel when component differences are examined.

The basic fallacy arises because we are dealing with components of a single vector. As discussed in Chapter II, sensors are only insensitive to rotations about the total vector. Rotations about one component are still sensitive to the orthogonal components, posing the problem of ambiguous data which must be resolved by other measurements. When dealing with components of a vector, one must keep track of all the components at all times.

Although vertical erection by vector matching in the null plane of \bar{g} has been shown improper, it is correct to consider the normal vertical erection process as a vector matching process in that one attempts to match the best estimate of the position of the gravity vector to a pre-determined attitude. It differs from the ordinary concept of vector matching in two ways: 1) the vector is naturally existing and 2) the desired relative orientation is known with respect to an independent reference frame, removing the need for a master system.

It follows from this latter property that the possibility exists to require no data transfer link between master and slave platforms during a vector matching alignment, even though the vector is artificially induced. This requires that the orientation of the vector be tightly controlled to a pre-determined orientation with respect to the master system reference axes. Since the vector is induced by a maneuver of the carrying vehicle, this is tantamount to precision control of the vehicle's dynamic path. A well known example of this type of control is maintaining the thrust vector of a missile through its center of gravity while adjusting the missile attitude with respect to the thrust vector.

The simplicity and reliability gained by use of this approach are due mainly to a reduction in data paths and system interconnections. These advantages come only at the high cost of an absolute restriction on discretionary maneuvers of the vehicle pilot or controller during the alignment period. The accuracy of alignment obtained with communication between master and slave would be somewhat degraded by discretionary deviations from a prescribed maneuver pattern but this error would be bounded; without master-slave communication the error is obviously unbounded.

3.6.5 General Formulation of Vector Matching

A single vector match is capable of fixing two degrees of angular freedom. The solution of the azimuth alignment problem by vector matching, since it reduces only one degree of angular freedom, is a special case. We investigate here the more general vector matching problem.

As shown previously, the inability of a system of sensors to perfectly indicate the direction of an existing physical vector can be resolved into a single normalized error angle, α . When the measurement apparatus is not directionally constrained about the measured vector, the constant probability density error locus is a cone of half-angle α (Figure 3-9a). The tip of the mis-indicated vector describes a circle in a plane normal to the measured vector. All points on this circle have a constant probability density. Normalizing the measured vector sets the circle's radius at α .

For separate systems using different instruments, the descriptions of the errors made in measuring the direction of the match vector have the identical geometrical interpretation and, insofar as the effects of environment can be ignored, are statistically independent. Assuming that the corrections have been made to ensure collinearity of the normalized match vector (Section 3.6.3) at all systems, the complete error analysis for

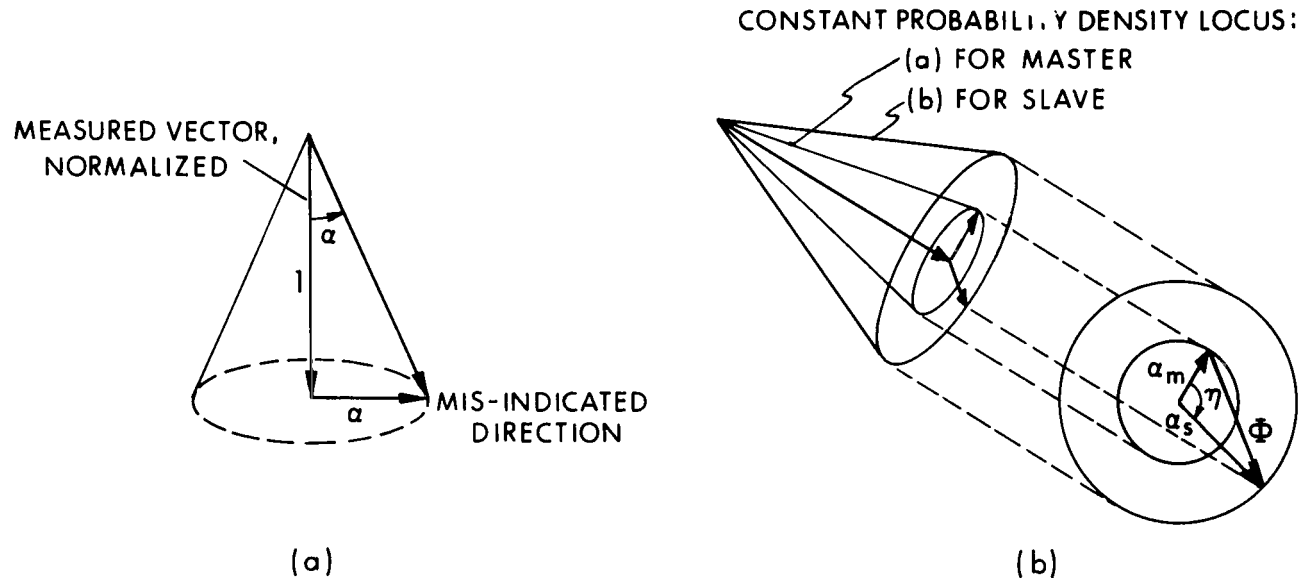


Figure 3-9 Error Geometry for Vector Matching

n systems may be carried out in a plane diagram consisting of n concentric circles centered about the match vector. The case of greatest practical interest is n = 2, which describes the alignment of a single slave to the master. The resultant misalignment Φ between the dependent and intermediate frames for this case is defined in Figure 3-9b. The angle η is identifiable as the difference of two independent angles, each uniformly distributed on 0-2 π . Application of the law of cosines to Figure 3-9b yields:

$$\Phi^2 = \alpha_m^2 + \alpha_s^2 - 2\alpha_m \alpha_s \cos \eta \quad 3.6-5$$

the statistics of which are evaluated in Appendix B with the results

$$\text{Mean Value: } \overline{\Phi} = \frac{2}{\pi} [(\alpha_m^2 + \alpha_s^2) \mathcal{E}(k^2)] \quad 3.6-6$$

$$\text{Mean Squared Value: } \overline{\Phi^2} = \overline{\alpha_m^2} + \overline{\alpha_s^2} \quad 3.6-7$$

where $\mathcal{E}(k^2)$ is a complete elliptic integral of the second kind and

$$k^2 = \frac{4\alpha_m \alpha_s}{(\alpha_m + \alpha_s)^2} \quad 3.6-8$$

Equation 3.6-6 cannot be further evaluated without complete knowledge of the probability density functions for α_m and α_s .

In keeping with the precedent established in Section 2.4.2.1., we will use the mean square misalignment as our performance index.

The master system will ordinarily make more accurate measurements than the slave, i. e. if we make the identification

$$\overline{\alpha_s^2} = q^2 \overline{\alpha_m^2} \quad 3.6-9$$

then $q \geq 1$. q may be thought of as a quality factor or figure of merit upon which systems are compared. It relates the RMS total vector measurement capability of systems of sensors as a

function of measurement method, number of sensors and quality of the sensors. q is very simply calculated by using Equation 2.4-49, Tables 2-2 and 2-3, and a little algebra. The mean-square misalignment resulting from a vector match is expressed as a function of q and the measurement capability of the master system as

$$\overline{\Phi^2} = (q^2 + 1) \overline{\alpha_m^2} ; \quad q \geq 1 \quad 3.6-10a$$

or in terms of RMS quantities

$$\frac{\text{RMS } \Phi}{\text{RMS } \alpha_m} = (q^2 + 1)^{1/2} ; \quad q \geq 1 \quad 3.6-10b$$

Note, for example, that with identical instrument configurations in the master and slave but with an across the board order-of-magnitude saving in instrument quality ($n = 10$) in the slave, the contribution of the master system to the total misalignment is almost negligible.

In order to consider full three degree-of-freedom alignment by two vector matches, one merely obtains the angle Φ for each of the vector matches and uses the results of Section 2.4.3 to calculate a composite misalignment for the entire system.

3.7 Gimbal Angle Matching

The generic term "gimbal angle matching" implies the comparison of signals from the attitude readout systems of each of two (or more) inertial platforms in order to bring the orientations of their stable members into angular coincidence. Here, as in all methods involving comparison, the inertial orientation of one platform (master) is taken as an absolute reference and all errors in alignment of the second platform (slave) are with respect to this reference. Since the only controlled function is the orientation of each system's stable member with respect to the base on which it is mounted, there is a strong dependence on the

fidelity of reference information transmission by the base. This dependence is the most significant limitation of gimbal angle matching. Knowledge of this limitation is not new. The method of developing it here, however, is a new approach.

Although a definite aid in the visualization of gimbal angle matching, there is no requirement that the systems have identical gimbal arrangements, nor must they even have an equal number of gimbals. Accurate computation of appropriate constant trigonometric transformations of the attitude drive signals is technologically feasible and can adequately compensate for this difference. The treatment of any desired non-coincident axis orientation follows similarly. An example of the latter situation is the alignment of a preferred-axis-orientation missile platform to a carrying vehicle's geographically oriented navigational platform.

Gimbal angle matching is the only alignment technique discussed in this thesis which is not applicable to "gimbal-less" or "strapdown" inertial measuring units. For what insights it may provide, however, the forthcoming analysis does apply to strapdown systems if the transformations T_1 and T_2 are replaced by the identity matrix.

3.7.1 Coordinate Transformations

Referring to Figure 3-10, an arbitrarily chosen set of orthogonal axes associated with the stable member of the dependent system is related to an orthogonal coordinate frame in its base by

$$\begin{bmatrix} d'_1 \\ d'_2 \\ d'_3 \end{bmatrix} = \begin{bmatrix} \\ \\ T_2 \\ \\ \end{bmatrix} \begin{bmatrix} d_1 \\ d_2 \\ d_3 \end{bmatrix} \quad 3.7-1$$

and further related to the coordinates at the base of the reference system by

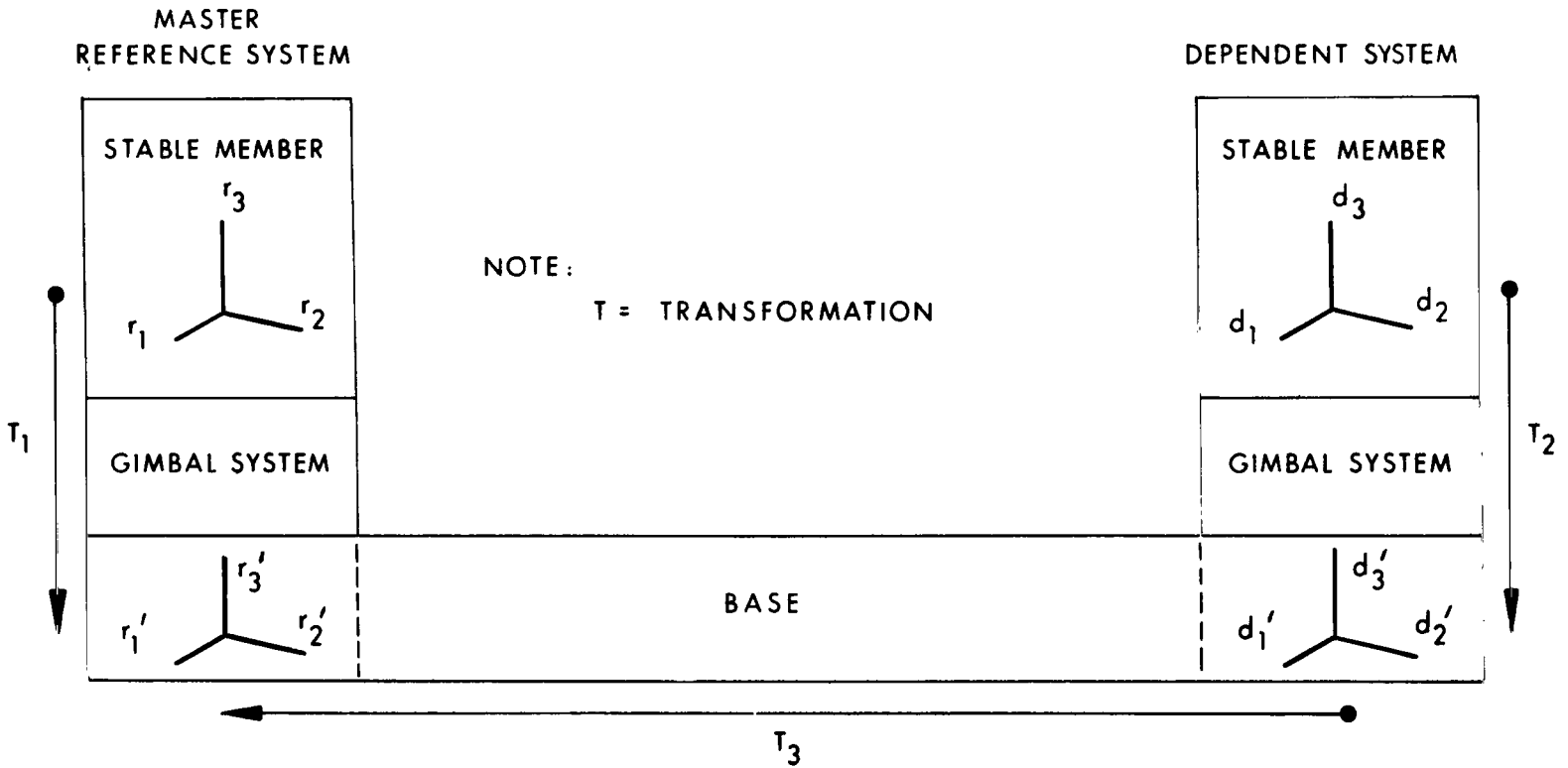


Figure 3-10 Symbolic Diagram of Gimbal Angle Matching Transformations

$$\begin{bmatrix} r_1 \\ r_2 \\ r_3 \end{bmatrix} = \begin{bmatrix} T_3 \end{bmatrix} \begin{bmatrix} d_1 \\ d_2 \\ d_3 \end{bmatrix} = \begin{bmatrix} T_3 \end{bmatrix} \begin{bmatrix} T_2 \end{bmatrix} \begin{bmatrix} d_1 \\ d_2 \\ d_3 \end{bmatrix} \quad 3.7-2$$

where T_2 and T_3 are square matrices of order three. For the master system we may write

$$\begin{bmatrix} r_1 \\ r_2 \\ r_3 \end{bmatrix} = \begin{bmatrix} T_1 \end{bmatrix} \begin{bmatrix} r_1 \\ r_2 \\ r_3 \end{bmatrix} \quad 3.7-3$$

Equating 3.7-2 and 3.7-3

$$\begin{bmatrix} T_1 \end{bmatrix} \begin{bmatrix} r_1 \\ r_2 \\ r_3 \end{bmatrix} = \begin{bmatrix} T_3 \end{bmatrix} \begin{bmatrix} T_2 \end{bmatrix} \begin{bmatrix} d_1 \\ d_2 \\ d_3 \end{bmatrix} \quad 3.7-4$$

relates the stable member coordinates of the two systems. The elements of T_1 and T_2 are functions of their respective system's attitude signals and possibly some constants; the elements of T_3 are functions of the parameters chosen to describe flexure of the base. This flexure may be divided into quasi-static and dynamic parts. The quasi-static flexure is an approximately constant deformation of the base which varies with the average stress conditions induced by conditions of motion. The "droop" of an aircraft wing as a function of fuel load, speed, etc. is an example of quasi-static flexure. All other base flexure constitutes the

dynamic portion. In addition to parameters of flexure it is convenient to include in the matrix T_3 those constants necessary to describe the initial relative misalignment of the bases occurring at the time of system installation.

Premultiplying both sides of 3.7-4 by the inverse of T_1 (denoted by T_1^{-1}) yields the more useful and traditional representation of gimbal angle matching

$$\begin{bmatrix} r_1 \\ r_2 \\ r_3 \end{bmatrix} = T_1^{-1} T_3 T_2 \begin{bmatrix} d_1 \\ d_2 \\ d_3 \end{bmatrix} \quad 3.7-5$$

where the unbracketed letters T_i represent the previously introduced 3×3 matrices. Without loss of generality we may assume that the desired alignment corresponds to parallelism between (r_1, r_2, r_3) and (d_1, d_2, d_3) respectively and also between (r'_1, r'_2, r'_3) and (d'_1, d'_2, d'_3) . Any transformation required to force the physical situation into agreement with this condition is constant, is assumed arbitrarily accurate, and hence does not enter the ensuing error analysis.

3.7.2 Error Analysis

The condition of angular coincidence between the two stable members is mathematically defined by

$$T_1^{-1} T_3 T_2 = I \quad 3.7-6$$

where I is the identity matrix. Under the simplifying restrictions of Section 3.7.1 and temporarily neglecting errors in the attitude systems we may specialize 3.7-6 to require

$$T_1 = T_2 \quad 3.7-7a$$

$$T_3 = I \quad 3.7-7b$$

With 3.7-6 and 3.7-7 as our definition of the desired alignment, we proceed to investigate the errors inherent in gimbal angle matching. The whole angle rotation concept of Chapter II will be useful here.

It is convenient to define the two attitude systems by

$$T_1 = T_1' + \epsilon_1 \quad 3.7-8a$$

$$T_2 = T_2' + \epsilon_2 \quad 3.7-8b$$

where a primed transformation corresponds to the ideal commanded attitude of a stable member and ϵ accounts for the difference between the actual and commanded attitudes caused by imperfect attitude readout equipment and imperfect attitude drives. The "matched" condition 3.7-7a is now $T_1' = T_2'$ and 3.7-8b may be written as

$$T_2 = T_1' + \epsilon_2 \quad 3.7-9$$

or using 3.7-8a

$$T_2 = T_1 + (\epsilon_2 - \epsilon_1) \quad 3.7-10$$

Substituting 3.7-10 into 3.7-5 gives

$$T_1^{-1} T_3 T_1 + T_1^{-1} T_3 (\epsilon_2 - \epsilon_1) \equiv T_{1-2} \quad 3.7-11$$

as the transformation between stable member coordinates when flexure of the base and an imperfect attitude system are considered. The transformation T_{1-2} is constrained to be orthogonal.

By Equation 2.4-15, the magnitude of the whole angle rotation described by T_{1-2} is evaluated from the trace of T_{1-2} .

Since the trace of a sum of matrices equals the sum of the traces of each matrix, the error contribution of each term of 3.7-11 to Φ may be calculated separately. For the first term of 3.7-11

$$\text{tr } T_1^{-1} T_3 T_1 = \text{tr } T_3 \quad 3.7-12$$

This follows by application of the similarity argument developed in Equations 2.4-12 through 2.4-15. The physical implication of this result is that for assumed perfect attitude systems ($\epsilon_1 = \epsilon_2 = 0$) the misalignment angle magnitude is only a function of the parameters of the base and the initial installation. This rather simple (but important) insight is emphasized by using the whole angle rotation for the error parameter. Although it is frequently a matter of engineering practice to neglect attitude system errors in the face of much greater base flexure errors, the alignment errors are still calculated as a function of the gimbal angles³. This results from carrying out the multiplication $T_1^{-1} T_3 T_2$ to obtain the direction cosines relating stable member reference axes and a subsequent appropriate combination of these elements to obtain azimuth and vertical errors. All that is accomplished by this lengthy calculation is to find one particular coordinatized representation of the basic misalignment angle Φ . Concern with the mathematical processes involved in multiplying three square third order matrices and the complexity of the resulting trigonometric error expressions can easily obscure the simple geometry of the problem. The misalignment angle and the axis about which it is defined can be determined by reference to the base alone and then treated as geometric entities in space. The reduction of this error into components in a particular coordinate system then proceeds directly without requiring reference to intermediate quantities. If the error axis is visualized as fixed in the carrying vehicle (base) and the attitude of the vehicle is specified with respect to a reference set of navigational coordinates then the decomposition

of the alignment error into components in the reference frame follows in a straightforward manner. This approach permits visualization of the change in alignment error as a function of vehicle attitude without resort to the substitution of "representative" numbers into a complicated trigonometric expression in order to further understanding of the result.

Perhaps more importantly, it suggests the possibility of dynamically compensating the errors due to installation and flexure. The measurement of inter-base angular phenomena could be achieved by an optical calibration link, such as a three-axis auto-collimation device which requires but a single light path. The cost-penalty of introducing equipment related only to alignment is minimized by affixing the relatively inexpensive passive portion of such systems to the dependent system. The more expensive active mechanism remains with the carrying vehicle. Because the link is between bases fixed relative to the vehicle, turns of the vehicle do not disrupt the optical path.

In the absence of a means for real-time base motion calibration, the accuracy realizable by gimbal angle matching is, for most vehicles, very crude (on the order of degrees). This technique then finds application only as a rapid, coarse alignment preceeding some other more accurate technique. The error bound for gimbal angle matching is then determined by the uncalibrated static and quasi-static portions of $\text{tr } T_3$; the dynamic portion of $\text{tr } T_3$ may be eliminated by filtering.

If compensation of $\text{tr } T_3$ is achieved to the order of a minute of arc or so, one must then undertake the algebra associated with the attitude system contribution to the total misalignment, Φ . From Equations 2.4-15 and 3.7-11 the relationship is

$$\cos \Phi = 1/2 \left[\text{tr } T_3 + \text{tr } T_1^{-1} T_3 (\epsilon_2 - \epsilon_1) - 1 \right] \quad 3.7-13$$

While evaluating $\text{tr } T_1^{-1} T_3 (\epsilon_2 - \epsilon_1)$ involves considerably more algebra than calculating $\text{tr } T_3$, it is only one third the work of calculating the triple matrix product $T_1^{-1} T_3 (\epsilon_2 - \epsilon_1)$.

3.7.3 An Observation Regarding System Installation

An observation regarding system installation on board a vehicle is prompted by the whole angle treatment. First, there are certain guidance system designs which can tolerate a cruder alignment about one axis than about the others. Second, the axis of the whole angle misalignment will have a statistically preferred location relative to the flexural mode axes of the vehicle. If the system axis mentioned above and the predominant flexural mode axis are made parallel, the alignment problem is reduced. This may require, however, that the platform be torqued to a different orientation prior to inception of a mission.

3.8 Optical Alignment

Optical alignment techniques are inherently very accurate, very rapid and simple in concept. They have proved their merit at fixed launch sites, particularly for azimuth alignment. In the moving base environment, they are an apparently attractive means for providing one, two or three axis alignment of a dependent frame to an intermediate frame (i. e., slave to master).

Optical comparison techniques circumvent the structural deflections of non-rigid bases. This is accomplished by establishing a light beam as a common reference between the systems. Provided a beam can be maintained between the master and slave systems, the systems need not even be carried aboard the same vehicle; the orientation of each is slaved to the electromagnetic vector. In truth, however, sufficient practical limitations exist that optical alignment on a moving base is normally dismissed as an impractical application. To this author's knowledge it has only been operationally employed in the submarine environment.

Not the least of the problem areas is the provision of a line-of-sight between the systems. Permanent obstacles require that the beam containing alignment information be directed around these obstacles. The use of prisms, mirrors or periscopes to direct the beam will reintroduce to some degree the very structural deflections of the base we are seeking to circumvent. Additionally, even in the absence of structural deflection every reorientation of the beam is accomplished at the expense of angular error and light loss. Personnel and portable equipment must also be kept out of the beam's path. This might prove a very unwelcome restriction on an aircraft carrier's flight deck. As with all alignment schemes, operational requirements and restrictions are a major basis for the pre-selection of feasible techniques.

The necessary provision of a suitable angular range is a significant restriction. A sufficient "window" must exist to 1) allow initial acquisition of the reflected beam and 2) maintain the beam, once acquired, in the face of angular vibrations of the vehicle. At least one application (Reference 3) foresees a 10° Master-Slave deflection. In an auto-collimating system, the angular range decreases as the separation of monitoring and monitored positions increases (See Figure 3-11).

The feasibility of slaving one stable platform to another utilizing polarized light techniques has been demonstrated on a limited scale²⁸. Although this procedure replaces the imaging problem of auto-collimation with simple light gathering, it is still restricted as to field of view. Both auto-collimating²⁹ and polarized systems²⁸ now have the ability to transmit three axis information over a single light path.

The heading of the vehicle carrying the two inertial systems must normally be restrained while employing optical alignments. As shown in Figure 3-12, unless the stable members of both the

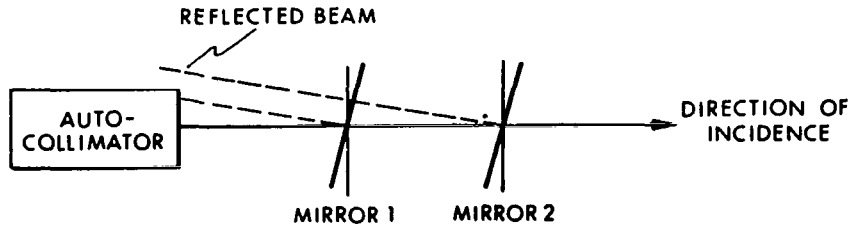


Figure 3-11 Demonstrating the Angular Range Decrease with Linear Range Increase for a Fixed Autocollimator

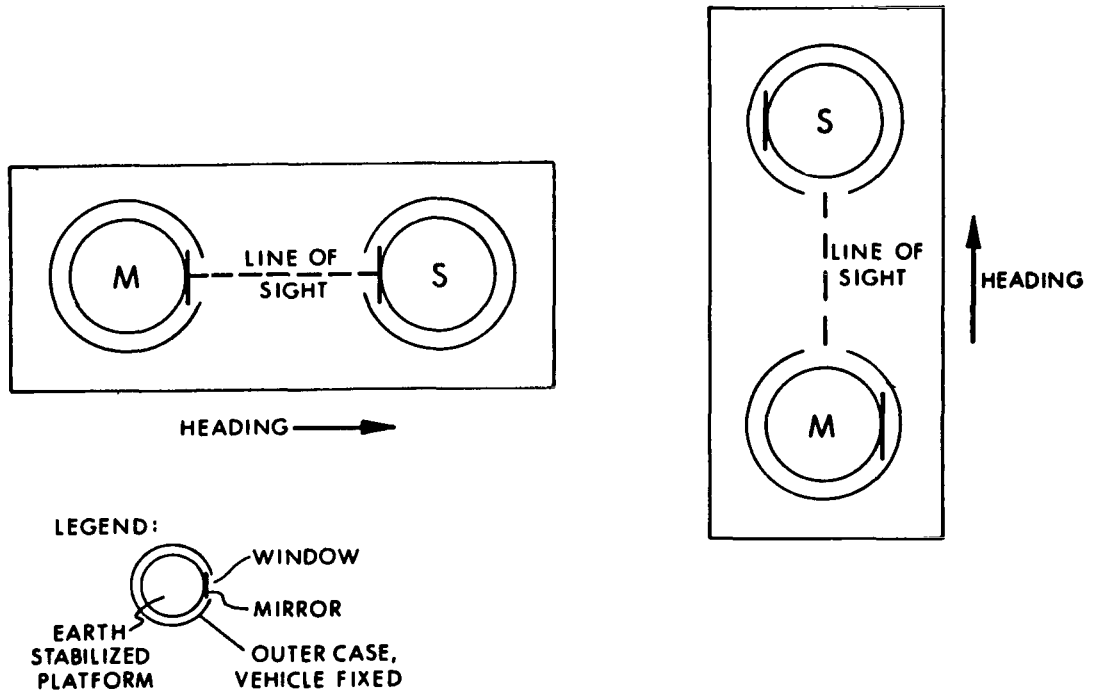


Figure 3-12 Demonstrating Loss of Mirror Line of Sight Under Heading Change

master and slave are caged to the vehicle structure during turns, it is impossible to keep the two mirrors in view. The caged mode of operation is an extremely unlikely one for a master navigator. If we are considering strapdown systems, of course, no restriction on the heading of the vehicle is necessary.

The accuracy achievable with optical slaving depends on the equipment selected, the maximum range, and the operating environment (windows, thermal gradients, vibration, etc.). Accuracies generally range from a few seconds of arc to about one minute of arc per axis. Equivalent whole angle misalignments are calculable from the formulas of Section 2.4.1 when a comparison with other schemes is desired.

3.9 Summary

The major accomplishments of this chapter are:

- 1) Presentation of the basic theory of seven distinct alignment measurement techniques;
- 2) Demonstration of the capacity of the unified alignment theory of Chapter II to properly include all the techniques;
- 3) Exposition within the context of Chapter II of the fundamental sensor and base motion limitations on alignment accuracy.

It has been shown for three of the direct measurement techniques (vertical indication, gyrocompassing, and star tracking) that base motion is responsible for an apparent deflection of the measured vector relative to the independent frame. Those filtering and compensation techniques required to restore a meaningful direction to the measured vector have been enumerated.

The fourth direct measurement technique (fix monitored azimuth) has been shown to successfully circumvent the problem of vector deflection by choosing to measure an earth referenced position vector. However, operational constraints, the time-limited validity of its basic model and its reliance on special equipment conspire to reduce its applicability.

The transfer techniques have been shown to circumvent the vector deflection problem by employing a master reference system. The vector inputs, rather than possessing an a priori significance in an independent frame, are calibrated by the master system.

In the case of vector matching, the instrument limitations have been shown to be of the same form as for vertical indication or gyrocompassing. The error magnitudes, however, vary with the amplitude of the match vector; the selection of a technique has set β to zero.

Angular deflections of the vehicle have been shown to limit the accuracy of gimballed angle matching. Although an old result, this was derived in a new fashion and provided additional insights regarding preferred installations.

Optical comparison techniques have been shown to circumvent the angular deflections of non-rigid vehicles. The only drawbacks to this technique, other than linear and angular range limitations, have been described as operational in nature. It remains, where feasible, an extremely attractive technique.

There has been introduced in Section 3.6 an important, relative-quality factor, q . This factor describes the relative sensor limited capability of systems of sensors to indicate the direction of a common vector. That it can be easily calculated for sensors of varying performance, non-identical configurations and varying orientations of the sensor configurations relative to the vector input is a result of the consistent error format of Chapter II.

CHAPTER IV

EXAMPLES OF UNIQUE OPERATIONAL SITUATIONS

4.1 Introduction

Two examples of unique operational situations are discussed in this chapter. The first case, that of simultaneously aligning several dependent systems in an airborne environment, reveals that measurements of a common input by multiple systems promises no simple improvement in the alignment of these systems over that obtained independently. The second case, that of aligning aircraft navigation systems on a carrier at sea, demonstrates the degree to which operational considerations act as a pre-filter on any alignment procedure selection.

4.2 Multiple Airborne Systems

A useful concept in weapons systems technology is that of a highly maneuverable aircraft capable of employing multiple missiles. The independent alignment of each missile's guidance system relative to a master system or to an independent reference frame follows straightforwardly from the techniques of the preceding chapter. We now inquire whether the simultaneous alignment of several systems is advantageous from the viewpoint of improving the alignment accuracy of each individual system.

This question is most relevant to the simultaneous alignment of n systems by measurement of a common physical vector, \bar{V} (See Fig. 4-1). It is perfectly true that this provides n independent measurements of a single quantity. It is also well known that multiple measurements of a scalar quantity reduce the effect of noise (or error) in the measurement process. To the extent

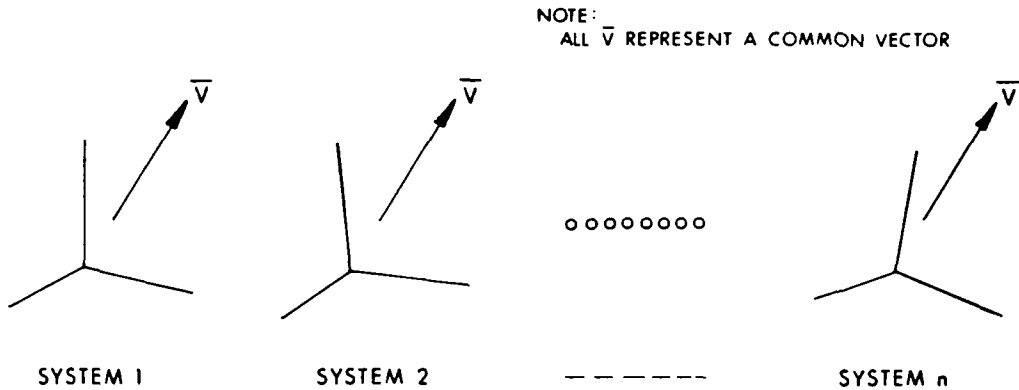


Figure 4-1 Measurement by n Systems of One Vector

that the errors in each measurement are independent and that their variances are equal. (i. e. "identical systems") the variance in the sample mean of a scalar quantity is reduced by $1/n$. Let us see how this applies to the case at hand, namely multiple measurements of a vector quantity.

The important parameters of \bar{V} are its magnitude, V , and its direction. V is not only scalar, it is invariant under coordinate transformations. Therefore, the measurements of V by each system represent independent estimates of the same quantity. Simple averaging provides an improved estimate of V which is meaningful to each system; the magnitude estimation capability of each individual system, however, has not been improved at all. Overall knowledge of V is improved only because the invariance of V under coordinate transformation makes the measurement of V independent of the frame of reference.

The direction of \bar{V} must be estimated in order to determine alignment. Although the direction of \bar{V} is representable by scalar quantities, these scalars (as opposed to V) are not invariant under a coordinate transformation; direction (i. e., alignment) is a relative quantity. Different systems' measurements of the direction

of \bar{V} are statistically independent estimates of unrelated variables. The fact that a common vector is being measured fails, in this case, to establish any dependency among the measurements. In the absence of additional measurements to establish some dependence among the variables, multiple alignment does not hold forth the promise of a simply achieved improvement in alignment accuracy (as by averaging measurements or "voting").

There is yet another reason why additional measurements are required to improve alignment accuracy. In the measurement of V , the quantity of interest (magnitude) is a physical observable. In the measurement of the direction of \bar{V} , however, the misalignment angle α is not a physical observable. Thus, the additional measurements required to improve alignment accuracy not only introduce some dependence among the variables but also serve the more basic purpose of rendering α physically observable.

In answering whether the simultaneous alignment of several systems is advantageous from the viewpoint of improved alignment accuracy for each system, we summarize here as follows:

- 1) The existence of a single vector which is measured by several systems allows us to improve easily our knowledge of the vector's magnitude but not of its direction; hence, alignment is not automatically improved by the existence of multiple systems measuring a common input.

- 2) Misalignments can be reduced by means of additional measurements.

The available magnitude improvement suggests the possibility of performing an on-board calibration of certain sensor coefficients. (There is a brief calibration discussion in Appendix A.) An improved knowledge of sensor coefficients, of course, implies an improved alignment capability. The precise feasibility

of this calibration and the operational restrictions required to achieve it will be revealed only by a detailed analysis of specific situations. This is not considered further here.

Let us consider, by means of a simplified example, an additional measurement which does make it possible to decrease the alignment uncertainty of each system. (Because each missile is likely to be separately targeted, an improved composite estimate of misalignment is valueless unless it provides the means to upgrade each system's alignment.) Consider the plane case of Figure 4-2, where each system's misalignment is described by α_i . Although α_1 is not a physical observable, we wish to reduce its variance by measurements additional to those of the vector. The additional measurement we choose is the $\theta_{i-1, i}$ between two systems' independent indications of \bar{V} . Note that if n is even, only $n/2$ additional measurements are implied. These measurements are between missile systems, not between the missile and a master or missile and the independent frame. When the missiles are close together, as in a magazine, this angle may be relatively easy to measure. We consider only the pair of systems shown in Figure 4-3 and assume the α_1 and α_2 have a known covariance matrix and a zero mean. The measurement of θ is imperfect, being corrupted by additive noise v of zero mean value and known variance σ_v^2 . v is independent of α_1 and α_2 .

Prior to measuring θ , our best estimates of α_1 and α_2 are zero (their means) with errors in these estimates whose variances are $\sigma_{\alpha_1}^2$ and $\sigma_{\alpha_2}^2$ (the variances of the alignment errors). After we measure θ and create new estimates $\hat{\alpha}_1$ and $\hat{\alpha}_2$ of α_1 and α_2 , the variances of the errors in our estimates of the misalignments are given by the results of Appendix D as

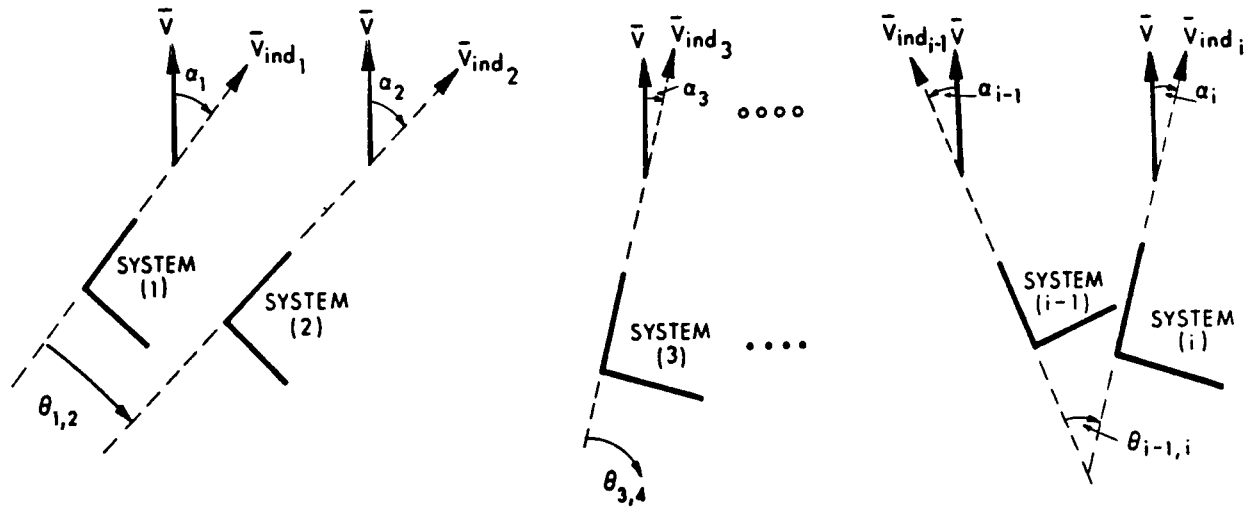


Figure 4-2 Definition of the Measured Angles $\theta_{i-1, i}$

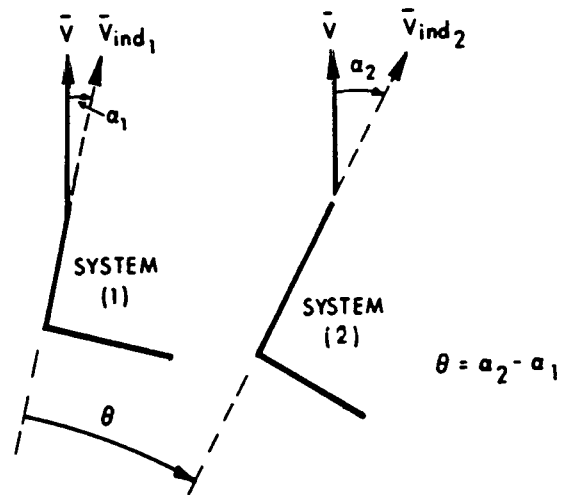


Figure 4-3 Definitions of Angles for Example of One System-Pair

$$\sigma^2(\hat{\alpha}_1 - \alpha_1) = \sigma_{\alpha_1}^2 \left(1 - \frac{1}{1 + \frac{\sigma_{\alpha_2}^2}{\sigma_{\alpha_1}^2} + \frac{\sigma_v^2}{\sigma_{\alpha_1}^2}} \right) \quad \text{D-9}$$

and

$$\sigma^2(\hat{\alpha}_2 - \alpha_2) = \sigma_{\alpha_2}^2 \left(1 - \frac{1}{1 + \frac{\sigma_{\alpha_1}^2}{\sigma_{\alpha_2}^2} + \frac{\sigma_v^2}{\sigma_{\alpha_2}^2}} \right) \quad \text{D-10}$$

The measurement of θ is seen to provide an improved estimate of the misalignments α_i of each system relative to the vector. The actual estimator for $\hat{\alpha}_i$ is found in Reference 4. We have merely shown here the reduced variances of the errors in the estimates of misalignment provided by a measurement of θ . Note that if the measurement noise variance σ_v^2 becomes too large, the measurement loses its effect. We plot D-9 and D-10 in Figure 4-4 for the special case $\sigma_{\alpha_1}^2 = \sigma_{\alpha_2}^2 = \sigma_{\alpha}^2$. For systems with equal variances the largest possible improvement in the variance of α_i is seen to be a factor of two. Whether or not this improvement warrants implementation of the measurement of θ and the computational routine which derives $\hat{\alpha}_1$ and $\hat{\alpha}_2$ is a judgment which cannot be made here.

In summary, this section has shown that multiple independent measurements of a single vector allow an improved estimate of the magnitude of the vector to be simply obtained. These measurements do not provide a corresponding simple improvement in the alignment of each measuring system relative to the vector. Additional measurements which relate the systems by pairs do make possible a significant alignment improvement for each system relative to the vector.

4.3 A Naval Situation

The Navy's constant emphasis on reducing pre-flight

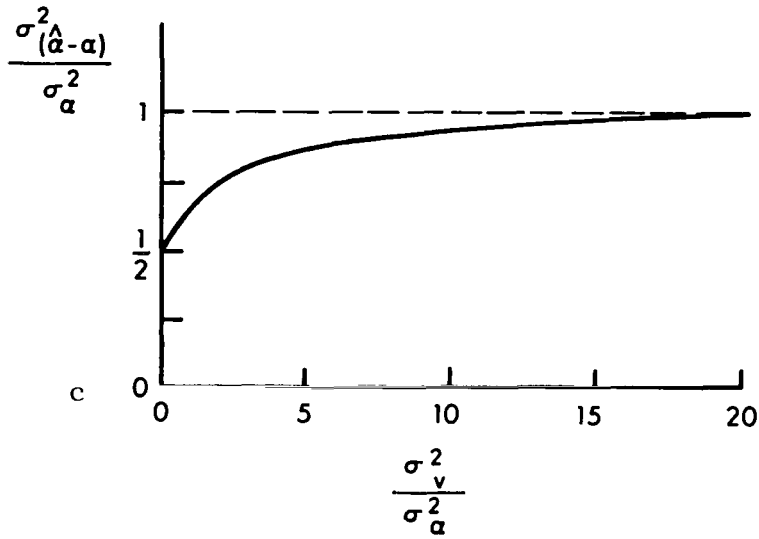


Figure 4-4 Variance of Error in Estimate of Misalignment as Function of Relative Measurement Noise

alignment times for carrier-based aircraft has resulted in two rather operationally unique alignment techniques. These techniques are known as the "Transfer Align" and the "Insertion Method."

The present alignment of an aircraft inertial system at sea is a two-phase procedure; first, the system must be warmed to its operating temperature; and secondly, the alignment is achieved by gyrocompassing (which here means tracking the horizontal component of earth rate from a pre-leveled platform; azimuth coupling is achieved via small platform tilts). The total time required for the two-step process is the "ready time." Personnel of the U.S. Naval Avionics Facility (Indianapolis) have expressed the opinion³⁰ that the ready time for gyrocompassing in a parked aircraft "probably will never be reduced to less than 15 or 20 minutes." At least half of this time period is devoted to gyrocompassing, during which the aircraft must be parked on the deck with uninterrupted power and reference signals. The length of time that the aircraft cannot be moved is considered a serious deck problem.

The insertion technique was proposed as a means of reducing the overall ready time. In this scheme, a thermally stabilized, pre-aligned system is brought from some remote location and inserted in the aircraft^{30, 31}; the dependent frame, in other words, is portable. Rather than aligning the dependent system on a time-constrained basis, it has been continuously gyrocompassing or navigating and its alignment has been carefully trimmed by comparison with SINS. (SINS is the intermediate reference frame aboard naval vessels.) The problem of aligning in a short time in the face of disturbing base motions has been traded for the strictly operational problems of hand carrying a system to the flight line and installing it in an aircraft without introducing severe thermal, mechanical or electrical transients. That this latter procedure can be consistently accomplished in a

short time has not, to this author's knowledge, been proved. It is, nonetheless, a very attractive possibility. Removal of the time constraint on alignment should permit greater gyrocompassing alignment accuracies with the same basic equipment.

The transfer align method reduces only the alignment time; the permanently installed aircraft system must still be brought to operating temperature. This method employs an active transfer reference frame (Section 2.2.4) which is pre-aligned relative to SINS by the techniques of Chapter III. The contractual transfer align effort³² in support of the F-111B aircraft inertial navigation system has chosen to use self-gyrocompassing of the transfer system with the assistance of SINS data. The transfer system is, therefore, an intermediary between SINS and the aircraft system; it may be thought of as an additional master system. Once aligned, the transfer system is carried to the aircraft (operating as a precision navigator on its own battery power) and attached to an external reference surface. Once mechanically attached, the alignment of the aircraft system is accomplished in less than one minute^{30, 32} by means of a technique such as gimbal angle matching.

In both the insertion and transfer align systems, the basic means of transferring alignment from one system to another (See Figure 2-1) is still chosen from those enumerated in Chapter III. But the emphasis is heavily on time. Time and accuracy are closely intertwined in this gyrocompassing mechanization, whereas the time scale is greatly reduced with several other alignment techniques.

The insertion and transfer techniques attack the time problem in distinctly different ways. The insertion method makes the time available for slow gyrocompassing by aligning completely "off line." The transfer technique uses an inherently rapid alignment transfer "on line." The rapid techniques (i. e., gimbal angle matching and optical comparison) require proximity between the

master and slave to eliminate base flexure and/or range problems. A preference for one technique over another is more likely to rest on operational considerations than on purely technical merit.

CHAPTER V

SUMMARY AND RECOMMENDATIONS

5.1 Summary

This study has attempted to develop a unified analysis of the alignment problem, with particular emphasis on the problems related to alignment on a moving base. The analysis facilitates a comparison and evaluation of the fundamental limitations of seemingly distinct techniques. It has described all alignment measurements as measurements of a vector quantity. Furthermore, it has demonstrated significant distinctions among "measuring a vector," "measuring a vector's magnitude," and "measuring a vector's direction," where only the latter is of ultimate significance to the alignment problem. The fundamental inability of a system of sensors to indicate the direction of a vector has been reduced in all cases to an equivalent angular uncertainty. This uncertainty was shown to be a useful figure-of-merit for comparing systems of sensors. Angular deviations of the measured vector for a desired nominal direction have been ascribed to vehicle motions relative to the earth and flexibility of the vehicle structure. The combined effects of sensor imperfection and base motion represent the fundamental limitations on moving base alignment.

It was desired that the basic figure-of-merit chosen for evaluating misalignments be insensitive to coordinate frame

transformation, thereby rendering system-level comparisons independent of system geometry. The magnitude of the whole-angle rotation between coordinate frames met this requirement and also enjoys other important properties. For example, the magnitude of a rotation specified by the arguments of the principal direction cosines is independent of the skewness of the coordinate frame, and the magnitude of a rotation specified by Euler angles is almost completely independent of the order of the rotations. The whole-angle concept made feasible a simply expressed evaluation of the sensitivity of misalignment to the angle between the two required vector inputs. In order to facilitate the adaptation of results expressed in terms of more familiar rotational parameters, the whole angle magnitude was developed in terms of many of these parameters.

The importance of distinguishing between magnitude measurements and directional measurements has been demonstrated in the case of multiple system alignment. Simultaneous measurements of a single vector by multiple systems were shown not to constitute multiple measurements of a common alignment parameter. Therefore, no simple improvement in alignment accrued from aligning the systems simultaneously vs. aligning them separately. It was further shown that any misalignment resulting from only one vector measurement is not physically observable. Viewing the alignment problem as a vector-direction-indication process was crucial to these deductions and to suggesting an additional measurement which both renders the misalignment observable and introduces a useful redundancy. The relative advantage of this measurement was calculated.

The utility of the unified theory of alignment as an analytical tool was demonstrated by application to seven distinct alignment measurement techniques drawn from the literature. In addition to providing a common basis for comparing these techniques, it has been shown to be a simpler way of treating old problems (particularly gimbal angle matching). It also serves an important purpose beyond analysis. It enumerates in detail the basic requirements for alignment, and does this in a standard form. A simple test of sufficiency is thereby available prior to any detailed analysis of a newly discovered technique.

5.2 Recommendations

The non-dimensional analysis of vector measurements has resulted in definite guidelines to minimize magnitude-indication and direction-indication errors as a function of instrument uncertainties and the orientation of the vector relative to the instruments. The results obtained are immediately applicable, yet this appears to be a profitable area for further study. Consideration of higher order instrument uncertainties is certainly appropriate, as well as whether redundant instruments (i. e., a fourth gyro or accelerometer) would contribute significantly to a system's alignment capability. Studies such as this have been made²⁰ where the performance index relates to terminal navigation error, but not, so far as this author knows, where misalignment is the figure-of-merit.

Another area of possible study relates to the calibration problem. In a crude sense, at least, the calibration problem may be viewed as the "inverse" of the alignment problem. That is, for alignment it is assumed that one has the best possible

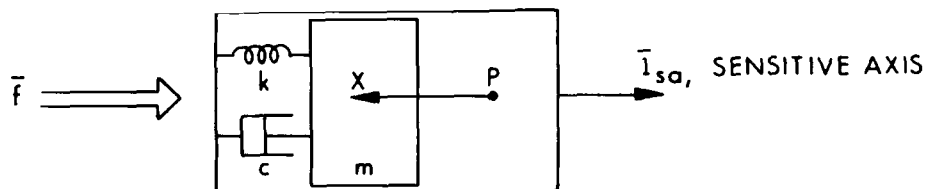
knowledge of his instruments and seeks to ascertain the direction of a vector (sometimes with the help of magnitude measurements). For calibration, on the other hand, it is assumed that one has excellent knowledge of a vector and seeks to ascertain by means of this vector a detailed knowledge of his instruments. For those cases where the misalignment angle is a physical observable during calibration, certain geometrical and analytical formulations of this thesis carry over directly to the calibration problem. The extent to which these formulations aid an understanding of the calibration problem is of interest. Another calibration study was suggested in Chapter IV. It was shown there that it is relatively simple to obtain improved knowledge of a vector's magnitude when the vector is measured simultaneously by several systems. The possibility of using this information to update one's knowledge of certain sensor coefficients appears to this author to be worthy of investigation. The degree to which this updating improves one's ability to align each system is the performance index of interest.

Finally, the author adds his voice to those who have previously emphasized the need for the improved availability of data concerning vehicle motions and descriptive models of this motion. The first requirement for a detailed dynamic study of any of the techniques described in this thesis is a set of representative models for motion of the various vehicles relative to the earth and for the relative linear and angular structural vibrations between inertial system locations.

APPENDIX A

Instrument Example The Linear Accelerometer

To clarify the definition of various instrument uncertainties, consider a simple linear accelerometer.



Point X is the center of mass of the "proof mass." Point P is fixed in the case. The proof mass is mounted so as to have only one degree of translational freedom. \bar{i}_{sa} is a unit vector parallel to the axis of translational freedom and defines the sensitive axis of the accelerometer. The output indication of the instrument, x_1 , is made proportional to the displacement of the proof mass relative to the case along \bar{i}_{sa} .

Let m = the mass of the proof mass.

k = the elastic coefficient of the spring.

c = the damping coefficient.

\bar{f} = the non-field (i. e. contact) specific force acting on the instrument.

p = the derivative operator $\frac{d}{dt}$

and write the governing equation

$$(p^2 + \frac{c}{m} p + \frac{k}{m}) x_i = -\bar{f} \cdot \bar{1}_{sa}$$

In the steady state for constant f

$$x_i = \frac{m}{k} (-\bar{f} \cdot \bar{1}_{sa}) + x_i(0)$$

where $x_i(0)$ is the zero setting of the scale. Choosing the nominal value $x_i(0) = 0$ permits $x_i(0)$ to represent directly any uncertainty in the scale zero. If the elastic coefficient of the spring should be capable of randomly varying by an amount Δk but the mass m remains well known.

$$x_i = -\frac{m}{k} (1 - \frac{\Delta k}{k}) \bar{f} \cdot \bar{1}_{sa} + x_i(0)$$

The foregoing equation describes an imperfect sensing mechanism which converts an input quantity of one set of dimensions (force per unit mass) to another (displacement). The uncertainties in this conversion are inherent to the transducer action referred to $\bar{1}_{sa}$. Hence the nomenclature "transducer uncertainty" to denote imperfections in knowledge of the basic conversion process.

Normalizing the steady state equation for unity gain

$$x_i^* = \frac{k}{m} x_i = - (1 - \frac{\Delta k}{k}) \bar{f} \cdot \bar{1}_{sa} + \frac{k}{m} x_i(0)$$

and comparing with Equation 2.4-55, the following identifications may be made

$$a_0 = \text{bias} = \frac{k}{m} x_i(0)$$

$$a_1 = \text{scale factor} = 1 - \frac{\Delta k}{k}$$

$$\Delta a_1 = \text{scale factor uncertainty} = -\frac{\Delta k}{k}$$

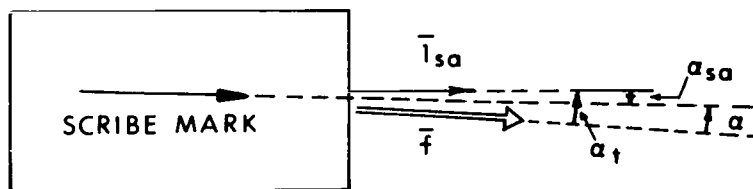
Under automatic operation which, for example, constrains $|x_i^*| = |\bar{f}|$ in order to place $\bar{1}_{sa}$ parallel to \bar{f} , the transducer

uncertainties a_0 and Δa_1 will cause the angle between \bar{f} and \bar{l}_{sa} to be non-zero.

Sensitive axis uncertainty problems arise simply because the accelerometer is typically a sealed unit. This requires knowledge of \bar{l}_{sa} to be transferred to the case exterior as, for example, a scribed line. If the scribed line and \bar{l}_{sa} are skew, the sensitive axis uncertainty numerically equals the skew angle.

Under automatic operation with no transducer uncertainty, \bar{l}_{sa} can be made exactly parallel with the vector input \bar{f} . To an external observer, however, the indicated vector direction is given by the direction of the scribed line. When the external observer role is assumed by the platform upon which the accelerometer is mounted, the platform becomes aligned imperfectly in spite of perfect transducer behavior.

In summary, sensitive axis uncertainty is measured from \bar{l}_{sa} to the scribe mark while transducer uncertainty is measured from the vector input, \bar{f} , to \bar{l}_{sa} . The total indicated misalignment is measured from f to the scribe mark.



- α = total angular indication error.
- α_{sa} = angular indication error contribution of sensitive axis uncertainty.
- α_t = angular indication error contribution of transducer uncertainty.

To further distinguish between transducer uncertainty and sensitive axis uncertainty, consider the calibration of the linear accelerometer. The determination of bias and scale factor requires precise knowledge of the magnitude of \bar{g} but relatively crude knowledge of its direction. Conversely, determination of the location of $\bar{1}_{sa}$ requires precise knowledge of the direction of \bar{g} but relatively crude knowledge of its magnitude. To fully calibrate an instrument, then, requires complete knowledge of the magnitude and direction of the vector used for calibration. Conversely, aligning an instrument with respect to a vector requires a complete knowledge of the magnitude and direction characteristics of the instrument. This contrast is the basis for viewing the calibration problem as the inverse of the alignment problem.

The determination of a_0 and a_1 involves placing $\bar{1}_{sa}$ both parallel and anti-parallel to \bar{g} and taking respective readings $(x_i^*)_1$ and $(x_i^*)_2$. Because the magnitude of \bar{g} sensed by the accelerometer varies as the cosine of the angle between \bar{g} and $\bar{1}_{sa}$, an uncertainty in this angle of up to 1 milliradian still guarantees knowledge of the input magnitude to at least five parts in 10^7 . a_0 is found from

$$a_0 = \frac{(x_i^*)_1 + (x_i^*)_2}{2}$$

and a_1 from

$$a_1 = \frac{(x_i^*)_1 - (x_i^*)_2}{2 |\bar{g}|}$$

Thus, very accurate transducer calibration is had in the face of crude angular alignment.

Having a_0 , the precise direction of $\bar{1}_{sa}$ is found by rotating $\bar{1}_{sa}$ until it is normal to \bar{g} (minimum indicated output). For an uncertainty (1σ) of $5 \times 10^{-7} |\bar{g}|$ in x_i^* , a_0 has an uncertainty (1σ) of $3.5 \times 10^{-7} g$.

This implies that \bar{I}_{sa} may be placed normal to \bar{g} within 3.5×10^{-4} milli radian (or somewhat less than 0.1 arc sec). An orthogonality accuracy of 1 milli radian can be had for a magnitude uncertainty of only 1 part in 10^3 . Placing \bar{I}_{sa} normal to \bar{g} within such tolerances is useful only if the direction of \bar{g} (or its normal plane) is known at least as accurately, for only by reference to this direction can \bar{I}_{sa} be located meaningfully.



APPENDIX B

A CERTAIN EVALUATION OF THE EQUATION

$$A^2 = B^2 + C^2 \pm 2 BC \cos \eta$$

From the equation

$$A^2 = B^2 + C^2 \pm 2 BC \cos \eta \quad (\text{B-1})$$

under the conditions that η is statistically independent of B and C and further that

$$\eta = \eta_1 - \eta_2 \quad (\text{B-2})$$

where η_1 and η_2 are independent variables, each uniformly distributed on the interval $0 - 2\pi$, we wish to evaluate the mean (\bar{A}) and mean-square (A^2) values of A for B and C fixed.

The probability density function for η is given by

$$f(\eta) = \begin{cases} \frac{1}{4\pi^2} (2\pi + \eta) & -2\pi \leq \eta \leq 0 \\ \frac{1}{4\pi^2} (2\pi - \eta) & 0 \leq \eta \leq 2\pi \end{cases} \quad (\text{B-3})$$

The mean of A is derived from

$$\begin{aligned} \bar{A} &= \int_{-2\pi}^{2\pi} A f(\eta) d\eta \\ &= \int_{-2\pi}^{2\pi} \sqrt{B^2 + C^2 \pm 2 BC \cos \eta} f(\eta) d\eta \end{aligned} \quad (\text{B-4})$$

In order to obtain an integrable form of (B-4), the integral is first treated in the following manner

$$\begin{aligned} \bar{A} = \frac{1}{4\pi^2} & \left\{ \int_{-2\pi}^{2\pi} 2\pi \sqrt{B^2 + C^2 \pm 2 BC \cos \eta} d\eta \right. \\ & \left. + \int_{-2\pi}^0 \eta \sqrt{B^2 + C^2 \pm 2 BC \cos \eta} d\eta - \int_0^{2\pi} \eta \sqrt{B^2 + C^2 \pm 2 BC \cos \eta} d\eta \right\} \end{aligned} \quad (B-5)$$

Suitable changes of variable reduce (B-5) to (B-6).

$$\bar{A} = \frac{1}{\pi} \int_0^{2\pi} \sqrt{B^2 + C^2 \pm 2 BC \cos \eta} d\eta - \frac{1}{2\pi^2} \int_0^{2\pi} \eta \sqrt{B^2 + C^2 \pm 2 BC \cos \eta} d\eta \quad (B-6)$$

If (B-4) is treated as

$$\begin{aligned} \bar{A} = \frac{1}{4\pi^2} & \left\{ \int_{-2\pi}^0 \sqrt{B^2 + C^2 \pm 2 BC \cos \eta} (2\pi + \eta) d\eta \right. \\ & \left. + \int_0^{2\pi} \sqrt{B^2 + C^2 \pm 2 BC \cos \eta} (2\pi - \eta) d\eta \right\} \end{aligned} \quad (B-7)$$

the substitutions $(2\pi + \eta) = \eta'$ and $(2\pi - \eta) = \eta''$ in the first and second integrals of (B-7) respectively yield

$$\bar{A} = \frac{1}{2\pi^2} \int_0^{2\pi} \eta \sqrt{B^2 + C^2 \pm 2 BC \cos \eta} d\eta \quad (B-8)$$

Equating (B-6) and (B-8) requires

$$\int_0^{2\pi} \sqrt{B^2 + C^2 \pm 2 BC \cos \eta} d\eta = \frac{1}{\pi} \int_0^{2\pi} \eta \sqrt{B^2 + C^2 \pm 2 BC \cos \eta} d\eta \quad (B-9)$$

which by comparison with the right hand side of (B-8) gives the desired result

$$\bar{A} = \frac{1}{2\pi} \int_0^{2\pi} \sqrt{B^2 + C^2 \pm 2 BC \cos \eta} d\eta \quad (\text{B-10})$$

The form of the integral (B-10) is elliptic. By appropriate changes of variable (B-10) can be reduced to a tabulated form.

For an example, consider the case where the plus sign occurs under the radical. The integral may be split as follows

$$\bar{A} = \frac{1}{2\pi} \left\{ \int_0^{\pi} \sqrt{B^2 + C^2 + 2 BC \cos \eta} d\eta + \int_{\pi}^{2\pi} \sqrt{B^2 + C^2 + 2BC \cos \eta} d\eta \right\} \quad (\text{B-11})$$

Operate on the second integral of (B-11) by first making the change of variable $\eta = (2\pi - n')$ and then interchanging the limits of integration. The two integrals of (B-11) are then identical with the result

$$\bar{A} = \frac{1}{\pi} \int_0^{\pi} \sqrt{B^2 + C^2 + 2 BC \cos \eta} d\eta \quad (\text{B-12})$$

Equation (B-12) also results from manipulations on (B-10) when the minus sign occurs under the radical.

If the substitution $\beta = \eta/2$ is made in (B-12), the tabulated form of (B-13) is obtained.

$$\begin{aligned} \bar{A} &= \frac{2}{\pi} (B + C) \int_0^{\pi/2} \sqrt{1 - k^2 \sin^2 \beta} d\beta \\ &= \frac{2}{\pi} (B + C) \mathcal{E} (k^2) \end{aligned} \quad (\text{B-13})$$

\mathcal{E} is the complete elliptic integral of the second kind¹⁷ with argument k^2

$$k^2 = \frac{4 BC}{(B + C)^2} \quad (\text{B-14})$$

The evaluation of the mean-square value of A follows much more directly. $\overline{A^2}$ is defined by

$$\begin{aligned} \overline{A^2} &= \int_{-2\pi}^{2\pi} A^2 f(\eta) d\eta \\ &= \int_{-2\pi}^{2\pi} (B^2 + C^2 \pm 2 BC \cos \eta) f(\eta) d\eta \end{aligned} \quad (\text{B-15})$$

which is simply integrated with the result

$$\overline{A^2} = B^2 + C^2 \quad (\text{B-16})$$

The results (B-11) and (B-14) are for B and C held constant. If they are random variables, the dependence of \overline{A} and $\overline{A^2}$ on the statistics of B and C would be calculated from (B-11) or (B-14) respectively.

APPENDIX C

AN INTERPRETATION OF STATISTICS ASSOCIATED WITH A TRIAD OF SENSORS

Relative to measuring a vector with a triad of similar instruments, we may make the interpretation of Figure C-1: instrument uncertainties result in a three-dimensional uncertainty in the location of the tip of the vector \bar{V} . The statistics of this uncertainty relative to the tip of the vector are obtained by affixing the x, y, z coordinate set to the tip of the vector such that it is a translated (but not rotated) representation of the x', y', z' frame. If we now assume for convenience that the instrument uncertainties of Equation 2.4-60 are normally distributed with zero mean, the statistics along x, y, and z are normally distributed with zero mean and standard deviations

$$\begin{aligned}\sigma_x &= \sqrt{\sigma_{a_0}^2 + V^2 \cos^2 \psi_1 \sigma_{\Delta a_1}^2} \\ \sigma_y &= \sqrt{\sigma_{a_0}^2 + V^2 \cos^2 \psi_2 \sigma_{\Delta a_1}^2} \\ \sigma_z &= \sqrt{\sigma_{a_0}^2 + V^2 \cos^2 \psi_3 \sigma_{\Delta a_1}^2}\end{aligned}\tag{C-1}$$

Note that although the statistics of each instrument are identical, the statistics of each axis are generally non-identical. This phenomenon results from scaling of the scale factor uncertainty contribution by the projected magnitude of the measured vector.

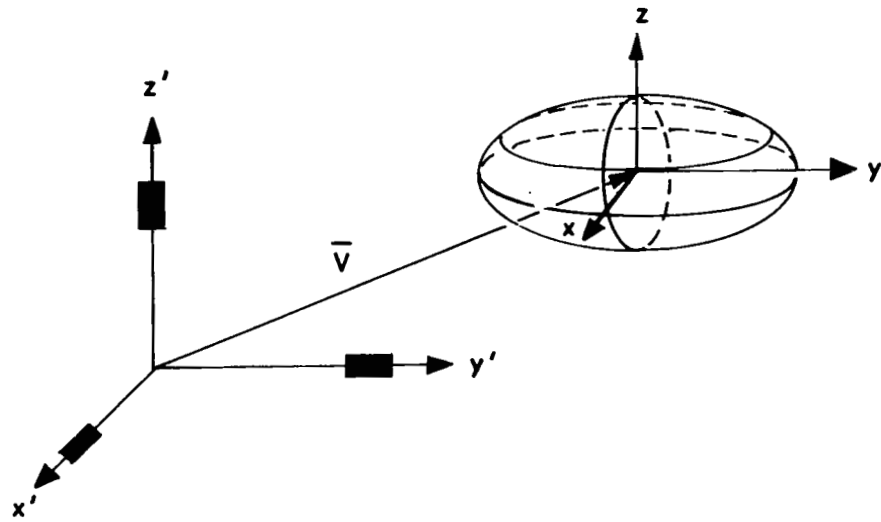


Figure C-1 Statistics Associated with a Triad of Sensors

It is of great interest to many people to plot contours of constant probability density in order to exploit certain geometrical interpretations of probability. Unfortunately, this problem does not lend itself to this technique. The contours of constant probability density in three-space are described by

$$\frac{x^2}{\sigma_x^2} + \frac{y^2}{\sigma_y^2} + \frac{z^2}{\sigma_z^2} = \text{Const.} \quad (\text{C-2})$$

The solid body described by C-2 is an ellipsoid, but one whose shape varies as its center is moved in three space. It becomes an ellipsoid of revolution if and only if two of the three direction cosines of the vector are equal. It becomes spherical if and only if all three direction cosines are equal. This, of course, only occurs when the vector is geometrically centered in the octant. There are exactly eight positions of the vector in all of three-space for which the contour of constant probability density is spherical! It should be obvious that for the majority of possible vector orientations with respect to the triad, the contours are not simple surfaces of revolution.

Results such as 2.4-66 are obtained without full calculation of the three dimensional error probability density functions for all vector orientations. The approach taken there is simpler and more direct. If one were to develop the three-dimensional probability density and evaluate the statistics of a vector tip's location, great care would have to be exercised to see that the result obtained related to directional uncertainties and not just the "total uncertainty" in measuring a vector.

APPENDIX D

OPTIMAL ESTIMATION APPLIED TO MULTIPLE SYSTEMS

Consider two independent random variables α_1 and α_2 , each of zero mean and respective variances $\sigma_{\alpha_1}^2$ and $\sigma_{\alpha_2}^2$.

By one measurement involving α_1 and α_2 we can make better estimates $\hat{\alpha}_1$ and $\hat{\alpha}_2$ of α_1 and α_2 such that our estimation error is improved

$$\sigma^2(\hat{\alpha}_1 - \alpha_1) \leq \sigma_{\alpha_1}^2 \quad (D-1)$$

$$\sigma^2(\hat{\alpha}_2 - \alpha_2) \leq \sigma_{\alpha_2}^2$$

even in the face of measurement noise. This is done here by a straightforward application of optimal estimation theory. We use here the formulation and notation of Bryson⁹.

The physical measurement is

$$z = \theta + v = \alpha_2 - \alpha_1 + v \quad (D-2)$$

$$= H \underline{x} + v \quad (D-3)$$

where the noise in the measurement is v and we have defined

$$H = [-1, +1], \quad \underline{x} = \begin{bmatrix} \alpha_1 \\ \alpha_2 \end{bmatrix} \quad (D-4)$$

v is assumed independent of \underline{x} with zero mean and known variance σ_v^2 . Using the known relation of θ to \underline{x} (Equation D-3), the known statistics of v , an initial estimate of \underline{x} , and the known uncertainty in this initial estimate, one can obtain an improved (in the least squares sense) estimate $\hat{\underline{x}}$ of \underline{x} (Reference 4).

The covariance matrix of the error in the estimate of \underline{x} is given by

$$P \equiv E(\underline{e}, \underline{e}^T) \equiv E\left[\left(\hat{\underline{x}} - \underline{x}\right) \left(\hat{\underline{x}} - \underline{x}\right)^T\right] \quad (D-5)$$

where E is the expected value operation. P is given by

$$P = M - M H^T (H M H^T + R)^{-1} H M \quad (D-6)$$

where M is the covariance matrix of our initial estimation error

$$M = E\left[\left(\underline{x} - \bar{\underline{x}}\right) \left(\underline{x} - \bar{\underline{x}}\right)^T\right] = \begin{bmatrix} \sigma_{\alpha_1}^2 & 0 \\ 0 & \sigma_{\alpha_2}^2 \end{bmatrix} \quad (D-7)$$

and R is the covariance matrix of the measurement error.

$$R = E(v^2) = \sigma_v^2 \quad (D-8)$$

Straightforward algebra yields for the variances in the errors in the estimates of α_1 and α_2

$$\sigma^2(\hat{\alpha}_1 - \alpha_1) = \sigma_{\alpha_1}^2 \left(1 - \frac{1}{1 + \frac{\sigma_{\alpha_2}^2}{\sigma_{\alpha_1}^2} + \frac{\sigma_v^2}{\sigma_{\alpha_1}^2}} \right) \quad (D-9)$$

and

$$\sigma^2(\hat{\alpha}_2 - \alpha_2) = \sigma_{\alpha_2}^2 \left(1 - \frac{1}{1 + \frac{\sigma_{\alpha_1}^2}{\sigma_{\alpha_2}^2} + \frac{\sigma_v^2}{\sigma_{\alpha_2}^2}} \right) \quad (D-10)$$

The results D-9 and D-10 fit the restrictions D-1.

REFERENCES

1. Brock, L. , "Application of Statistical Estimation to Navigation Systems," M. I. T. Ph. D. Thesis, 1965.
2. Hovorka, J. , "Damping of Inertial Navigation Systems," M. I. T. Sc. D. Thesis, May 1961.
3. Nauman, R. L. , and Oestreich, J. W. , "Alignment of Inertial Guidance Systems on a Non-Rigid Body," M. I. T. S. M. Thesis, 1961.
4. Gulland, C. K. , "The Rapid Transference of Stable Coordinates on a Moving Craft," M. I. T. S. M. Thesis, 1957.
5. O'Donnell, C. F. , ed. , "Inertial Navigation, Analysis and Design," McGraw-Hill, New York, 1964.
6. Broxmeyer, C. , "Inertial Navigation Systems," McGraw-Hill, New York, 1964.
7. Pitman, G. R. , Jr. , ed. , "Inertial Guidance," John Wiley and Sons, New York, 1962.
8. Draper, C. S. , Wrigley, W. , and Hovorka, J. , "Inertial Guidance," Pergamon, London, 1960.
9. Bryson, A. E. , and Ho, Y. , "Optimal Programming, Estimation, and Control," (To be published), Harvard University, Cambridge, 1966.
10. Aviation Week and Space Technology, McGraw-Hill Publications, New York, August 17, 1964, p. 84.
11. Halfman, R. L. , "Dynamics," Vol. I, Addison-Wesley, Reading, Massachusetts, 1959.
12. Goldstein, H. , "Classical Mechanics," Addison-Wesley, Reading, Massachusetts, 1959.
13. Wrigley, W. , "An Investigation of Methods Available for Indicating the Direction of the Vertical from Moving Bases," M. I. T. Sc. D. Thesis, 1941.
14. Wrigley, W. , and Hollister, W. , Notes for Course 16.41, "Space Dynamics and Gyroscopic Instruments," M. I. T.

15. Ball, R. S., "A Treatise on the Theory of Screws," University Press, Cambridge, England, 1900.
16. Hildebrand, F. B., "Methods of Applied Mathematics," Prentice-Hall, Englewood Cliffs, New Jersey, 1952.
17. Markey, W. R., and Hovorka, J., "The Mechanics of Inertial Position and Heading Indication," Methuen, London, 1961.
18. Abramowitz, M., and Stegun, I. A., eds., "Handbook of Mathematical Functions," U. S. Government Printing Office, Washington, D. C., 1964.
19. Cooper, J. R., "A Statistical Analysis of Gyro Drift Test Data," M. I. T. S. M. Thesis, 1965.
20. Gunckel, T. L., II, and Vander Stoep, D. R., "Optimizing Accelerometer Orientations," Paper presented to SAE/NASA Aerospace Vehicle Flight Control Conference, Los Angeles, July, 1965.
21. Cannon, R. H., Jr., "Kinematic Drift of Single Axis Gyroscopes," Paper 57-A-72 ASME, Journal of Applied Mechanics, September, 1958.
22. Goodman, L. E., and Robinson, A. R., "Effect of Finite Rotations on Gyroscopic Sensing Devices," Paper 57-A-30 ASME, Journal of Applied Mechanics, June, 1958.
23. Weinstock, H., "Effect of Angular Vibration on Gyroscope Performance," Inertial Navigation Equipment Evaluation Techniques, (Notes from M. I. T. '63 Summer Program, 16.39S), M. I. T., 1963.
24. Thomas, I. L., "Notes on the Fundamental Problems Involved in Determining True North by Gyroscopic Methods," Tech Note I. E. E. 56, Royal Aircraft Establishment, London, August, 1964.
25. Quasius, G., and McCanless, F., "Star Trackers and System Design," Spartan Books, Washington, 1966.
26. "Proposal for An Optical/Inertial Guidance Study," TRW Systems, Redondo Beach, California, TRW Sales No. 7398.000, May, 1966.
27. Sutherland, A., "Application of Optimal Linear Estimation to the Alignment of Inertial Guidance Systems," M. I. T. Sc. D. Thesis, September, 1966.
28. Loeber, A. P. and Del Carlo, C., "Development of Three-Axis Electro-Optical Synchro Transmission Techniques," Technical Documentary Report No. ASD-TDR-63-178, Chrysler Corporation Missile Division, Detroit Michigan, March, 1963.
29. U. S. Patent Office, Patent No. 3241430, "Three Axis Optical Alignment Device," 22 March 1966.

30. Snare, L. E., Loser, J. L., and Wisehart, W. R., "Discussion of Various Alignment Methods," U. S. Naval Avionics Facility, Indianapolis, 9670/6760, 1 May 1964.
31. Aviation Week and Space Technology, "USAF to Test Suitcase Navaid for F-111," 23 August 1965, p. 52, McGraw-Hill.
32. Berke, L. C., "Master Reference for Rapid At-Sea Alignment of Aircraft Inertial Navigation Systems," AIAA/JACC Guidance and Control Conference, Seattle, Washington, 16 August 1966.

Electronics Research Center
National Aeronautics and Space Administration
Cambridge, Massachusetts, April 1967
180-17-01-05

"The aeronautical and space activities of the United States shall be conducted so as to contribute . . . to the expansion of human knowledge of phenomena in the atmosphere and space. The Administration shall provide for the widest practicable and appropriate dissemination of information concerning its activities and the results thereof."

—NATIONAL AERONAUTICS AND SPACE ACT OF 1958

NASA SCIENTIFIC AND TECHNICAL PUBLICATIONS

TECHNICAL REPORTS: Scientific and technical information considered important, complete, and a lasting contribution to existing knowledge.

TECHNICAL NOTES: Information less broad in scope but nevertheless of importance as a contribution to existing knowledge.

TECHNICAL MEMORANDUMS: Information receiving limited distribution because of preliminary data, security classification, or other reasons.

CONTRACTOR REPORTS: Scientific and technical information generated under a NASA contract or grant and considered an important contribution to existing knowledge.

TECHNICAL TRANSLATIONS: Information published in a foreign language considered to merit NASA distribution in English.

SPECIAL PUBLICATIONS: Information derived from or of value to NASA activities. Publications include conference proceedings, monographs, data compilations, handbooks, sourcebooks, and special bibliographies.

TECHNOLOGY UTILIZATION PUBLICATIONS: Information on technology used by NASA that may be of particular interest in commercial and other non-aerospace applications. Publications include Tech Briefs, Technology Utilization Reports and Notes, and Technology Surveys.

Details on the availability of these publications may be obtained from:

SCIENTIFIC AND TECHNICAL INFORMATION DIVISION
NATIONAL AERONAUTICS AND SPACE ADMINISTRATION

Washington, D.C. 20546